THE ROLE OF IL-17RA- AND IL-17RC-DEPENDENT SIGNALS ON NON-HEMATOPOIETIC CELLS IN SHAPING THE HOST IMMUNE RESPONSES DURING *CHLAMYDIA* RESPIRATORY TRACT INFECTION

by

Cynthia Tram

Submitted in partial fulfilment of the requirements
for the degree of Master of Science

at

Dalhousie University
Halifax, Nova Scotia
August 2016

For my mom, dad, and brother,

thank you for all of your support!

TABLE OF CONTENTS

LIST OF TABLES

LIST OF FIGURES

ABSTRACT

The role of IL-17-family cytokines and their receptor-mediated signaling in host defense is complex. During my graduate study, I investigated the specific role of non-hematopoietic IL-17 receptor A (IL-17RA) and IL-17RC in controlling bacterial replication and host immune responses to intracellular *Chlamydia* infection *in vitro* and *in vivo*. A series of *in vitro* studies using mouse embryonic fibroblasts (MEFs) revealed that exogenous IL-17A, IL-17C, or IL-17E do not have inhibitory effects on intracellular *Chlamydia* replication in in MEFs. However, endogenous IL-17A is required to control *Chlamydia* replication as loss of IL-17RA in MEFs results in heightened bacterial burden. While *Chlamydia* infection stimulated production of cytokines and chemokines in MEFs, including IL-1α, IL-1β, IL-6, TNF, IL-10, IL-22, CXCL1, CCL3, CXCL2, TSLP, and GM-CSF, the cytokine profile was markedly altered in IL-17R-unresponsive MEFs, particularly in IL-17RA-knockout (KO) MEFs. In parallel with *in vitro* studies, bone marrow chimeric (BMC) mice were constructed using IL-17RAKO and IL-17RCKO mice as recipients for wild-type (WT) hematopoietic cells. Compared to WT-BMC mice, IL-17RAKO-BMC and IL-17RCKO-BMC mice displayed greater clinical disease upon respiratory *Chlamydia* infection, which was associated with significantly higher bacterial burden, enhanced rates of apoptosis, and heightened mononuclear cell infiltration in the lungs. A unique IL-17A-producing population with characteristic features of type 3 innate lymphoid cells (ILC3) was markedly induced in the BMC mice containing IL-17R-unresponsive tissue structure cells, particularly in IL-17RAKO-BMCs, indicating a relationship between IL-17RA and ILC3 induction in *Chlamydia* infection. Of interest, while IL-17RAKO-BMC mice displayed a type 17-biased immune profile, IL-17RCKO-BMC mice had enhanced type 1 immune responses compared to WT-BMC mice. Collectively, our results highlight an important role of non-hematopoietic IL-17RA and IL-17RC in host defense against *Chlamydia* infection and explicitly demonstrate distinct roles of IL-17RA and IL-17RC in tissue stromal cells in shaping host immune responses. To my knowledge, this is the first study in the *Chlamydia* research field that provides in-depth characterization of an animal model upon *Chlamydia* infection that will be useful in dissecting the nature of immunopathology associated with persistent *Chlamydia* infection.

LIST OF ABBREVIATIONS USED

ACK	ammonium-chloride-potassium
Act1	NFκB activator 1
AmpR	ampicillin resistance gene
ANOVA	analysis of variance
APC	antigen-presenting cell
ASF	alternative splicing factor
BAL	bronchoalveolar lavage
BCG	bacillus Calmette- Guérin
BMC	bone marrow chimeric
bp	base pair
BS	bovine serum
CCL	CC-chemokine ligand
CD	cluster of differentiation
cDC	conventional dendritic cell
C/EBP	CCAAT-enhancer-binding protein
cHSP60	chlamydial heat shock protein 60
Cm	*Chlamydia muridarum*
COX	cyclooxygenase
CPAF	chlamydial-proteasome/protease-like factor
CXCL	CXC-chemokine ligand 1
DAPI	4',6'-diamidino-2-phenylindole
DC	dendritic cell

DMEM	Dulbecco's modified Eagle medium
dUTP	deoxyuridine triphosphate
EB	elementary body
ELISA	enzyme-linked immunosorbent assay
ERK	extracellular signal-regulated kinases
FACS	fluorescence-activated cell sorting
FBS	fetal bovine serum
Foxp3	forkhead box P3
FRET	fluorescence resonance energy transfer
GATA	GATA-binding protein
gDNA	genomic deoxyribonucleic acid
GFP	green fluorescent protein
GM-CSF	granulocyte/monocyte colony-stimulating factor
HBSS	Hank's balanced salt solution
H & E	hematoxylin and eosin
HK	heat-killed
HK-*Cm*	heat-killed *Cm*
HSP	heat-shock protein
ICAM	intracellular adhesion molecule
ICCS	intracellular cytokine staining
IDO	indoleamine-2,3-dioxygenase
Ig	immunoglobulin
IFN	interferon

IFU	inclusion forming unit
IKK-ε	nuclear factor kappa-B kinase subunit-epsilon
IKK-γ	nuclear factor kappa-B kinase subunit-gamma
IL	interleukin
IL-17R	IL-17 receptor
IL-17RA	IL-17 receptor A
IL-17RC	IL-17 receptor C
ILC	innate lymphoid cell
iNKT	invariant natural killer T
iNOS	inducible nitric oxide synthase
i.p.	intraperitoneal
JAK	Janus-activated kinase
KIR	killer immunoglobulin-like receptor
KD	knockdown
KO	knockout
LB	lysogeny broth
LPS	lipopolysaccharide
Lin-	lymphoid lineage negative
LTi	lymphoid tissue inducer
MAPK	mitogen-activated protein kinase
MEF	mouse embryonic fibroblast
MEM	minimal essential medium
MHC	major histocompatibility complex

MIP	macrophage inflammatory protein
MLN	mediastinal lymph node
MOI	multiplicity of infection
MOMP	major outer membrane protein
mRNA	messenger ribonucleic acid
MyD88	myeloid differentiation factor 88
NFκB	nuclear factor kappa-light-chain-enhancer of activated B cells
NCR	natural cytotoxicity receptor
NK	natural killer
NKT	natural killer T
NLR	NOD-like receptors
NO	nitric oxide
NOD	nucleotide-binding oligomerization domain
PAMP	pathogen-associated molecular pattern
PBS	phosphate-buffered saline
PCR	polymerase chain reaction
pDC	plasmacytoid dendritic cell
PGN	peptidoglycan
p.i.	post infection
PI3K	phosphoinositide 3-kinase
PMA	phorbol myristate acetate
PRR	pattern-recognition receptor
P/S	penicillin/streptomycin

qPCR	quantitative polymerase chain reaction
RAG	recombination-activating genes
RB	reticulate body
RNA	ribonucleic acid
ROR	retinoid-related orphan receptor
RPMI	Roswell Park Memorial Institute medium
rRNA	ribosomal ribonucleic acid
RT	room temperature
RT-PCR	reverse transcription-polymerase chain reaction
SCID	severe combined immunodeficiency
SD	standard deviation
SEFIR	similar expression to FGF receptor/IL-17R
SEM	standard error of the mean
SPG	sucrose-phosphate-glutamic buffer
STAT	signaling transducer and activator of transcription
TAK1	TGFβ-activated kinase 1
Tc	T cytotoxic
TCR	T cell receptor
TGF	transforming growth factor
Th	T helper
TL1A	TNF-like protein 1A
TLR	toll-like receptor
TNF	tumor necrosis factor

TRAF	tumor necrosis factor receptor-associated factor
Treg	T regulatory cell
TSLP	thymic stromal lymphopoietin
TUNEL	terminal deoxynucleotidyl transferase dUTP nick end labeling
WT	wild-type

ACKNOWLEDGEMENTS

First and foremost, I would like to thank my supervisor Dr. Jun Wang for her utmost support, encouragement, and guidance as her student for the past few years. Under her training, I have gained a surpassing amount of knowledge and I am incredibly thankful for her help in guiding me through my research and getting to where I am today. I would also like to thank my co-supervisor Dr. Scott Halperin for his support, and my supervisory committee Dr. Brent Johnston and Dr. Andrew Stadnyk for their time and feedback throughout my research project.

My MSc program would not have been complete without the help and support of past and present lab members and colleagues. I would like to thank the numerous past lab members of Dr. Wang's lab especially Hyun, Sheren, and Bassel for helping me get started in the lab. I would also like to thank the present lab members, especially Rachel, Chi, and Emily for giving me a great amount of support in the lab. Also, I would like to thank the students from other labs and departments for their time and resources throughout my program. I am thankful for all other lab personnel, technicians, and staff that have helped me throughout my program with special thanks to Derek Rowter for many hours of cell acquisition.

Last but not least, I would like to thank my mother, father, and brother who have always supported from the beginning. I am extremely thankful for their encouragement and patience throughout my years of school.

CHAPTER 1 INTRODUCTION

1.1 *Chlamydia* infection and associated diseases

1.1.1 Prevalence of *Chlamydia* infection and disease worldwide

Chlamydiae is a class of intracellular bacterial pathogens that infect the mucosal epithelium lining the respiratory, ocular, and genital tracts of humans and animals leading to a wide spectrum of diseases (1). Serovars D-K (2) of the species *Chlamydia trachomatis* causes genital tract infections and mainly infect the urethra in men and the endocervix in women (1). *C. trachomatis* genital tract infections are the most common bacterial sexually transmitted disease in humans (3). The disease is highly asymptomatic in males and females and, therefore, these individuals are often left untreated. In 2012, there were an estimated 131 million new cases of *Chlamydia* infections globally (3), which is higher than the number of gonorrhoea and syphilis cases. Approximately 30-50% of men and 70-90% of women that are infected with *C. trachomatis* do not develop symptoms (4, 5). This infection may cause inflammation, edema, and mucosal discharge from the genital tract (6). If the infection is diagnosed, genital infections can be treated with doxycycline and azithromycin (7). Untreated genital tract infections with *C. trachomatis* may lead to infertility, pelvic inflammatory disease, and ectopic pregnancies in women (2). With a high prevalence of asymptomatic *C. trachomatis* genital infections, neonatal *Chlamydia* infections by vertical transmission from infected mothers (8, 9) are a significant health concern. The genital serovars of *C. trachomatis* can also cause neonatal conjunctivitis and pneumonia and are commonly acquired during childbirth from infected mothers (2). Of the neonates that are born to *Chlamydia*-infected mothers, 8% to 44% develop conjunctivitis and up to 17% develop pneumonia (10). Of all deaths in children that are less than 6 months of age, 16%

are caused by *pneumoniae* (11). The trachoma serovars (A-C) of *C. trachomatis* causes ocular infections and is the leading cause of preventable blindness worldwide (12). Also, the invasive lymphogranuloma venereum serovars (L1-L3) of *C. trachomatis* can cause severe infection of mononuclear phagocytes of lymph nodes and disseminates via the lymphatic system in humans leading to areas of necrosis within the lymph nodes, followed by the formation of abscess (13, 14).

Chlamydia pneumoniae is transmitted between humans through infected aerosol droplets (15). *C. pneumonia* is a common human respiratory disease which leads to community-acquired pneumonia, pharyngitis, bronchitis, and sinusitis (16). This human respiratory pathogen is responsible for approximately 10% of all community-acquired pneumonia and 5% of bronchitis and sinusitis cases (17). Approximately 50% of healthy young adults and 75% of the elderly have serological evidence of previous *C. pneumoniae* infection (18). Additionally, *C. pneumoniae* has been associated with atherosclerosis, chronic obstructive pulmonary disease, and asthma (19, 20). In one study, patients with antibody specific for *C. pneumoniae* had an increased risk for myocardial infarction and coronary heart disease, as the difference in the frequency of antibody in patients versus controls were significantly different (21). *C. pneumoniae* gains access to the vasculature during inflammation of the local respiratory tract (22). Also, *C. pneumoniae* infects vascular endothelial cells *in vitro* and stimulates the secretion of proinflammatory cytokines and expression of leukocyte adhesion molecules (23). Smoking has also been associated with increased levels of *C. pneumoniae* serum antibodies in patients that had chronic obstructive pulmonary disease (24). As summarized by Hahn (20), 15 out of 18 controlled epidemiologic studies found significant associations between *C. pneumoniae* infection and asthma.

Chlamydia psittaci is primarily transmitted between birds and is associated with epizootic outbreaks (25). Humans can get infected by *C. psittaci* by inhaling droplets or dust particles containing the urine, respiratory secretions, or dried feces of infected birds (25). *C. psittaci* infection in humans causes minor to severe systemic disease resulting in pneumonia and encephalitis (25). Another animal pathogen, *Chlamydia pecorum,* is a widespread pathogen of livestock including cattle, goats, and pigs (26). *Chlamydia suis* is also a natural pathogen of pigs causing a range of diseases (27). The role of *C. pecorum* and *C. suis* in human disease has not been reported.

Chlamydia muridarum (Cm) is a distinct biovar of *C. trachomatis* (28). *Cm* was originally isolated from the lungs of mice and this strain has been extensively propagated and passaged in the laboratory setting (28, 29). The first successful infection in the urogenital tract of mice showed that *Cm* infection mimics many aspects of human *Chlamydia* infection including *Cm*-induced infertility (30). Since then, *Cm* has been widely utilized for studying the immune responses and pathogenesis of respiratory and/or genital tract *Chlamydia* infection in mice (31–33).

1.1.2 *Chlamydia* replication cycle

The growth of *Chlamydia* species is unique in that it consists of a biphasic life cycle (Figure 1.1). The bacterial forms involved are the small (~0.3 μm) elementary body (EB), which is infectious but metabolically inactive, and the larger (~0.8 μm) reticulate body (RB), which is non-infectious but metabolically active (34). The EB attaches to the cell surface and enters the cell via endocytosis. The infected cell forms a phagocytic compartment which is rapidly altered by *Chlamydia*-derived proteins to form a vacuole

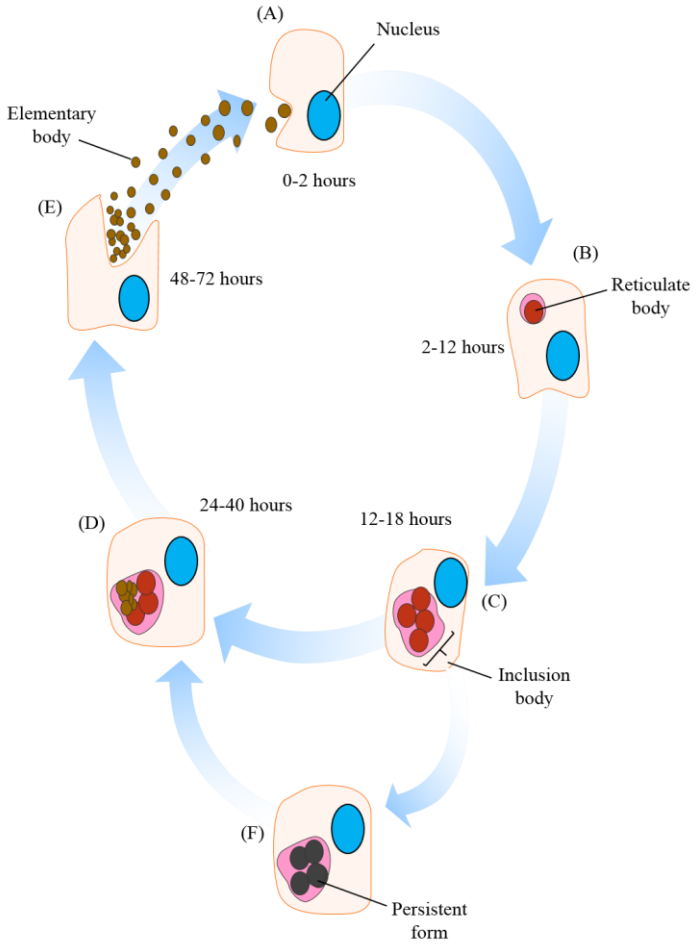

Figure 1.1 The *Chlamydia* growth and replication life cycle. (A) *Chlamydia* elementary bodies (EBs) attach to epithelial cells by receptor-mediated endocytosis. Two hours post internalization into the cells, the EBs fuse together to form a nascent inclusion body. (B) Between 2 to 12 hours post internalization, the EBs begin to differentiate into reticulate bodies (RBs) and divide by binary fission (C). The increasing numbers of RBs differentiate back into EBs at approximately 24 hours post infection (D) and continue differentiating until the cell lyses (E) or releases the EBs at around 48 to 72 hours post infection. (F) In the presence of stimuli or inhibitors such as IFN-γ, penicillin, or amino acid deprivation, *Chlamydia* will be driven into a persistent state where RB division stops until the stimuli or inhibitor is removed (35, 36).

called the inclusion body (6). The inclusion body quickly dissociates from the endolysosomal pathway and avoids fusing with lysosomes (37). The EBs then differentiate into the RBs and multiply with the maturation of the inclusion (37). The RBs continue to divide by binary fission and at approximately 24-40 hours after initial infection, they transition back into EBs (6). The newly formed EBs are released from the cell via host cell lysis or exocytosis at approximately 48-72 hours post infection and infect neighboring cells (6, 38).

The phenomenon of chlamydial persistence has been studied extensively *in vitro* (36). Persistent chlamydial infection is defined as viable but non-replicating bacteria which is believed to be a key cellular mechanism leading to chronic disease (36). *Chlamydia* persistence can be induced *in vitro* by treating the cells with antibiotics and/or cytokines or by removing essential nutrients (36), which often lead to altered ultrastructural characteristics of the inclusion body (39). IFN-γ is the most extensively studied of the cytokines that can cause persistent *C. trachomatis* infection (36). High levels of IFN-γ suppress *Chlamydia* growth but low levels of this cytokine have been shown to induce morphological aberrant intracellular forms (39). Molecular studies of persistence have mainly involved the major outer membrane protein (MOMP) and the chlamydial heat shock protein 60 (cHSP60) (36). *C. trachomatis* infection of HeLa cells and exposure to IFN-γ cause cHSP60 to increase and MOMP levels to decrease, which were indicative of molecular changes during *Chlamydia* infection (40). Alternatively, *Chlamydia* can become spontaneously persistent after infection of monocytes via a cytokine-independent mechanism (41). Also, after lytic infection by bacteriophages, enlarged, distended RBs have been observed that had the basic characteristics of aberrant bodies seen in other cell culture models of persistence (42, 43). The abnormally large reticulate bodies eventually

lyse, releasing phage progeny and mature EBs in the inclusion into the cytosol of the cell when the inclusion membrane is lysed (43). Additionally, when host cells and *Chlamydia* are able to multiply in the absence of stresses, continuous cultures can become spontaneously persistent (36) and have been shown to contain enlarged RB resembling those described in other persistent *Chlamydia* infections (44). Continuous cultures are defined as cycles of inclusion-free host cell multiplication eventually leading to partial (45) or almost complete (46) host cell destruction. Some continuous cultures have been suggested to be established by a genetic block instead of blocks by inhibitors or deficiencies (36) indicating that *Chlamydia* or the host cells may have favoring genotypes that lead to a persistent relationship.

Some evidence for chlamydial persistence *in vivo* comes from experimental animal infections via observation of morphologically aberrant chlamydial forms (47). Clinical data from human disease suggest that recurring *Chlamydia* infections are due to reactivation of persistent infections rather than reinfection (48). However, these data do not confirm persistent infection, hence there is currently no recent direct evidence of persistent *Chlamydia* infection *in vivo*.

1.1.3 The mouse model of respiratory and genital tract *Chlamydia* infection

The mouse model of *Cm* infection is widely utilized to study the host immune responses because the course of infection in mice resembles *C. trachomatis* or *C. pneumoniae* infections in humans (49). However, there are important differences to consider in human and mouse *Chlamydia* infections. One difference is that infections in mice are self-limiting and mice resolve the infection by approximately 1 month (50). In contrast, humans can potentially develop chronic infections and may not spontaneously

clear the infection for several months (50). Immune evasion mechanisms also differ in that there are currently no direct *in vivo* data linking *Chlamydia* infections in humans to persistence of infection (36).

Studying the cellular immune responses to *C. trachomatis and C. pneumoniae* are important because of the chronic diseases that occur in the genital tract and lungs of humans. However, it is important to consider the differences in the immunological features of the lung and the female genital tract. The immune response induced at the mucosal inductive sites in the lungs are common to other mucosal sites (51). On the other hand, the genital tract mucosa lacks organized mucosal lymphoid structures that are found in the lung (52). The female genital tract is divided into immunologically different lower and upper genital tracts as opposed to the multi-lobed upper and lower lung (53). Nonetheless, the mouse model has provided substantial information about the immunobiology of *Chlamydia* infection.

1.2 Host responses to *Chlamydia* infection

1.2.1 Innate immune responses

1.2.1.1 Mucosal epithelial cells

Chlamydia infection is initiated at the mucosal surface of the epithelium (54) and causes intense local inflammation orchestrated by the induction and release of antimicrobial peptides, cytokines, and chemokines by the mucosal epithelial cells (2). This leads to the recruitment of innate immune cells to the site of infection, which in turn, activate adaptive immune responses (2). The mucosal epithelium acts as a first line of host defence via pattern-recognition receptors (PRRs) (55). Toll-like receptors (TLRs) are a class of PRRs and are the most widely studied (56). TLR activation initiates downstream myeloid

differentiation factor 88 (MyD88) (56) which activates nuclear factor kappa B (NFκB) and mitogen-activated protein kinase (MAPK) pathways leading to production of chemokines and proinflammatory cytokines (56). In turn, the proinflammatory cytokines and chemokines induce secretion of antimicrobial peptides and defensins (56). In particular, TLR2 and TLR4 are believed to sense *Chlamydia* infection, mainly recognizing heat shock proteins (HSP) and cell wall components like lipopolysaccharides (LPS), respectively (57).

It has been shown that a greater amount of EBs were attached in coated pits and vesicles when *C. trachomatis* was inoculated onto the apical surfaces of polarized cells than in unpolarised cells (58). This suggests that *Chlamydia* organisms spread from one cell to another at the apical surface and are mainly exposed to the mucosal extracellular environment. In doing so, the organisms get exposed to antimicrobial peptides, among other host immune effectors, that potentially eliminate the bacteria. Multiple antimicrobial peptides are induced during infection including the cathelicidin LL-37 (59) which potentially inhibits *Chlamydia* infection (60). A unique serine protease called chlamydial-proteasome/protease-like activity factor (CPAF) can block LL-37 anti-chlamydial activity and restore chlamydial infection (59). This suggests that CPAF, pre-stored in the host cell cytoplasm, would be able to rapidly come upon extracellular antimicrobial peptides when the host cell undergoes lysis (59), promoting the growth of *Chlamydia.* This indicates that *Chlamydia* has evolved an immune evasion strategy to overcome this important form of host immune response and potentially leading to persistent infection.

Nucleotide-binding oligomerization domain (NOD) proteins and NOD-like receptors (NLRs) are intracellular PRRs that recognize peptidoglycan (PGN) and other danger signals (61). Activation of NLRs, by molecules associated with danger signals, leads to the formation of inflammasomes (62). In turn, inflammasomes generate active Caspase-

1 which is required to produce the mature cytokine interleukin-1β (IL-1β) (61). Caspase-1 dependent IL-1β signaling and NLRP3 inflammasome activation are important for host defence against *C. pneumoniae* infection (61). Previous studies have shown that NOD1 is also important in the induction of inflammation during *Cm* and *C. trachomatis* infection*s* (63). NOD1 is involved in the induction of inflammatory cytokines like IL-6 and macrophage inflammatory protein 2 (MIP-2) (also known as CXCL2) in mouse epithelial cells upon *Chlamydia* infection (63). Autophagy, a self-degradative and house-keeping mechanism in the cell, targets cellular components and then fuses with the lysosome to degrade its contents (64). During *Chlamydia* infection, the chlamydial vacuole does not fuse with the lysosome and in turn can block autophagy completion but the mechanism of this process is unclear (64).

1.2.1.1.1 Cytokine responses

Following *in vitro C. trachomatis* infection of cervical and colonic epithelial cells, many proinflammatory cytokines and chemokines were released including CXC-chemokine ligand 1 (CXCL1), CXCL10, CC-chemokine ligand 5 (CCL5), IL-8, granulocyte/monocyte colony-stimulating factor (GM-CSF), IL-6, and IL-1α (54). Cytokines, like IFN-α and IFN-β, are further secreted from *Cm*-infected epithelial cells that lead to production of interferon-γ (IFN-γ) (65, 66). Some of these cytokines are involved in chemoattraction and activation of immune cells like neutrophils, monocytes and T cells. Other cytokines induce adhesion molecules on endothelial cells or induce acute phase proteins from epithelial cells and macrophages (54). Overall, the production of proinflammatory cytokines by epithelial cells during *Chlamydia* infection is likely to recruit inflammatory cells to the site of infection and elicit a protective immune response.

Additionally, the cross-talk between epithelial cells and the leukocytes is important for inducing a controlled immune response during infection (54). Hence, the cytokine environment is able to shape the adaptive immune response.

1.2.1.1.2 Cell death responses

Cell death processes are tightly regulated during inflammation and infection with pathogens but often times the processes can be dysregulated in ways which may be detrimental to the host (67). Cell death can be complicated in *Chlamydia* infections because apoptosis, necrosis, or pyroptosis can be induced or inhibited (68, 69). Oncosis and necroptosis are other forms of cell death (70, 71) but have not been associated with *Chlamydia* infection. When cells undergo apoptosis, phosphatidylserine receptors on phagocytic cells interact with the apoptotic bodies and reduce the inflammatory response via release of transforming growth factor β (TGF-β) and IL-10 (72). If cells die by necrosis, molecules that are normally in the nucleus, organelles, or the cytosol may get released into the extracellular environment (73). In turn, this may trigger danger signal receptors located on macrophages and dendritic cells leading to inflammatory responses (68). The pathogen can also be released at the same time from the necrotic cells which could interact with TLRs or stimulate danger signal receptors to induce inflammatory responses if they are coated with host-cell debris (68). The type of cell that is being infected with *Chlamydia* may also dictate the balance between apoptosis and necrosis. For example, primary fibroblasts are more sensitive to apoptosis than the HeLa epithelial cell line (74). Pyroptotic cell death is mediated by caspase-1, which is a protease that activates IL-1β and IL-18 (70). Pyroptosis eventually leads to cell lysis and the release of inflammatory contents (70). In one study,

the staining and secretion of *C. pneumoniae*-infected T cells by caspase 1 and IL-18 respectively suggest that the pyroptosis pathway was activated (69).

Overall, cells infected with *Chlamydia* can undergo pyroptosis, apoptosis and/or necrosis in an attempt to control the infection but in turn can also lead to detrimental outcomes for the host when there is potentially spread of the bacteria or excess inflammation.

1.2.1.2 Innate immune cells

1.2.1.2.1 Neutrophils

Neutrophils are a major cellular component of acute inflammation and bind to pathogens through TLRs, lectins and lectin receptors, scavenger receptors, C-reactive protein, and complement and their receptors (55, 75). Classically, neutrophils have been classified as phagocytes because of their ability to engulf and eliminate bacteria (76). Tumor-associated neutrophils can have antitumorigenic or protumorigenic functions, also known as N1 and N2 phenotypes, respectively (77). The specific role of N1 or N2 neutrophils during *Chlamydia* infection are unknown. Neutrophils generate extracellular fibers, also known as neutrophil extracellular traps, which are composed of granule and nuclear components that kill bacteria extracellularly (78). However, the role of neutrophil extracellular traps in intracellular *Chlamydia* infection has not been shown. Additionally, neutrophils are producers of cytokines in mice and humans some of which are TNF, IL-1α, IL-1β, IL-6, G-CSF, and also M-CSF and IL-10 which is produced in mice only (79). Cytokine expression and production from neutrophils are either constitutive or activated by microenvironmental stimuli (80). Neutrophils also produce chemokines including CXCL1 and CXCL2 in mice and humans and CCL5 in mice that attract other immune cells to the

affected areas (79). Neutrophils have been shown play an important role in recruiting, activating, and programming antigen presenting cells (APC) (75). Monocytes, dendritic cells, and lymphocytes are recruited and activated by neutrophils through cell to cell contact and secreted products (75). Importantly, activated neutrophils undergo respiratory burst leading to production of anti-microbial reactive oxygen intermediates (75). In addition, neutrophils respond to different stimuli which allow them to progressively release distinct sets of granules. This leads to activation of a killing cascade at the plasma membrane and the release of nuclear proteins and cytosolic contents (75). Peroxidase-negative granules are released initially followed gradually by peroxidase-positive granules which contain α-defensins and myeloperoxidase (75). Neutrophils have been shown to be important players in the early stages (76) of different types of *Chlamydia* infection including genital tract (2), respiratory (81, 82), and eye infection (76). Mice infected with respiratory *Cm* results in pronounced neutrophil recruitment to the lung which correlates with the height of infection (83). Another study showed that neutrophils played a pathological role in ocular pathology during *Chlamydia caviae* infection in guinea pigs (76). Overall, the role of neutrophils during *Chlamydia* infection may be complex in that they may help to shape the adaptive immune response while promoting detrimental effects in the host as well.

1.2.1.2.2 Dendritic cells

Dendritic cells (DCs) are immune cells that sense microbial antigens in the tissues and play an important role in bridging the innate and adaptive immune responses (84). These cells transition from an immature state to a mature stage while upregulating major histocompatibility complex-class II (MHC-II) and costimulatory molecules (85). DCs eventually migrate to the local draining lymph nodes to present antigens to T cells and

secrete cytokines like IL-12 and IL-10 (86). DCs that produce IL-12 are more efficient at inducing type 1 T cell responses (87). DCs are subdivided into three main subtypes which consists of two main lineages of conventional DCs (cDCs) plus plasmacytoid DCs (pDCs) (86). The two lineages of cDCs are cDC1 which includes cluster of differentiation 8α (CD8α+) and CD103+ DCs, and cDC2 which includes CD11b+ and CD172a+ DCs (86). In *C. pneumoniae* infection, it was found that pDCs are activated in the lung and elicit protective CD4+ T regulatory cells (Tregs)/IL-10 responses that regulate T cell responses for optimal immunity (88). Studies have also shown that natural killer (NK) cells and DCs play an important role in mucosal immunity to various lung infections (89, 90), including *Chlamydia* infection where NK cells modulate lung dendritic cell-mediated T helper (Th) 1 and Th17 immune responses (84).

1.2.1.2.3 Innate lymphoid cells

Innate lymphoid cells (ILCs) populate the mucosal epithelium and are a family of cells that are important in innate mucosal immunity to bacteria, viruses, fungi and intracellular and extracellular parasites (91). These cells are found in a variety of organs such as the gut, lung, and mucosal membranes, and are recruited to the barrier tissues which occurs during embryonic development (91). Epithelial cells and myeloid cell lineages have to cooperate and sense infection or tissue damage in turn to produce cytokines and alarmins that recruit specific ILCs (92). ILCs share phenotypic, morphological, developmental, and functional features with CD4+ T helper cells but do not express the lymphoid lineage markers expressed on Th cells (93). There are three main innate lymphoid cell types as shown in Figure 1.2. All mouse ILCs express IL-2R (CD25), IL-7Rα (CD127) (some subsets of NK cells), CD90 (alloantigen Thy-1) (some subsets of NK cells), and the

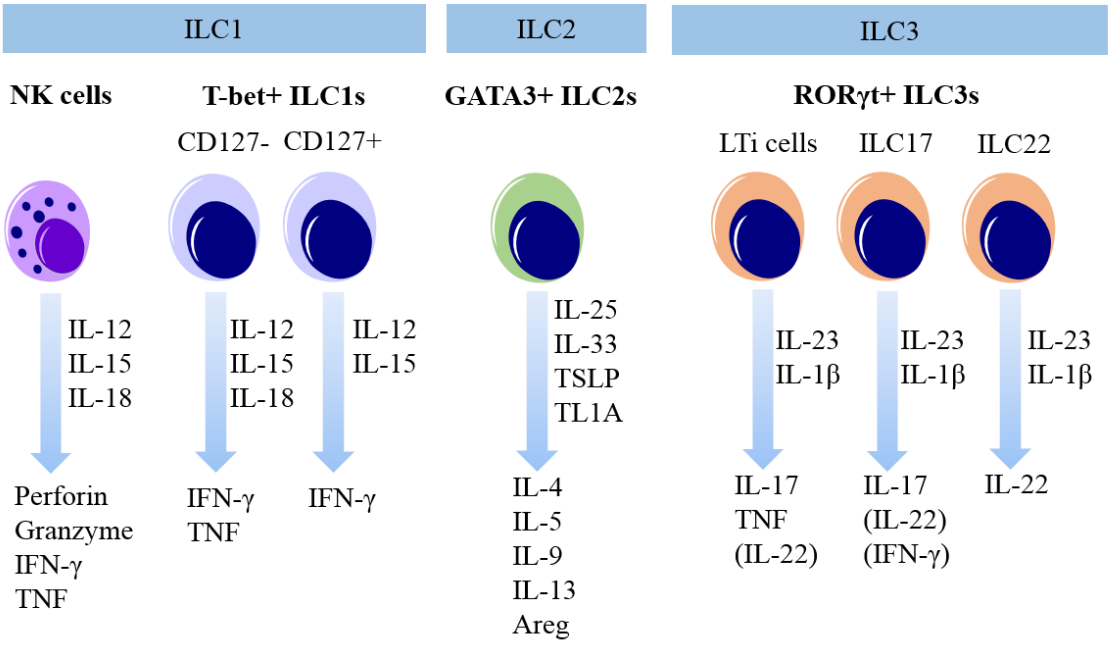

Figure 1.2 Overview of the innate lymphoid cell family. The group 1, group 2, and group 3 innate lymphoid cells (ILC) are categorized into subsets of cells based on their cell surface marker expression, transcription factor expression, and different patterns of effector cytokines produced by the cells. Group 1 ILCs are defined by their ability to produce IFN-γ, group 2 ILCs are defined by their ability to produce type 2-associated cytokines, and group 3 ILCs are able to produce IL-17A and IL-22. A subset of ILC3s, ILC17s, may produce IL-17A alone or they may co-express IL-22. In addition there is a subset of ILC17s that may co-express IL-17A and IL-22. Areg, amphiregulin; IFN-γ, interferon-γ; IL, interleukin; LTi, lymphoid tissue inducer; NK, natural killer; TNF, tumor necrosis factor; TL1A, TNF-like ligand 1A; TSLP, thymic stromal lymphoietin (91–93).

common γ chain (CD132) (92). ILCs are positioned to be activated rapidly by host-derived cytokines and growth factors. Epithelial cells and myeloid cell lineages act together to sense infections and tissue damage produce cytokines and alarmins that mobilize and activate ILCs (92). Specifically, IL-12, IL-15, and IL-18 activate NK cells and ILC1s and IL-4, IL-2, IL-25, IL-33, thymic stromal lymphopoietin (TSLP), IL-9 and TNF-like protein 1A (TL1A) activate ILC2s (91). IL-1β and IL-23 are required for stimulation of ILC3 cells (91).

NK cells are considered part of the ILC1 group of cells but conventional NK cells and non-NK ILC1s are separate lineages according to recent analysis of the developmental pathways of ILCs (91). NK cells play an important role in innate immunity due to their rapid activity and their role in connecting the innate and adaptive immune response (94). NK cells form synapses at infected cells and other immune cells like macrophages and dendritic cells (94). The NK cell integrates the balance of activing and inhibitory signals on these cells and determines whether to kill the associated cell or not (94). Activating receptors include the natural cytotoxicity receptors (NCRs) and inhibitory receptors include some of the killer immunoglobulin-like receptors (KIRs) (KIR2DL and KIR3DL) (94). Once NK cells are activated, they can direct their cytolytic granule contents towards the synapse to directly kill the cell (94). In addition to having the ability to act as direct killing cells of the innate immune system, NK cells also have a role in bridging the innate and adaptive responses (84). In *Chlamydia* genital tract infection, NK cells are important for the early IFN-γ production, and play a role in the development of the Th1 response to control the infection (95). Also, there is *in vivo* evidence that NK cells stimulate Th1/Th17 responses by modulating the lung DC function during respiratory *Chlamydia* infection (84). Non-NK ILC1s produce IFN-γ which is the signature T-helper 1 (Th1) cytokine (96).

ILC1s are distinguishable from NK cells as they express CD127 and depend on the transcription factor T-bet, whereas NK cells depend on the transcription factor Eomes (97). ILC2s are dependent on GATA3 for their development and function and RORα for their development (91) and secrete the Th2 cytokines IL-5, IL-9, IL-13 (93). ILC2s are important in helminth infections and asthma (98) which are in line with the role of Th2 responses.

ILC3s express the hormone nuclear receptor retinoid-related orphan receptor (RORγt) which is required for their development and function (92). ILC3s are subdivided into 3 subsets that are NKp46- and CCR6+ including lymphoid tissue inducer (LTi) cells which produce IL-17A and IL-22 under some conditions, IL-22-producing ILCs (ILC22) which produce only IL-22, and IL-17A producing or IL-17A/IL-22 producing ILCs (ILC17) (93). There are other ILC3 subsets can be characterized based on their expression of NKp46 and CCR6 (91). LTi cells are able to promote the formation of secondary lymphoid nodes in addition to Peyer's patches during embryonic development (93). While most studies on ILC3s focus on their role in the intestine in the context of bacterial infection, one study showed enhanced production of IL-17A and IL-22 production by lung ILC3 upon *Streptococcus pneumoniae* infection (99). In this study, most of the lung ILC3s coexpressed RORγt and CCR6 which are hallmarks of spleen, tonsil, and gut ILC3 (100, 101). These cells are implicated as an important source of IL-22 in the lungs during infection with *S. pneumoniae* or the fungus *Candida albicans* (91). IL-22 targets local non-hematopoietic cells to promote inflammation and tissue repair, and to stimulate an antimicrobial response (102). In addition, mice that received bacillus Calmette-Guérin (BCG) vaccination had an innate source of IL-17A and IFN-γ from ILC3s which provided protection against challenge with *Mycobacterium tuberculosis* (103). Overall, ILC3s may not be limited to bacterial infection in the intestine and are important in host defense against

respiratory microbial infections. However, ILCs have not been described in *Chlamydia* infection.

1.2.1.3 The complement system

The complement system is a network of proteins which are tightly regulated and have an important role in host immunity and inflammation (104). Activation of complement occurs through the alternate, classical, or lectin pathways which involve proteins that are mainly inactive zymogens and then cleaved and activated along the pathways (104). All three pathways lead to the cleavage of the anaphylatoxins C3a and C5a (104). C5a activates tissue-infiltrating neutrophils while C3a limits neutrophil mobilization from bone marrow (105). Also, C5a is a potent activator of granulocytes and monocytes/macrophages whereas these cells are weakly affected by C3a (106). The membrane attack complex, which is downstream of C5, lyses extracellular pathogens (104). There is evidence that the complement system orchestrates adaptive immune responses and has a role in controlling intracellular pathogens (107, 108). In a previous study, it was reported that mice deficient in C5 did not develop any hydrosalpinx upon genital *Cm* infection which is a hallmark of tubal infertility as seen in WT mice (109). It was also confirmed that the role of C5 in promoting hydrosalpinx was not due to ascending infection of the genital tract by *Cm* (109). Another study showed that C3a receptor-deficient mice had prolonged pneumonia with greater overall clinical disease compared to WT mice upon lung infection with *C. psittaci* (107). *C. psittaci* infection of C3a receptor-deficient mice caused reduced numbers of B cells, CD4+ T cells, and antigen-specific IFN-γ-producing T cells (107). Taken together, these studies indicate that some of the components from the complement system are important in the immune response against *Chlamydia* infection.

1.2.2 Adaptive immune responses

1.2.2.1 Humoral responses

The first evidence showing that antibody production from B cells might play a role in *Chlamydia* infection was in women with chlamydial cervical infection (110). It was observed that the bacterial load of *C. trachomatis* was inversely correlated with the amount of immunoglobulin (IgA) A antibody from the patients (110). The results from this study suggests that greater humoral responses may be directly linked to reduced bacterial shedding during infection (110). However, high titres of *Chlamydia*-specific antibody in another study did not correlate with resolution of the infection in humans, and in turn may be correlated with heightened sequelae of infection (111). Moreover, mice that lacked B cells did not have an altered course of primary *Chlamydia* genital tract infection (112). It has been suggested that B cells may play a bigger role in resistance to re-infection with *C. trachomatis* (113). Neutralization of CD4+ or CD8+ T cells and subsequent genital re-infection with *C. trachomatis* in mice had a limited effect on resistance (113). However, secondary *C. trachomatis* infection in B-cell deficient mice could not be resolved when CD4+ T cells, but not CD8+ T cells, were depleted (113). This model suggests a synergistic effect of B cells and CD4+ T cells in the host response against *C. trachomatis* secondary infection *in vivo*. Overall, B cells may not have a decisive role in resolving primary *Chlamydia* infections but they may be more important in controlling secondary infections. Underlying mechanisms include antibody-mediated neutralization and opsonization, antigen presentation to T cells, and Fc-receptor-mediated uptake of antigen-antibody complexes (113–115).

1.2.2.2 Cell-mediated responses

There has been extensive research on the protective and detrimental T cell responses that can occur during different types of infection. Naïve T cells differentiate into different potential lineages of effector or memory cells after recognizing antigen presented by APCs (116). CD4+ T cells are a major T cell subset that is responsible for the function of the adaptive immune response (116). DCs are responsible for bridging the innate and adaptive arms of immunity and induce various CD4+ T cells responses against infectious agents (116). In addition to the classic type 1 and type 2 paradigm, multiple other CD4+ T cell types have been reported such as, follicular helper T cells, Tregs (natural or induced), type 3 and type 1 T regulatory cells (117), type 17 cells, type 9 cells, and type 22 cells (118–120).

1.2.2.2.1 Type 1 responses

T-helper 1 (Th1) cells are one lineage of cells that naïve CD4+ T cells can differentiate into and they are characterized by their production of IFN-γ. The differentiation of these cells depends on IL-12, the master transcription factor T-bet, and the signaling transducer and activator of transcription 4 (STAT4) (116) after antigen encounter presented by DCs and specific cytokine environments that regulate the expression of transcription factors. Through mainly IFN-γ production, Th1 cells, and in certain cases tumor necrosis factor (TNF), are involved in controlling intracellular bacterial infections like *Francisella tularensis* (121), *C. pneumoniae* (122), and *M. tuberculosis* (123) and also viral infections (124).

Studies of *Chlamydia* infection using mouse models have proven that T cells, specifically the Th1 responses, are important in resolving the infection (1, 2, 125). There is

in vitro evidence showing that IFN-γ controls the growth of *C. trachomatis* through induction of the enzyme indoleamine-2,3-dioxygenase (IDO) production (126). IDO, is ubiquitously expressed outside the liver and the expression can be heightened by LPS, virus infection, or IFN-γ (127, 128). IDO induction degrades tryptophan which consequently deprives the bacteria of an essential amino acid (126). IFN-γ can also induce other immune mechanisms to suppress *Cm* growth such as induction of nitric oxide (NO) production (129) and further promotion of Th1 protective immune responses which would downregulate the non-protective Th2 responses (130).

CD8+ T cells are another major subset of cells in the type 1 response. These cells are part of the T cytotoxic 1 (Tc1) response because of their cytotoxic abilities but also produce IFN-γ (131). Cytotoxic mechanisms include granule exocytosis of perforin and granzymes or Fas/Fas ligand pathways and production of antimicrobial peptides (132). The importance of CD8+ T cells in *Chlamydia* infection has been controversial. MHC class I peptide presentation to CD8+ T cells is not essential to clear *Chlamydia* infection because mice deficient in β-microglobulin (113), perforin, or FAS (133) were still able to clear *Cm* infection. Although these deficiencies would affect NK cells as well, which were previously mentioned as important in modulating T cell subsets in *Chlamydia* infection (134), these results suggest that their cytotoxic mechanisms are not important for resolving the infection. There are several mouse studies showing that CD8+ production of IFN-γ protects mice against *Chlamydia* infection. For instance, *Chlamydia*-specific CD8+ T cells that were derived from WT mice but not IFN-γ-deficient mice and then transferred into naïve recipient mice protected against *C. pneumoniae* infection (135). Moreover, depletion of CD8+ T cells, but not CD4+ in mice, suppressed protection against *C. psittaci* infection in mice (136), and increased the severity of disease in primary and secondary infection with

C. pneumoniae (131). CD8+ T cells may also have immunopathological functions in the context of *Chlamydia* infection. In one example, patients that had an increased history of *C. trachomatis* infection and who also expressed the MHC class I allele HLA-B27 were associated with an increased risk of developing reactive arthritis (137) suggesting an immunopathological role of CD8+ T cells. In mice, the antigen-specific CD8+ T cells were reported to be specifically responsible for upper genital tract pathology after primary genital *C. muridarum* infection (138). Due to the controversial role of CD8+ T cells in *Chlamydia* infection, further work needs to be conducted to fully elucidate their role during infection.

1.2.2.2.2 Type 2 responses

For T-helper 2 (Th2) cell differentiation, IL-4 is required and is controlled by the master transcription factors GATA-binding protein 3 (GATA3) and STAT6 (116). Immune responses by Th2 cells are characterized by production of the cytokine IL-4 which can act as an autocrine mediator for Th2 differentiation (116). In *Chlamydia* infection, Th2 responses are linked to pathological responses in the host. In one study, *Cm*-specific Th2 cells were important for serum and vaginal antibody production, and accumulated in the genital tract during chronic infection (139). The mRNA expression levels for Th2 cytokines are markedly higher in women with infertility caused by *Chlamydia* (140), indicating that Th2 responses are detrimental to the host during *Chlamydia* infection.

1.2.2.2.3 Type 17 responses

Th17 cells are another T helper lineage that was discovered in a mouse model of experimental autoimmune encephalopathy which at that time was thought to be a Th1-

associated disease (141). The role of Th17 responses have been implicated in many infectious diseases, mainly involving extracellular bacteria and fungi (142). The pathogenic role of Th17 cells in autoimmune diseases have been implicated in multiple sclerosis, rheumatoid arthritis, and psoriasis (143). Th17 cells are CD4+ effector T cells that express the αβ T cell antigen receptor and have high expression of the transcription factors RORα and RORγt, low expression of T-bet and GATA-3, and high surface expression of CCR6 the chemokine receptor (144). These cells produce primarily the cytokines IL-17A, IL-17F, and IL-22, the IL-23 receptor, and the chemokine CCL20 (145). In mice, Th17 cells are differentiated from naïve CD4+ T cells in the presence of IL-6 and TGF-β via STAT3 activation (144). T-cell polarization in response to pathogen-associated molecular patterns (PAMPs) have been studied and shows a variety of fungal components (146) and bacterial stimuli (147) that induce the Th17 lineage. Th17 cells play an important role in extracellular bacterial and fungal infections by production of effector molecules that largely recruit neutrophils to the site of infection and the induction of antimicrobial peptides (144).

On the other hand, intracellular bacterial infections usually require Th1 responses for resolution of the infection (116), but emerging evidence suggests that IL-17A/Th17 are important in *Chlamydia* infection. *Cm* infection of the genital tract in IL-17A-/- mice elicited higher levels of *Chlamydia*-neutralizing antibody in the serum and had reduced infection and pathology than WT mice (148). However, vaccination in IL-17A-/- mice did not reduce the infection or pathology further, in contrast to WT mice (148). In another study, *Cm* infection caused Tregs to convert into Th17 cells and also promoted Th17 differentiation from CD4+ T cells resulting in heightened pathology in mice (149). In men that were PCR-positive for *C. trachomatis*, IL-17A levels were increased in seminal levels compared to control samples (150). There are numerous other reports highlighting the

controversial role of Th17 responses in the clearance of *Chlamydia* infections which warrants further investigation of this host immune response in *Chlamydia* and other intracellular bacteria.

1.3 IL-17 and IL-17 receptor family cytokines

1.3.1 Overview of IL-17 family cytokines and their receptors

The IL-17-family of cytokines consists of IL-17A, IL-17B, IL-17C, IL-17D, IL-17E (IL-25), and IL-17F (Figure 1.3) (151). The IL-17 cytokines generally function as homodimers while IL-17A and IL-17F can also form a heterodimer (152, 153). Immune responses are induced by the binding of these IL-17 family cytokines to heterodimers of specific IL-17 receptors. IL-17 receptors A through E have been identified (154). IL-17 receptor (IL-17R) A (IL-17RA) is shared by several different IL-17 cytokines, specifically IL-17A, IL-17C, IL-17 E, and IL-17F, and pairs with different receptor subunits (154). More specifically, IL-17A, IL-17F, and IL-17A/F transduce signals through the IL-17RA/RC complex, whereas IL-17C and IL-17E signal through IL-17RA/RE and IL-17RA/RB complexes respectively (154). IL-17B can associate with IL-17RB but it is not known whether it also signals in a complex with IL-17RA. The receptor for IL-17D is unknown (155) and IL-17RD is an orphan receptor (155).

IL-17A and IL-17F are the best characterized out of the IL-17 family of cytokines and have similar biological functions (154). Both IL-17A and IL-17F induce the production of antimicrobial peptides (defensins and S100 proteins) (156, 157), cytokines (IL-6, G-CSF, and GM-CSF) (158), chemokines (CXCL1, CXCL5, IL-8, CCL2, and CCL7) (159), and matrix metalloproteinases (MMP1, MMP3, and MMP13) (159, 160) from fibroblasts, endothelial cells, and epithelial cells. In addition, IL-17A induces intracellular cell adhesion

molecule 1 (ICAM-1) in keratinocytes (161), IL-1 and TNF in macrophages, inducible nitric synthase (iNOS) and cyclooxygenase-2 (COX-2) in chondrocytes (162), and COX-2-dependent-prostaglandin E2-mediated receptor activator of NF-κB ligand (RANKL) expression in osteoblasts (163). Mice that are deficient in both IL-17A and IL-17F, but not single deficient mice, are susceptible to systemic *Staphylococcus aureus* infection (164), suggesting that IL-17A and IL-17F have redundant functions in host defense. Expression of both IL-17A and IL-17F is required for β-defensin production for immunity against oral *Citrobacter rodentium* infection (164). However, IL-17F triggers markedly decreased strength of signaling compared to IL-17A which could lead to distinct biological effects (165). Together, IL-17A and IL-17F are important cytokines in maintaining the mucosal barrier integrity and inducing proinflammatory responses from tissue epithelial cells and fibroblasts (166).

Th17 cells are the main producers of IL-17A, but CD8+ T cells are also able to produce IL-17A upon TGF-β and IL-6 stimulation (89). As well, innate cells like γδ T cells, NK cells, natural killer T (NKT) cells, and some sub-populations of ILC3s can also produce IL-17A (168). Innate IL-17A-producing cells are important sentinels of the immune system and provide an early line of defence against pathogens at mucosal surfaces (168). Additionally, neutrophils (169), macrophages, and Paneth cells (170, 171) are potential IL-17A-producers. γδ T cells, which produce a high amount of IL-17A, varies between 0.2-20% of total T cells in the peripheral blood of humans (172). These cells are localized to mucosal tissues that come into contact with the external environment and often respond rapidly to pathogens. IL-17A-producing γδ T cells have been shown to be important in *Listeria monocytogenes* and *M. tuberculosis* infection (173, 174).

IL-17RA and IL-17RC are expressed ubiquitously among non-hematopoietic cells such as fibroblasts and epithelial cells and innate immune cells such as macrophages and neutrophils (154). Although both subunits are expressed ubiquitously, there are still some specific differences. IL-17RA is expressed highly in the hematopoietic tissues while IL-17RC is expressed highly in non-hematopoietic cells (175). This expression pattern may indicate that IL-17A may have differential impacts on epithelial, endothelial, fibroblast cells and immune subsets (154). Although the actual stoichiometry of the IL-17A-binding complex is not defined, it has been suggested that the IL-17A receptor may consist of two IL-17RA subunits and one IL-17RC subunit (154). Using fluorescence resonance energy transfer (FRET), it has been shown that IL-17RA may exist as a preformed homodimer on the cell surface that goes through a conformational change when IL-17A binds and forms a signaling complex with IL-17RC (176).

IL-17C mainly targets epithelial cells due to the preferential expression of IL-17RE on these cells (166). IL-17C acts in an autocrine manner and triggers similar pathways as IL-17A and IL-17F in the protection against bacterial infections (91). IL-17A and IL-17C have been suggested to be functionally similar because of the similarity in the genes that are upregulated by these cytokines (177).

In comparison, IL-17E mainly acts on leukocytes and after binding to the IL-17RA-IL-17RB complex, type 2 responses are induced (166). The IL-17RA/IL-17RB complex is expressed on innate and adaptive immune cells like CD4+ Th2 and Th9 cells, fibroblasts, basophils, invariant natural killer T (iNKT) cells, macrophages, and ILC2s (178). IL-17E induces eosinophilia and also induces the expression of IL-13 by DCs (145). However, IL-17E inhibits IL-23 production by macrophages to limit Th17 cell development (145). Overall, allergen and parasitic infections induce IL-17E production which promotes Th2

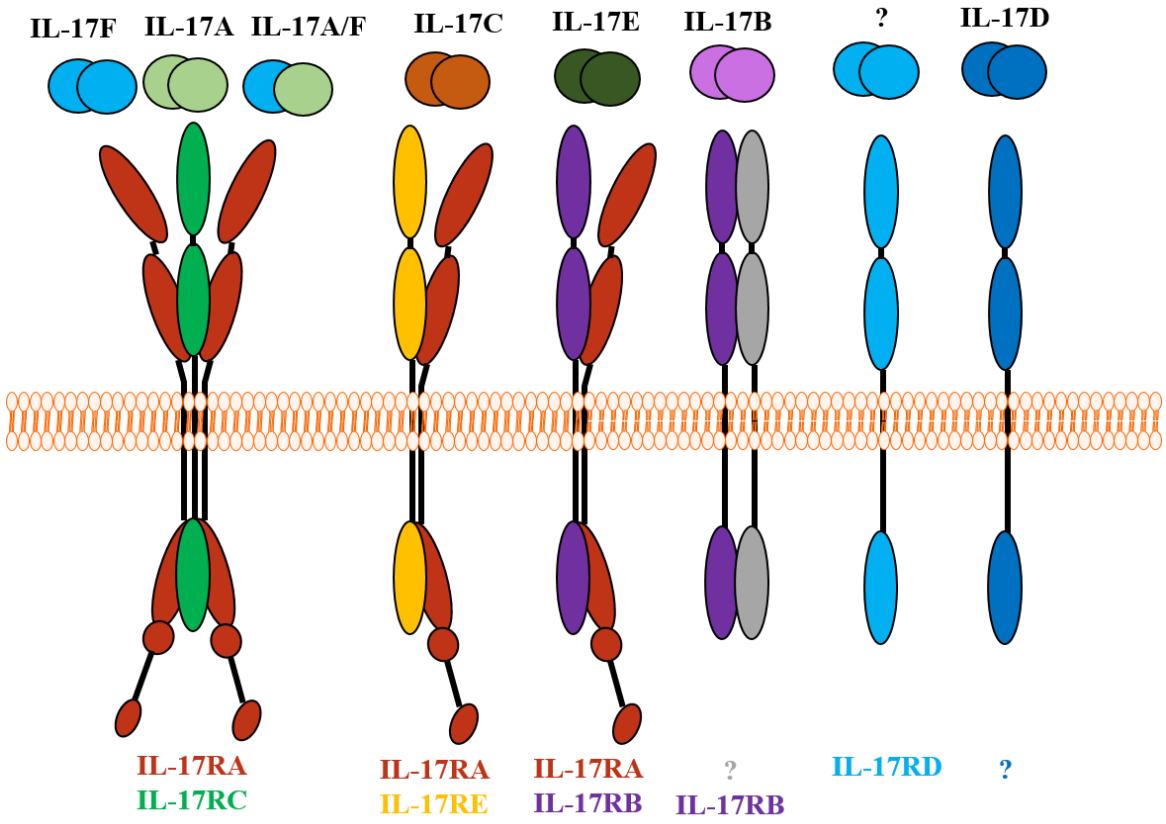

Figure 1.3 The IL-17 family cytokines and corresponding IL-17 receptors. There are six identified IL-17 cytokine family members to date, named IL-17A, B, C, D, E, and F. There are also five identified IL-17 receptor family members, IL-17RA to RE. IL-17A and IL-17F forms a homodimer or heterodimer with each other and binds to IL-17RA and IL-17RC together for signal transduction. IL-17C associates with the IL-17RA and IL-17RE heterodimer to activate signal transduction for host defense as well while IL-17E binds to the IL-17RA and IL-17RB heterodimer for signal transduction. As such, IL-17RA is shared by IL-17A, IL-17F, IL-17C, and IL-17E. The ligand for IL-17RD and the receptor for IL-17D has yet to be identified (154, 179).

differentiation and is also involved in the regulation of effector and memory Th2 cells (145). Therefore, compared to IL-17A, IL-17F, and IL-17C, IL-17E has a unique function of initiating and promoting Th2 responses (180) and also inhibits Th1 (181) and Th17 (182) responses.

1.3.2 IL-17 receptor A (IL-17RA) and IL-17 receptor C (IL-17RC) signaling pathways

Binding of IL-17A to the IL-17RA/IL-17RC complex activates multiple signaling pathways which include the NFκB, MAPK, and the CCAAT-enhancer-binding proteins (C/EBPs) pathways (Figure 1.4) (183). There is a conserved region on the C-terminal of the IL-17RA and IL-17RC subunit called the similar expression to FGF receptor/IL-17R (SEFIR) domain and the IL-17RA subunit has two additional domains called the TILL and distal domain (154). Upon binding of IL-17A, IL-17F, or IL-17A/IL-17F to the IL-17RA/IL-17RC receptor, NFκB activator 1 (Act1), which is a cytosolic adaptor molecule, is recruited to the SEFIR domain (179). Act1 recruits tumor necrosis factor receptor-associated factor 6 (TRAF6), which is an E3 ubiquitin ligase, to the receptor subunits since they do not have a TRAF6 binding site (154). Act1 polyubiquitinates TRAF6 and may possibly polyubiquitinate TGFβ-activated kinase 1 (TAK1) (184). The complex of TRAF6, TAK1, and Ubc13, which is part of a dimeric ubiquitin-conjugating enzyme complex, catalyzes the formation of K63-linked ubiquitination of nuclear factor kappa-B kinase subunit-gamma (IKK-γ) and leads to the activation of the transcription factor NFκB.

Another Act1-dependent pathway that is activated by IL-17A signaling is the MAPK p38 pathway which leads to the activation of AP-1 transcription factors (185). In addition, C/EBPβ and C/EBPδ transcription factors are activated by Act1-dependent and

Figure 1.4 IL-17RA/RC signaling pathways. IL-17RA and IL-17RC have the SEFIR domain and IL-17RA has two extra domains called the TILL and distal domain. Upon binding of IL-17A, IL-17F, or IL-17A-IL-17F to the IL-17RA/IL-17RC receptor, Act1 is recruited to the SEFIR domain of IL-17RA. Act1 exerts E3 ligase activity to mediate K63-linked ubiquitination of TRAF6, allowing its interaction with TAK1 where it may also be polyubiquitinated by TRAF6. TAK1, TRAF6 and Ubc13, part of a dimeric ubiquitin-conjugating enzyme complex, catalyzes the formation of K63-linked ubiquitination of IKK-γ which leads to the activation of NFκB. The Act1 signaling complex also activates MAPKs and activation of transcription factor AP1. Act1-dependent and Act1-independent pathways of IL-17RA/RC signaling contribute to the activation of transcription factors C/EBP-β and C/EBP-δ. The Act1-independent pathway involves PI3K and JAK1 but the activation of this pathway is unclear. Activation of IL-17RA/RC can also form another complex which consists of Act1-IKKε-TRAF2-TRAF5-ASF to mediate TRAF6-independent mRNA stability for chemokines and cytokines induced by these pathways. TRAF3 is a negative regulator of IL-17RA/RC signaling by interfering with the formation of the Act1-TRAF6 complex. Act1, NFκB activator 1; AP1, activator protein 1; ASF, alternative splicing factor; C/EBP, CCAAt/enhancer-binding protein; IKKε, inhibitor of nuclear factor kappa-B kinase subunit epsilon; IL-17RA, interleukin-17 receptor A; IL-17RC, interleukin-17 receptor C; JAK1, Janus kinase 1; K63, Lys 63; PI3K, phosphoinositide 3-kinase; SEFIR, SEF/IL-17R; TILL, TIR-like loop; TNFR-associated factor 6; TRAF, IKK, IκB kinase (179, 184, 186).

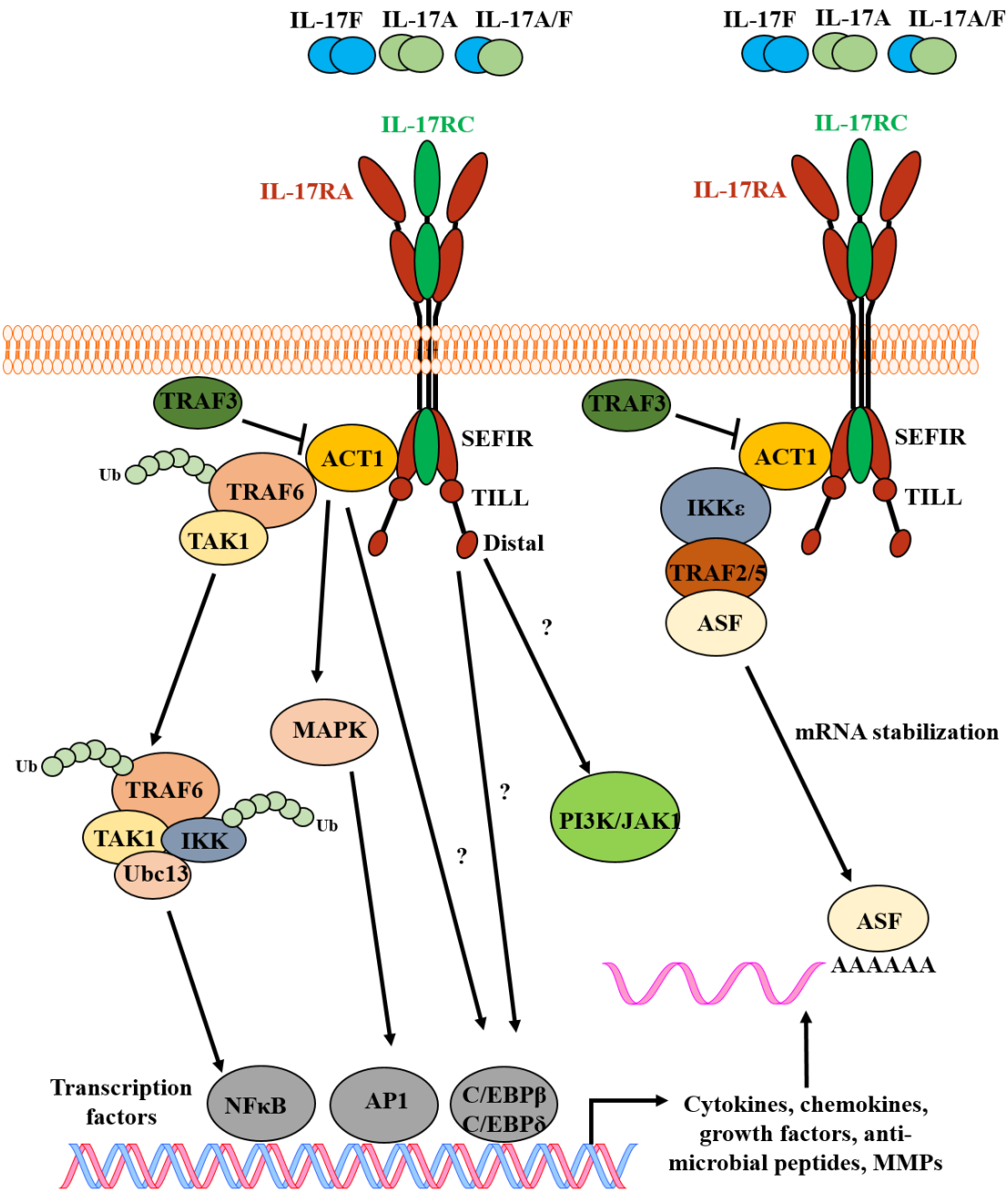
IL-17F
IL-17A
IL-17A/F
IL-17F
IL-17A
IL-17A/F
IL-17RC
IL-17RA
IL-17RC
IL-17RA
TRAF3
ACT1
SEFIR
TILL
Distal
Ub
TRAF6
TAK1
TRAF3
ACT1
SEFIR
TILL
IKKε
TRAF2/5
ASF
?
MAPK
mRNA stabilization
Ub
TRAF6
TAK1
IKK
Ubc13
Ub
?
?
PI3K/JAK1
ASF
AAAAAA
Transcription factors
NFκB
AP1
C/EBPβ
C/EBPδ
Cytokines, chemokines, growth factors, anti-microbial peptides, MMPs

independent pathways via IL-17A signaling (187). There is evidence showing that C/EBPδ or C/EBPδ is essential for the expression of IL-6 and that the C/EBP family members are important for the functional cooperation between IL-17 and TNF (187). In addition to these pathways, IL-17A also cooperates with TNF-α to activate the Janus-activated kinase-phosphoinositide 3-kinase (JAK-PI3K) and JAK-signal transducers and activators of transcription (JAK-STAT) pathways (183) although the complete pathway is still unclear. Activation of IL-17RA/IL-17RC can also form the complex of Act1-inhibitor of nuclear factor kappa-B kinase subunit epsilon (IKKε)-TRAF2-TRAF5-alternative splicing factor (ASF) to mediate TRAF6-independent mRNA stability for cytokines and chemokines induced by these pathways (184). Lastly, TRAF3 is a negative regulator of IL-17RA/RC signaling by interfering with the formation of the Act1-TRAF6 complex (184). Despite extensive research on the various pathways involved in IL-17A signaling, the full pathway is not fully understood and still require more specific experiments to reveal additional mechanisms involved.

1.3.3 Role of IL-17A/IL-17R in the host defence against pathogens

IL-17A and the IL-17A receptor have been implicated in many previous studies identifying their protective or pathogenic role mainly in response to extracellular bacterial or fungal infections (188). IL-17A has been shown to induce protective effects in the host defence against bacterial pathogens like *Klebsiella pneumoniae.* This was initially demonstrated by comparing the susceptibility of IL-17R-deficient with control mice upon intranasal *K. pneumoniae* infection although the authors did not indicate which IL-17A receptor subunit was affected (189). After infection, IL-17R-deficient mice had increased bacteria burden in the lungs, dissemination to other organs, and reduced overall survival

(189). These outcomes were directly associated with delayed neutrophil recruitment and reduced expression of G-CSF and CXCL2 in the lungs (189). More recently, it was shown that IL-23 was responsible for triggering IL-17A production during this infection (190). IL-17A and IL-23, play an important role in early recruitment of neutrophils to provide protective immunity to *K. pneumoniae* infection (190). In a different bacterial infection with *Porphyromonas gingivalis,* a pathogen of the oral mucosa, IL-17RA-deficient mice were also shown to be more susceptible (191). IL-17RAKO mice of both male and female gender displayed increased susceptibility to *P. gingivalis,* while only female IL-17RAKO mice showed more severe disease, largely due to defects in neutrophil recruitment (191). This study demonstrated a gender-dependent effect of IL-17A signaling in the protection against *P. gingivalis* infection through induction of neutrophil-recruiting chemokines (191). Taken together, IL-17A plays an important role in the protective responses to extracellular bacteria via early recruitment of neutrophils.

The protective roles for IL-17A and the IL-17A receptor in fungal infections have been well characterized in experimental infections with *Candida* and other fungal species (192). In one example, intravenous *C. albicans* infection induces IL-17A expression in mice (193). In this study, mice that were defective in the IL-17A receptor had increased fungal burden in tissues and decreased survival (193). This observation was associated with impaired recruitment of neutrophils (193). In addition to protective IL-17A and IL-17A signaling roles during fungal infections, detrimental responses have also been associated with IL-17A or Th17 responses (192). In one example, fungal burden is reduced during intragastric *C. albicans* or intranasal *Aspergillus fumigatus* infection in mice by blocking IL-23 via targeted deficiency or antibody neutralization (194). It was demonstrated that IL-17A can inhibit the fungicidal activity of neutrophils in a dose-dependent manner (194)

indicating that IL-23 and Th17 responses promote inflammation and impair the antifungal immunity. Also, human IL-17RC is essential for immunity against chronic mucocutaneous candidiasis caused by *C. albicans* (195). Taken together, these studies suggest that some degree of IL-17A and Th17 responses are required for protection against fungal infections but may also be detrimental to the host and promote inflammation in some conditions.

For intracellular bacteria, IL-17A has less of a defined role. For example, IL-17A-deficient mice and control mice both survived infections with *Salmonella enterica* (196). However, there was higher bacterial burden in the spleen and liver of IL-17A-deficient mice (196). Early neutrophil recruitment directly associates with IL-17A-mediated protection against this bacterium (196) but whether this is the sole mechanism of protection is unclear. In *M. tuberculosis* infection, IL-17RA-deficient mice were defective in exerting long-term control of the bacterial infection, exhibiting impaired neutrophil recruitment to the lung at early stages of infection (197). Pulmonary TNF, IL-6, and IL-10 were decreased while IL-1β was increased in IL-17RA-deficient mice during *M. tuberculosis* infection (197). In contrast, production of IFN-γ and iNOS were not effected in IL-17RA-deficient mice during this infection (197). Overall, IL-17A and the IL-17A receptor have been widely studied in a broad range of infectious diseases and are important players in both beneficial and detrimental host immune responses.

1.3.4 Current knowledge of the role of IL-17A/Th17 in *Chlamydia* infection

Within the past decade there has been extensive research looking at Th17 and IL-17A responses in the context of *Chlamydia* infections. Initially, there was evidence that IL-17A was produced early during the innate immunity phase following intranasal *Chlamydia* infection in mice (32). The induction of IL-17A, likely via MyD88-mediated signaling

pathways, correlated with the increase in live replication of the bacteria (32). This first line of evidence suggested that IL-17A in innate immunity plays a protective role in host defence against respiratory chlamydial infection. *In vitro* experiments in this study showed that IL-17A did not affect *Chlamydia* growth directly, but instead enhanced inflammatory cytokine and chemokine induction by *Chlamydia*-infected mouse L929 cells (32). In contrast, a more recent study showed that IL-17A synergizes with IFN-γ to enhance iNOS expression and NO production in murine epithelial cells and macrophages to directly inhibit growth (129). Therefore, the role of IL-17A in directly controlling *Chlamydia* replication is highly controversial.

IL-17A has also been shown to indirectly control *Chlamydia* replication *in vivo* by the induction of protective responses. A study revealed that neutralization of endogenous IL-17A in mice delayed clearance of respiratory chlamydial growth and showed more severe disease (198). The DCs from IL-17A-neutralized mice showed reduced CD40 and MHC class II expression and IL-12 production which led to a failure to induce protective Th1 responses (198). It remains to be determined whether IL-17A protects the host from *Chlamydia* infection directly through inhibiting bacterial replication or through promoting protective Th1 responses.

Aside from having a protective role in the host defence against *Chlamydia* infection, exacerbated IL-17A/Th17 responses are observed in mouse strains with increased susceptibility to *Chlamydia* infection (81, 82). *Chlamydia*-susceptible C3H/HeN mice displayed a significantly higher IL-17A/IL-17R-associated response than the *Chlamydia*-resistant C57BL/6 mice did and this was evident from the increases in airway neutrophils, Th17-associated cytokines, IL-17A mRNA expression, and a higher IL-17A recall response from antigen-restimulated splenocytes from the mice (82). Similarly, the immune responses

to intranasal *Chlamydia* infection in BALB/c mice (a different susceptible strain to *Chlamydia*) (81) indicated that BALB/c mice display significantly higher levels of IL-17A production and lower IFN-γ production than the C57BL/6 mice during *Cm* infection of the lungs (81). These data collectively showed that there is a complex relationship between susceptibility to *Chlamydia* infection and IL-17A/Th17 responses in terms of when, where, and how much IL-17A/IL-17R-mediated signaling are induced. Considering the importance of Th1 response in *Chlamydia* infection and the role of IL-17A in inducing Th1 response during infection (198), the ratio of Th1 to Th17 responses might be important instead of absolute levels of the individual responses. Also, exacerbated Th1 or Th17 responses may lead to dysregulation of additional immune responses that may not be beneficial for the host if they are not induced in the correct timing (early or late) during *Chlamydia* infection.

Interestingly, a *C. pneumoniae*-specific inclusion membrane protein called CP0236 has been shown to sequester Act1 (199). CP0236 caused alteration of the distribution of Act1 in the cytoplasm of HeLa cells infected with *C. pneumoniae,* and led to the association with the chlamydial inclusion membrane (199). Therefore, Act1 could not be recruited to IL-17RA in *Chlamydia*-infected cells *in vitro* (199). Since innate IL-17A signaling is suggested to be important in controlling early infection, this method of NFκB pathway inhibition by *C. pneumoniae* may delay adaptive immune responses induced by IL-17A and in turn allow the bacteria to replicate more sufficiently in the epithelial cells. In a more recent study from the same group, *C. pneumoniae* was shown to degrade TRAF3, a signaling molecule important for type I IFN production and IL-17A signaling (200). Therefore, *C. pneumoniae* prevents downstream TRAF3 signaling during infection to impair the innate immune response in infected cells. With this knowledge, it is therefore

important to not only characterize the innate and adaptive type 1 and type 17 responses during *Chlamydia* infection but we are in need of re-defining the role of IL-17A and IL-17A signaling in the direct control of *Chlamydia* infection.

1.4 Rationale, objective, and hypothesis of the study

1.4.1 Rationale

As previously mentioned, IL-17A signaling requires the IL-17RA subunit and the IL-17RC subunit for signal transduction to occur. However, IL-17RA is shared by IL-17C and IL-17E, and is also required for their signaling as it pairs with IL-17RE and IL-17RB respectively. A respiratory *Cm* infection model was established in bone marrow chimeric WT, IL-17RAKO, and IL-17RCKO mice. Therefore, loss of IL-17RC would be a specific loss of IL-17A signaling whereas loss of IL-17RA would be a loss of IL-17A, IL-17C, and IL-17E signaling. This way, the model would allow us to examine the role of IL-17RA/IL-17RC, IL-17A, and other potential IL-17 family members in the tissue stromal cells in controlling bacterial replication and host responses to *Chlamydia* infection. A respiratory, instead of genital, *Cm* infection model was established because of the acute infection that is caused the by the bacteria in the lungs. This provided a useful model to study the immune response without the complications of hormones and other unique immune structures in the genital tract. Additionally, body weight loss caused by acute respiratory *Cm* infection is a useful determinant of clinical disease in mice.

My thesis focused on the suboptimum initial host defence against *Chlamydia* infection via IL-17RA or IL-17RC deficiency in tissue stromal cells and investigating how this affects the adaptive immune response leading to subsequent immunopathology. IL-17RA or IL-17RC deficiency in tissue stromal cells leave the IL-17RA and IL-17RC

function intact in hematopoietic cells and therefore, leaving a fully functional adaptive immune response that is driven by initial immune responses from the tissue stromal cells in this model.

1.4.2 Objective

The objective of this study was to determine the role of IL-17RA and IL-17RC in non-hematopoietic tissue stromal cells in controlling *Chlamydia* replication and induction of subsequent immune responses *in vitro* and *in vivo*.

1.4.3 Hypothesis

Based on the current literature, I hypothesized that IL-17A/IL-17R has a multi-faceted role in critically controlling host responses to *Chlamydia* infection.

CHAPTER 2 MATERIALS AND METHODS

2.1 *Chlamydia* and cell lines

2.1.1 Propagation, purification and quantification of *Chlamydia*

2.1.1.1 McCoy cell culture

McCoy cells were obtained from American Type Culture Collection (Manassas, VA, USA) and used to propagate *Cm* for the experiments. McCoy cells are mouse originated fibroblast cells that are susceptible to *Chlamydia* strains (201). The cells were grown in a T175 flask in McCoy medium (minimum essential medium (MEM); Earle's salts, L-glutamine, non-essential amino acids (Invitrogen, Oakville, Ontario), 2.2 g sodium bicarbonate, 5% fetal bovine serum (FBS) (Sigma Aldrich, Oakville, Ontario), gentamicin (10 μg/ml) (Invitrogen), fungizone (2 μg/ml) (Invitrogen).

2.1.1.2 Purification of *Chlamydia muridarum (Cm)*

Cm was obtained from Xi Yang (University of Manitoba, Winnipeg, Manitoba) and expanded in McCoy cells following procedures by Li *et al.* (112). McCoy cell monolayers were grown in 10-20 150 mm tissue culture dishes until confluent. McCoy medium was removed from the culture dishes and the cells were infected with crude *Cm* supernatant (2-3 ml, left undisturbed for 10 minutes) and a total of 20 ml of growth medium (MEM (Invitrogen), 5% FBS (Sigma Aldrich), 10.06% Glucose (BioShop, Burlington, Ontario), 7.5% sodium bicarbonate (Bioshop), 10 mM HEPES (Wisent Bio Products, Saint-Jean-Baptiste, Québec), 200 mM L-Glutamine (Wisent Bio Products), 1X vitamins; choline chloride, D-calcium panthothenate, folic acid, nicotinamide, pyridoxal hydrochloride, riboflavin, thiamine hydrochloride, i-Inositol (Invitrogen), 50 mg/ml gentamicin

(Invitrogen), 10 µg/ml cyclohexamide (Sigma Aldrich)) was added back to the culture dishes. The infected cells were incubated at 37°C with 5% CO_2 for approximately 40 hours.

The culture supernatants were centrifuged (335 g, 10 min at 4°C) to remove tissue debris. Then, the supernatant was collected in chilled centrifuge tubes and centrifuged (22,500 g, 1 hour at 4°C) to pellet the bacteria. The pellet was washed with 10 ml sucrose-phosphate-glutamic buffer (SPG) (220 mM sucrose, 4 mM potassium phosphate monobasic, 7 mM potassium phosphate dibasic, 5 mM monosodium glutamate (L-glutamic acid monosodium salt hydrate, pH 7.3)) and tubes were combined to make a larger volume for fewer tubes. The suspensions were centrifuged again (22,500 g, 1 hour at 4°C). The pellet was resuspended in SPG buffer, aliquoted in small volumes, and stored in -80°C. The bacteria prepared from culture supernatant were designated as sup-derived *Cm* and the same batch was consistently used for conducting *in vivo* experiments.

The remaining cell monolayers were detached in 5 ml of SPG buffer per culture dish using a sterile cell scraper. The suspension was sonicated on ice and debris were removed by centrifugation (335 g, 10 min, 4°C). The supernatant was centrifuged (22,500 g, 1 hour at 4°C). The EB in the pellet were purified by a discontinuous density gradient with 30% Isovue-370 (Bracco Diagnostics, Princeton, NJ, USA) in 30 mM Tris-HCl and 50% sucrose (Sigma Aldrich) in 30 mM Tris-HCl. After centrifugation, the pellet was resuspended in 10 ml SPG buffer and loaded onto the two-layer cushion as described above and centrifuged (22,500 g, 1 hour at 4°C, slow acceleration, deceleration off). The pellet was washed once with SPG buffer, centrifuged (22,500 g, 1 hour at 4°C) and then the pellet was resuspended in SPG buffer. The samples were designated as monolayer-derived *Cm* and consistently used for *in vitro* experiments and were aliquoted in small volumes and

stored in -80°C. The titer of purified EBs was determined by using quantitative PCR (qPCR) and the inclusion forming unit (IFU) assay as described below.

2.1.1.3 Bacterial quantification by real-time quantitative PCR (qPCR)

To quantify the bacteria burden or the titer of purified EBs, total nucleic acid from the 100 µl sample was extracted using DNAzol (Invitrogen) following the manufacturer's protocol. The amount of bacteria in each sample was measured by qPCR with *Chlamydia*-specific the primers specific for the genomic sequence encoding *Cm* 16s rRNA (forward primer was 5'-CGCCTGAGGAGTACACTCGC-3' and the reverse primer was 5' -CCAACACCTCACGGCACGAG-3'). All primers were produced by Integrated DNA Technologies, Inc. (Montreal, Quebec, Canada). The sample and primers were mixed with 2X RT^2 SYBR Green FAST Mastermix (Qiagen, USA) (10 µl/reaction) and then processed using a 7900H fast real-time PCR machine (Applied Bioscience, Foster City, CA, USA). The bacterial copy number was calculated based on a standard that was generated using genomic DNA (gDNA) from a known titer of purified *Cm* and was expressed as log10 of copies of 16S rRNA per ml.

2.1.1.4 Inclusion forming unit (IFU) assay

McCoy cells were seeded into a 96-well flat-bottom plate in McCoy medium at a density of 70,000 cells per well and incubated at 37°C overnight. The culture medium was aspirated from the wells and *Cm* samples were added to the wells. The *Cm* stock was diluted 1:500 initially and then 1:2 serial dilutions were generated in duplicate from wells 1 to 11 in a 96-well plate. This was repeated for all *Cm* stocks that needed the titer to be established. The last well in each row was used as a negative control and no *Cm* was added. The culture

plate was incubated at 37°C for 1 hour and then centrifuged (1300 g, 1 hour at 36°C). Finally, the culture plate was incubated at 37°C for 40 hours.

After infection and incubation of the McCoy cells, the supernatant was aspirated and 200 µl of 100% methanol was added to each well to fix the cell monolayer. The plate was then incubated in a fume hood for 20 minutes. The methanol was then removed and the plate was incubated uncovered in the fume hood for 30 minutes and then stained or stored in 4°C for up to one week.

For cytological staining of *Cm,* Giménez working solution was prepared by mixing 2 ml Giménez stock solution (Sigma Aldrich) and 5 ml Giménez phosphate buffer (Sigma Aldrich). The working solution was filtered into a 100 mm Petri dish using a 10 ml syringe with a 0.2 µm filter. Using a multichannel pipette, 60 µl of Giménez working solution was added to each well and incubated at room temperature for 20 seconds (Giménez stains the inclusion bodies purple) (202). The stain was discarded and the plate was rinsed with tap water. Then, 60 µl of 0.8% Malachite Green solution was added to each well and incubated for 1.5 minutes (Malachite Green will stain the cells green). The stain was discarded and rinsed with tap water and another 60 µl of 0.8% Malachite Green was added to each well for 30 seconds. After discarding the stain and rinsing again with tap water, the wells were checked under the microscope to identify green cells containing purple inclusion bodies. If required, the Malachite Green staining was repeated. Dilutions with countable inclusion bodies to count were selected and the inclusion bodies were counted for the whole well with a cell counter. The average of duplicate wells were taken and this was multiplied by the respective dilution factor to achieve the correct *Cm* titer.

2.2 Mice

Congenic C57BL/6 CD45.1 mice were purchased from the Jackson Laboratories (Bar Harbor, ME, USA) and were bred in house. Breeding pairs of IL-17RAKO (CD45.2) and IL-17RCKO mice (CD45.2) were supplied by Amgen (Thousand Oaks, California) and Genentech (San Francisco, California) respectively. Forkhead box P3 (Foxp3)-IRES-eGFP knock-in (Foxp3-GFP) mice were provided by Dr. Mohamed Oukka (Harvard Medical School, MA, USA) and bred in house. The Foxp3-GFP mice were used as WT C57BL/6 (CD45.2) and will be referred to as WT mice. Mice were typically used between 4 to 6 weeks of age for bone marrow chimeric experiments and between 6 to 10 weeks for all other experiments.

To genotype the IL-17RAKO mice, ear punches were taken and the gDNA was extracted and processed for genotyping by polymerase chain reaction (PCR) using the REDExtract-N-Amp™ Tissue PCR Kit (Sigma Aldrich). Extraction Solution (100 µl) was mixed with 25 µl of Tissue Preparation Solution for each sample. The ear of each mouse was notched using sterile utensils and the tissue was placed in the solution and mixed. The sample was incubated at room temperature for 10 minutes and then at 95°C for 20 minutes. Neutralization Solution B (100 µl) was added to each sample and mixed by vortexing. PCR was run with the REDExtract-N-Amp PCR Reaction Mix following the manufacturer's instructions. The cycling parameters were as follows: initial denaturation at 95°C for 5 minutes, 40 cycles of denaturation-annealing-extension at 95°C for 40 seconds, 61.2°C for 30 seconds, 72°C for 1 minute respectively, and final extension at 72°C for 10 minutes. Primers for IL-17RA were synthesized by Integrated DNA Technologies, Inc. (Montreal, Quebec). The following primers were used for IL-17RA: forward primer 5'-AGG CCA TAC ACC CAC AGG GGA-3', reverse primer 5'TTG CAT GTT GAG TGG ACC CTG

CA-3'. The primers target the exon 3 and 4 of the RA gene and display a band at 698 base pairs (bp).

Mice were housed at the Isaak Walton Killam Health Centre animal facility under pathogen-free conditions. All animal procedures were approved by the Ethics Committee according to the Canadian Council for Animal Care guidelines.

2.3 *In vitro* studies

2.3.1 Mouse embryonic fibroblast (MEF) cell isolation

T175 flasks were coated with 0.2% bovine gelatin (Sigma Aldrich) in sterile distilled water prior to the procedure for two hours. Pregnant mice were euthanized 2 weeks post coitum and uterine horns containing the embryos were removed entirely, rinsed briefly in 70% ethanol briefly, and then submerged in 5% BS Roswell Park Memorial Institute 1640 Medium (RPMI 1640 medium). All of the following procedures were performed using sterile equipment and techniques. Individual embryos were removed from the yolk sac in a Petri dish and the head and red organs were removed and discarded. The rest of the embryo was set aside or placed in 5% BS RPMI medium until all embryos were processed. The embryos were mechanically disrupted with sterile glass slides until the pieces were able to be pipetted. A mixture of 0.05% trypsin/EDTA (Wisent Bio Products), 10 µg/ml DNase I (Sigma Aldrich), and 300 µg/ml collagenase II (Sigma Aldrich) (1 ml/embryo) was added to the suspension and then pipetted into a tube. The sample was incubated at 37°C for 20 minutes with gentle vortexing every 5 minutes. The reaction was stopped with at least one volume of complete Dulbecco's modified Eagle medium (DMEM) (10% FBS, 2mM L-glutamine, 1% 100 U/ml penicillin and 100 µg/ml streptomycin (P/S), 10mM HEPES) and then centrifuged (525 g, 10 min at 4°C). The supernatant was carefully

aspirated with a pipette and the pellet was suspended in complete DMEM. The suspension was plated onto the gelatin coated flasks (3-4 embryos per flask) and then incubated at 37°C until confluent. Cells were then detached, filtered, and passaged for experiments.

2.3.2 Assessing the impact of IFN-γ, IL-17A, IL-17C and IL-17E in controlling *Cm* infection in primary MEFs and McCoy cell line

MEF cells were plated in triplicate for each stimulation condition in a 48-well plate at a density of 100,000 cells per well. The cells were allowed to settle and attach to the plate overnight in 200-300 µl of complete DMEM. *Cm* was prepared from frozen stocks by diluting the bacteria in complete DMEM without addition of 1% P/S to achieve the multiplicity of infection (MOI) for the particular experiment. Once the *Cm* was prepared, the original medium was removed from the culture and replaced with medium alone, or medium containing *Cm* (100 µl). The plate was then incubated at 37°C for 4 hours, washed 3 times with DMEM lacking 1% P/S (400 µl per individual well), and DMEM lacking 1% P/S was added back to the cells (300 µl) and incubated at 37°C. Supernatant amounts of 100 µl, for extraction of gDNA for bacterial quantification, and 200 µl for cytokine measurement were collected at 4, 20, or 40 hours post infection and stored in -80°C. The attached cells were also stored at -80°C for any future experiments by wrapping the culture plate in parafilm and then freezing the entire plate.

For MEF experiments with cytokine stimulation in addition to *Cm* infection, instead of adding back antibiotic-free DMEM, DMEM containing IFN-γ, IL-17A, IL-17C or IL-17E or combinations of two cytokines were added. IFN-γ stimulation was at 20 ng/ml and IL-17A, IL-17C, and IL-17E were added at 10 ng/ml. Combinations of IFN-γ (20 ng/ml) were also made with IL-17A, IL-17C, or IL-17E (all at 10 ng/ml). These stimulations were

added after *Cm* infection and washing and after any initial supernatants were collected for early samples within 4 hours post infection. For *Cm* infection experiments with WT, IL-17RAKO, and IL-17RCKO MEFs, the cells were isolated from corresponding mice as described above. MEFs were infected with *Cm* at MOI of 0.5 and 100 µl of the culture supernatant was collected at 6 and 24 hours and stored at -80°C for further gDNA isolation to measure *Cm* levels post infection.

For cytokine experiments with McCoy cells, in addition to *Cm* infection (MOI 1, 100,000 cells in 48-well plate), instead of adding back antibiotic-free McCoy medium, McCoy medium containing IFN-γ (20 ng/ml), IL-17A (10 ng/ml), or a mixture of both were added. These stimuli were added after *Cm* infection and washing and after any initial supernatants were collected for early samples within 4 hours post infection. Culture supernatants (100 µl) were collected at 4 and 40 hours and stored at -80°C for further gDNA isolation to measure *Cm* levels post infection.

2.4 *In vivo* models

2.4.1 Generation of IL-17RA knockout (KO) and IL-17RCKO bone marrow chimeras (BMC)

For preparation of bone marrow cells, all techniques were performed under sterile conditions. C57BL/6 CD45.1 congenic donor mice were euthanized and the femurs and tibia were removed, rinsed in 70% ethanol, and placed in RPMI medium containing 5% bovine serum (BS). After removing connective tissue, both ends of the femur and tibia were carefully removed. The bone marrow was extracted by inserting a syringe with a 23 gauge needle into the bone marrow cavity and flushed with 3 to 5 ml of 5% BS RPMI into a Petri dish. The extracted bone marrow was dissociated by flushing repeatedly with a syringe.

The sample was centrifuged (525 g for 10 min at 4°C) and then the cell pellet was suspended in ammonium-chloride-potassium ACK buffer (0.1 mM EDTA, 0.15 M NH_4Cl, 1mM $KHCO_3$) for red blood cell lysis for 5 min at room temperature. The reaction was stopped by the addition of at least one volume of 5% BS RPMI medium. The suspension was centrifuged (525 g for 10 min at 4°C) and the cell pellet was suspended in 5% BS RPMI medium. The cells were counted by the trypan blue-dye exclusion method using a hemacytometer and then centrifuged (525 g, 10 min at 4°C) and resuspended in sterile PBS at a concentration of 1 x 10^8 cells/ml.

Recipient mice (C57BL/6 WT, IL-17RAKO, or IL-17RCKO) (4 to 6 weeks old) were administered 0.2% w/v neomycin antibiotic-laced drinking water *ad libitum* 2 weeks prior to irradiation. Recipient mice were exposed to 750 rads and 450 rads of γ-irradiation from a cesium source delivered approximately 4 hours apart. Within 30 minutes following the second dose of irradiation, the mice were placed in a restraint device and were administered tail vein injections of approximately 10 x 10^6 of WT CD45.1 congenic donor bone marrow cells in 100 µl of sterile phosphate-buffered saline (PBS). Recipient mice were monitored by measuring their body weight daily and were provided with 0.2% neomycin-laced drinking water *ad libitum* for two weeks. Softened food pellets were provided in this time period and, when necessary, intraperitoneal (*i.p.)* injection of sterile PBS was administered to the mice to prevent severe dehydration. At 4 weeks post irradiation, peripheral blood was obtained from the mice by submandibular bleeding, and was analyzed for the presence of donor-derived cells. CD45.1 and CD45.2 expression were analyzed by flow cytometry and only the mice with over 80% reconstitution of donor cells were used in further experiments.

2.4.2 Respiratory tract *Cm* infection model

Six weeks post bone marrow reconstitution, a respiratory infection was established in the bone marrow chimeric mice. The mice were immobilized with an *i.p.* injection of ketamine (37.5 mg/kg) (Bioniche, Lavaltrie, Québec) and Rompun (xylazine) (7.5 mg/kg) (Bayer Healthcare, Mississauga, Ontario) anesthesia, and inoculated intranasally with 4 x 10^3 IFU of *Cm* in 25 µl of SPG buffer with a P100 micropipette and 250 µl pipette tip. The body weight was measured daily at approximately the same time starting on the day of inoculation. Mice that lost more than 20% of their original body weight before the scheduled end point were euthanized. Intact WT, IL-17RA-, and IL-17RC-knockouts were also infected with *Cm* at a dose of 4 x 10^3 IFU in 25 µl of SPG buffer as described above.

2.4.3 Tissue sample processing

An overview of the parameters collected during sacrifice of mice for *in vivo* experiments are shown in Figure 2.2. At 3, 5, and 11 days post infection, the mice were euthanized and the bronchoalveolar lavage (BAL) fluid was collected. The trachea was exposed and a small incision was made to insert a 23 gauge needle (with polypropylene tubing on the needle). A small piece of suture was tied around the trachea and needle to secure it in place. Using a syringe, approximately 1 ml of 1X PBS was delivered into the lung. The chest area was then massaged gently for approximately 30 seconds before the fluid was withdrawn into the syringe. The sample was then centrifuged (10,500 g, 10 mins, 4°C) and the supernatant was stored at -80°C for cytokine measurements.

The lungs were excised and the upper and lower left lobes were placed in SPG buffer on ice. One kidney and a section of the liver (adjusted to the same concentration as the kidney sample by weighing the tubes post organ collection and adjusting the SPG

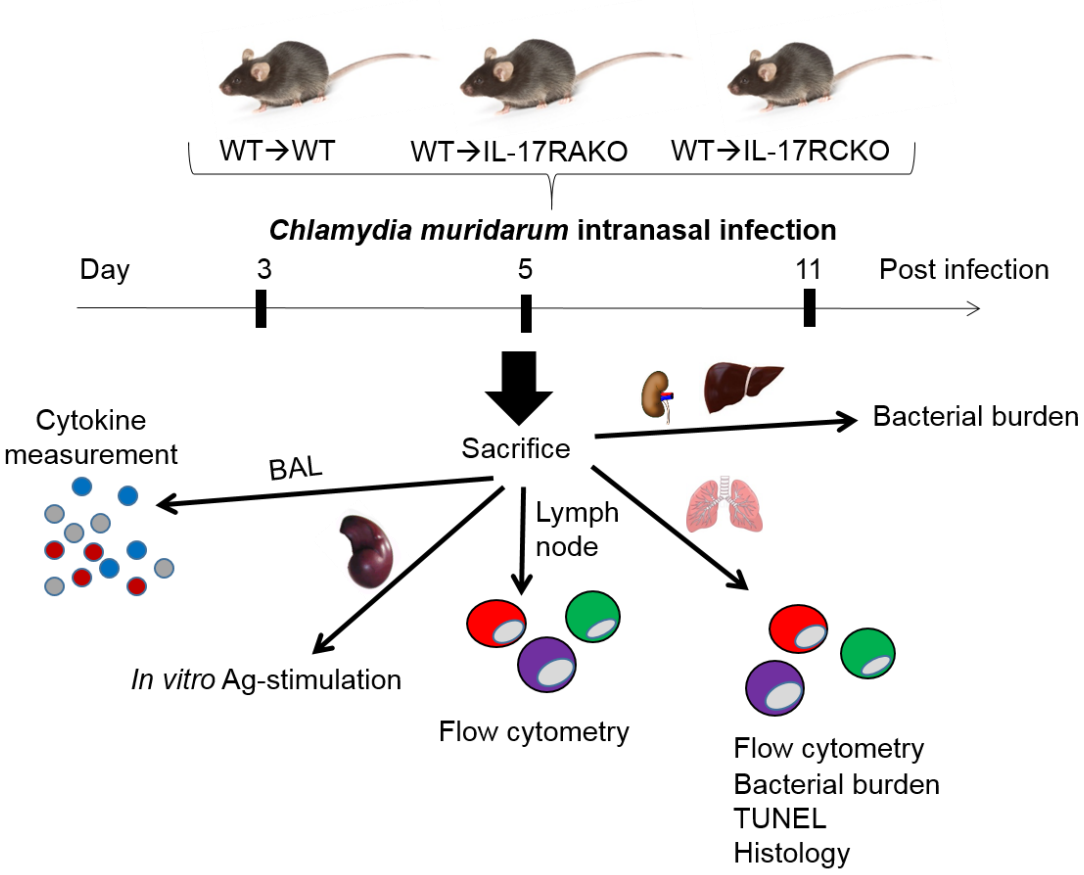

Figure 2.1 Overview of parameters collected and analyzed during *in vivo* experiments. WT-BMC, IL-17RAKO-BMC, and IL-17RCKO-BMC mice were euthanized at the indicated time points post respiratory *Cm* infection. The BAL fluid was collected for cytokine measurement, spleen for *in vitro* recall response, mediastinal lymph node for flow cytometry analysis, lung for flow cytometry analysis, bacterial burden measurement, TUNEL staining, and H & E staining, and kidney/lung for bacterial burden measurement.

volume after organ collection to the same weight as one kidney) were also collected in SPG buffer on ice. The samples were homogenized with a tissue homogenizer at the highest speed for approximately 30 seconds repeatedly until the whole tissue was completely homogenized. The tissue suspension was centrifuged (1000 g, 10 minutes at 4°C) and two 100 µl aliquots of the supernatant were collected and stored at -80°C for bacterial quantification. The remaining sample for the lung was centrifuged (21,000 g, 10 minutes at 4°C) and the supernatant was separated into two aliquots and stored at -80°C for cytokine measurement. If the lung was to be processed for RNA extraction, the tissue was homogenized in Buffer RLT from RNeasy Plus Mini Kit (Qiagen) according to the manufacturer's protocol. For analysis of IL-17C, IL-17E, IL-17RE, and IL-17RB mRNA expression levels in the lung, subsequent RT-PCR and PCR was performed as described above.

The remaining lung tissue was placed in 1 ml of Hanks balanced salt solution (HBSS) and minced into small pieces with sterile surgical scissors. Then, a final concentration of 200 µg/ml of collagenase II was added to the suspension and incubated for 20 mins at 37°C with occasional vortexing. The reaction was stopped with 1 volume of 5% BS RPMI and the solution was pressed through a 40 µm cell strainer. The cell suspension was washed once with 5% BS RPMI and the number of cells was counted with a hemacytometer via Trypan blue exclusion assay using a cell sample diluted with 4% Trypan blue.

For lymph node isolation, the mediastinal lymph node (MLN) was placed in 1 ml of 5% BS RPMI medium in a 60 mm dish. The organ was mechanically disrupted using two sterile glass slides and then the cell suspension was pipetted through a 40 µm cell strainer. The glass slides and dish were washed with 1 ml of 5% BS RPMI pipetted through

the cell strainer. The suspension was centrifuged (525 g, 10 mins at 4°C), and resuspended in complete RPMI medium, and counted as described above.

For splenocyte isolation, the spleen was placed in 10 ml of 5% BS RPMI medium in a Petri dish and mechanically disrupted using two sterile glass slides. The cell suspension was pipetted into a tube and the glass slides and Petri dish were washed with an additional 10 ml of 5% BS RPMI medium and also pipetted into the tube. The cell suspension was centrifuged (525 g, 10 mins at 4°C) and then the cell pellet was suspended in ACK buffer (4 ml per organ) for 6 mins at room temperature. The red blood cell lysis reaction was stopped with at least one volume of 5% BS RPMI medium and centrifuged (525 g, 10 mins at 4°C). The cell pellet was suspended in 10 to 20 ml of 5% BS RPMI medium and pipetted through a 40 µm cell strainer, resuspended in complete RPMI medium, and counted as described above.

2.5 *In vitro* antigen restimulation assay

Heat-killed *Cm* (HK-*Cm)* was used as an antigen for *in vitro* stimulations. To prepare HK-*Cm,* purified *Cm* were incubated at 65°C for 30 minutes and then stored at 4°C for future experiments. Splenocytes were seeded into 96-well flat-bottom plates at a density of 1 x 10^6 cells/well and then stimulated with HK-*Cm* at a final dose of 4.8 x 10^6, 2.4 x 10^6, and 1.2 x 10^6 IFU/ml (1:50, 1:100, 1:200 of *Cm* used, diluted in complete RPMI medium) or medium alone. The plate was incubated at 37°C for 72 hours and then the culture supernatant was collected and frozen at -20°C for cytokine enzyme-linked immunosorbent assay (ELISA).

2.6 Immunofluorescence staining and flow cytometry

All of the primary antibodies used for staining and flow cytometry are listed in Table 2.1. If cells were grown in a tissue culture plate, 4-6 µl of 0.1M EDTA was added to each well and pipetted and left at room temperature for 5-10 mins. Cell suspensions were transferred to a 96-well v-bottom plate with approximately 1 x 10^6 cells/well and centrifuged (755 g, 3 mins at 4°C) to pellet the cells. The supernatant was quickly discarded and the cell pellets were suspended in 200 µl fluorescence-associated cell sorting (FACS) wash buffer (0.5% BS in 1X PBS) and centrifuged (755 g, 3 mins at 4°C) to wash the cells. The cells were blocked with 50 µl of 10% filtered heat-inactivated rat serum in FACS wash buffer for 15 mins at 4°C. Without removing the rat serum, 50 µl of the corresponding fluorochrome-conjugated anti-mouse monoclonal antibodies were added to each sample for cell-surface staining and incubated for 20 mins at 4°C. After incubation, 100 µl of FACS wash buffer was added to each sample and then the plate was centrifuged (755 g, 3 mins at 4°C) and washed with FACS wash buffer two additional times. If the cells were only stained for surface markers, the samples were fixed in 200 µl of 1% formalin in PBS and stored at 4°C in the dark until they were ready for analysis within 2 days.

If the cells were to be stained for intracellular cytokines, the single cell suspensions (prior to surface staining) were stimulated in 96-well flat-bottom plates containing 200 µl of complete RPMI with 50 ng/ml phorbol myristate acetate (PMA) (Sigma Aldrich), 2 µg/ml ionomycin (Sigma Aldrich), and 10 µg/ml of Brefeldin A (eBioscience, San Diego, CA, USA) at 37°C. After 4-6 hours, the plate was moved to 4°C overnight and the staining was continued the next morning. The cells were harvested and surface stained as described above until the last wash step. The cells were fixed with intracellular fixation buffer (eBioscience), permeabilized with permeabilization buffer (eBioscience) according to the

Table 2.1 List of fluorochrome-conjugated primary antibodies used in immunofluorescence staining

Specificity	Host	Isotype	Clone	Manufacturer
Anti-mouse CD4 FITC Anti-mouse CD4 PE	Rat	IgG2b κ	GK1.5	eBioscience
Anti-mouse CD8α PE	Rat	IgG2a κ	53-6.7	eBioscience
Anti-mouse CD19 PE-Cy7	Rat	IgG2a κ	MB19-1	eBioscience
Anti-mouse CD3 FITC	Armenian Hamster	IgG	145-2C11	eBioscience
Anti-mouse CD11c FITC	Armenian Hamster	IgG	N418	eBioscience
Anti-mouse CD11b FITC	Rat	IgG2b κ	M1/70	eBioscience
Anti-mouse Gr1 FITC	Rat	IgG2b κ	R56-8C5	eBioscience
Anti-mouse/human CD45R (B220) PE	Rat	IgG2a κ	RA3-6B2	eBioscience
Anti-mouse TCRβ APC-eFluor 780	Armenian Hamster	IgG	H57-597	eBioscience
Anti-mouse γδ TCR PerCP-eFluor 710	Armenian Hamster	IgG	eBioGL3	eBioscience
Anti-mouse CD45.2 PE	Mouse	IgG2a κ	104	eBioscience
Anti-mouse NK1.1 PE	Mouse	IgG2a κ	PK136	eBioscience
Anti-mouse NKp46 PE	Rat	IgG2a κ	29A1.4	eBioscience
Anti-mouse IL-17RA PE	Rat	IgG2a	PAJ-17R	eBioscience
Anti-mouse IL-17RC APC	Goat	IgG	-	R & D
Anti-mouse/rat IL-17A APC	Rat	IgG2a κ	eBio17B7	eBioscience
Anti-mouse IFN-γ APC Anti-mouse IFN-γ PE-Cy7	Rat	IgG1 κ	XMG1.2	eBioscience
Anti-mouse CD127 PE-Cy7	Rat	IgG2a κ	A7R34	eBioscience
Anti-mouse IL-22 PerCP-eFluor 710	Rat	IgG1 κ	IH8PWSR	eBioscience
Anti-mouse RORγt PerCP-eFluor710	Rat	IgG1 κ	B2D	eBioscience
Rat IgG2a κ isotype control APC	Rat	IgG2a κ	eBR2a	eBioscience
Rat IgG1 κ isotype control PerCP-eFluor 710	Rat	IgG1 κ	eBRG1	eBioscience
Anti-Goat IgG APC	Goat	IgG	-	R & D

manufacturer's protocol. The cells were intracellularly stained with 50 µl of corresponding intracellular fluorochrome-conjugated anti-mouse monoclonal antibodies or isotype-matched control antibody (diluted in permeabilization buffer) for 20 minutes at room temperature. The cells were then washed with permeabilization buffer once and fixed with 1% formalin in PBS. If the cells were to be stained for the intracellular transcription factor RORγt, the Transcription Factor Staining Buffer Set (eBioscience) was used according to the manufacturer's protocol. Cells were stimulated with PMA, ionomycin, and Brefeldin A as described above, blocked with rat serum, and stained with the Fixable Viability Dye eFluor®506 (eBioscience). Cell samples were then stained as described above for intracellular staining.

The samples were collected on a FACSCalibur (BD Biosciences, Mississauga, ON, Canada) or FACSFortessa (BD Biosciences). The data was analyzed using FCS Express 4 Flow Cytometry software (De Nova Software, Los Angeles, CA, USA).

2.7 Cytokine ELISA assay

The concentrations of cytokines and chemokines in culture supernatants were determined by ELISA using antibody pairs specific for mouse IFN-γ, IL-17A, IL-17E, IL-4, IL-13, IL-10, IL-1β, CXCL1, IL-6, TNF, IL-12p70, IL-23, and IL-27 (eBioscience). The optimal concentration of each antibody was specified by the manufacturer.

96-well flat-bottom Costar Maxisorp plates were coated with 50 µl of the specific capture antibody per well for each cytokine or chemokine of interest. The capture antibodies were all initially diluted in Coating Buffer (eBioscience). Each plate was incubated for 24 hours at 4°C and then washed 3 times. To wash the plates, 200 µl of 0.01% Tween-20/PBS buffer was added to each well and then dumped out and patted dry on paper

towel. Alternatively, an automatic plate washer was used for this process (BioTek, ELx405). Blocking buffer (100 µl) (Assay Diluent) (eBioscience) was added to each well and the plates were incubated for 2 hours at room temperature (RT). The plates were then washed three times as described above. The cytokine standards were prepared in a 1:2 serial dilution in Assay Diluent starting at 2000 pg/ml, with the exception of IL-10 which started at 8000 pg/ml. At least 8 dilutions were performed to generate a standard curve. Samples were diluted in Assay Diluent if the concentration of the cytokine being measured exceeded the upper limit of quantitation of the standard curve. Standards and samples were added to each plate (50 µl each) and plates were incubated overnight at 4°C. After incubation, 50 µl of biotinylated detection antibody diluted in Assay Diluent was added to each well and the plates were incubated for 2 hours at RT and then washed 3 times. After washing, 50 µl of streptavidin-horse radish peroxidase (eBioscience) diluted in Assay Diluent was added to each well and incubated for 20 minutes in the dark at RT. Plates were then washed 5 times and 50 µl of 1X tetramethylbenzidine substrate solution (eBioscience) was added to each well. Assays were monitored for color change and the reaction was stopped with 50 µl of 0.2M H_2SO_4. Within 30 minutes, plates were read on an ELISA plate reader (BioTek Synergy HT) at 450 nm wavelength and the data was analyzed using Gen5 software (BioTek).

2.8 Luminex assay

The concentrations of cytokines and chemokines in the mouse BAL and *in vitro* MEF *Cm* infection supernatants were measured by a Luminex assay using the ProcartaPlex Multiplex Immunoassay (eBioscience, San Diego, CA, USA) with antibody magnetic beads specific for CCL3, CXCL1, CXCL2, GM-CSF, IFN-γ, IL-1α, IL-1β, IL-2, IL-6, IL-

7, IL-9, IL-10, L-12p70, IL-13, IL-15/IL-15R, IL-17A, IL-18, IL-21, IL-22, IL-23, IL-25, IL-31, IL-27, TSLP (all from eBioscience).

The Luminex assay was performed following the manufacturer's instructions. Samples were thawed on ice before the preparation of the Luminex plate. The antigen standard was prepared to the optimal concentration specified by the manufacturer. Antibody magnetic beads were diluted to 1X in multiple mixtures of solutions and 50 µl of each solution were added to each well until all mixtures of magnetic beads are added. The plate was washed with ProcartaPlex wash buffer (eBioscience) and the BAL or supernatant samples were added to the plate at 50 µl per sample. The corresponding standards and controls were also added to the plate at 50 µl per sample. The plate was sealed and incubated with shaking (800 rpm) for 2 hours at RT. After incubation, the beads were washed 3 times and detection antibody was added to the plate (25 µl of 1X detection antibody mix). The plate was sealed and incubated with shaking (800 rpm) for 30 minutes at room temperature. After incubation the beads were washed 3 times and 50 µl of Streptavidin-PE was added to each well. The plate was sealed and incubated with shaking (800 rpm) for 30 minutes at RT and then the beads were washed 3 times. The beads were then resuspended in 120 µl of reading buffer, and the plate was sealed and incubated with shaking (800 rpm) for 5 minutes at RT. The data was acquired on a Bio-Rad BioPlex200 System (BioRad, California, United States).

2.9 Histology

Mice were euthanized post *Cm* infection and the lower right lobe of the lung was removed and stored in 10% buffered formalin. The samples were embedded in paraffin and 3-5 µm sections were cut and stained with hematoxylin and eosin (H & E) by technicians

from the pathology lab in the IWK Health Centre. I examined the slides at 50X and 400X magnification for apparent cellular infiltration and overall pathology of the lung using a Leica DM 2500 microscope (Leica Microsystems, Wetzlar, Germany). Five random fields were analyzed for each tissue sample per time point and the representative images were shown.

2.10 Fluorescent TUNEL staining

For fluorescent apoptosis staining in the lung, 3-5 μm thick paraffin-embedded lung tissue sections on glass slides were processed and stained using the ApopTag Red *In Situ* Apoptosis Detection Kit S7165 (EMD Millipore, Temecula, CA, USA) according to the manufacturer's protocol. Briefly, the tissue sections were deparaffinised in a coplin jar, pretreated with protein digesting enzyme, equilibrium buffer, and then working strength TdT enzyme. The reaction was stopped by adding working strength stop/wash buffer. Then, working strength anti-digoxigenin conjugate was added to the sample and washed in PBS. The samples were then counterstained with 4',6'-diamidino-2-phenylindole (DAPI). The slides were examined at 630X magnification using a Zeiss Imager Z2 microscope and analyzed by AxioVision Rel. 4.8 software (Zeiss, Oberkocken, Germany). Five different fields were chosen at per lung section per mouse strain that had the highest visible amount of rhodamine stain (Texas Red). Images were taken with the Texas Red filter and also in the DAPI filter and overlaid automatically. Terminal deoxynucleotidyl transferase deoxyuridine triphosphate (dUTP) nick end labeling positive (TUNEL) positive signals that were associated with DAPI positive staining were counted as apoptotic cells (showing a purple color). The average number of counted cells was taken from the five different fields per sample.

2.11 Statistical analysis

All tests for statistical significance were performed using GraphPad Prism 4 software. The two-tailed unpaired Student's *t* test was used to determine significant differences between two groups. For comparison of more than two groups, the one-way analysis of variance (ANOVA) test followed by multiple comparison of means (Bonferroni) was applied. All of the data are shown as the mean ± standard error of the mean (SEM) or standard deviation (SD) and P values < 0.05 were considered statistically significant.

CHAPTER 3 RESULTS

3.1 IFN-γ, but not IL-17A, IL-17C, or IL-17E directly suppresses *Cm* growth in C57BL/6 or BALB/c MEFs or McCoy cells

Given the controversial reports concerning the role of IL-17A in the direct control of *Chlamydia* growth (32, 129), we wanted to revisit the issue using primary MEFs. C57BL/6 MEFs were used to establish the *in vitro* model of *Cm* infection and replication. Consistent with the understanding that *Chlamydia* normally takes at least 40 hours to complete their intracellular life cycle (35), we did not observe significant changes in bacterial levels at 20 hours post infection (p.i.) of C57BL/6 MEFs at MOI of 0.5. However, bacterial levels were increased markedly by 40 hours (Figure 3.1A), validating that primary MEFs are able to support intracellular replication of *Cm* and are a suitable cell type for directly evaluating the impact of IL-17 cytokine family members in controlling *Chlamydia* replication. Subsequently, we tested whether IFN-γ or IL-17A, individually, or in combination, could reduce *Cm* growth in MEFs. Consistent with a well-established protective role of IFN-γ (126, 129), recombinant IFN-γ at 20 ng/ml exerted a significant suppressive effect on *Cm* replication compared to *Cm* alone (Figure 3.1A). In comparison, recombinant IL-17A did not significantly inhibit *Cm* growth in C57BL/6 MEFs. We did not observe synergistic suppressive effects of IL-17A and IFN-γ in this experiment (Figure 3.1A). Also, IL-17C or IL-17E, which share the IL-17RA receptor subunit with IL-17A (154), did not exhibit any suppressive effect on *Cm* growth in C57BL/6 MEFs by 40 hours p.i. (Figure 3.1B).

We next sought to determine whether the lack of effect of IL-17A on *Cm* growth might be strain-dependent. To this end, we utilized MEFs from BALB/c mice and repeated the experiments. IFN-γ (20 ng/ml) had a significant inhibitory effect on *Cm* growth in

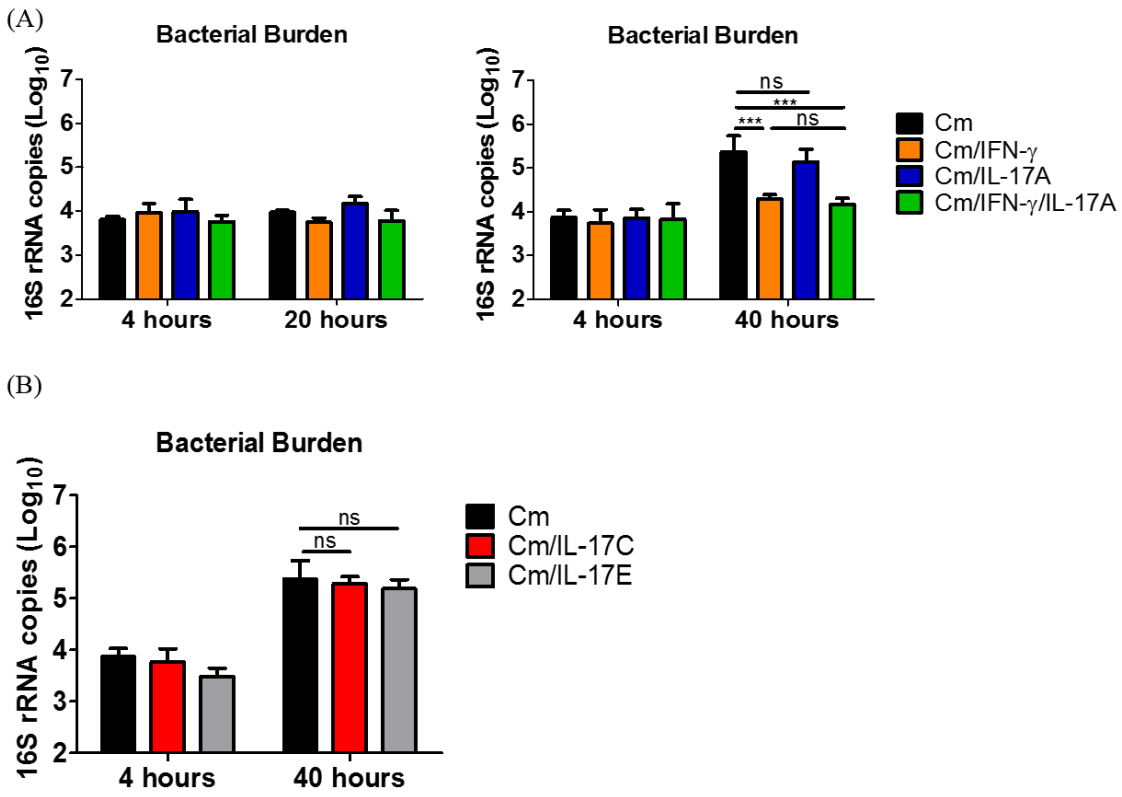

Figure 3.1 IFN-γ, but not IL-17A, IL-17C, or IL-17E, suppress *Cm* growth in C57BL/6 MEFs *in vitro.* Cultured C57BL/6 MEFs were infected with *Cm* at MOI of 0.5 and treated with medium alone, IFN-γ (20 ng/ml) and/or IL-17A (10 ng/ml), IL-17C (10 ng/ml), or IL-17E (10 ng/ml). (A) For *Cm*, IFN-γ and/or IL-17A experiments, the culture supernatant was collected at 4 and 20 hours post infection for each condition in one culture plate and 4 and 40 hours post infection for each condition in a separate plate and gDNA was isolated. The amount of *Cm*-specific gDNA encoding 16s rRNA in each sample was measured by qPCR and the total IFU was calculated and presented as Log_{10} copy number for each condition. Data for 4 and 20 hours post infection are from one experiment with triplicate wells for each condition. Data for 4 and 40 hours post infection are from 2 pooled experiments with 6 independent samples for each condition. (B) For the *Cm*, IL-17C, or IL-17E experiment, the culture supernatant was collected at 4 and 40 hours and the gDNA was isolated from the samples as described above. Data shown are from two pooled experiments with 6 independent samples for *Cm,* and one experiment with triplicate samples for *Cm*/IL-17C and *Cm*/IL-17E. Data are graphed as mean±SD. ***$p<0.001$ using one-way ANOVA per time point.

BALB/c MEFs compared to *Cm* alone (Figure 3.2A). In contrast, IL-17A did not suppress *Cm* growth in the BALB/c MEFs compared to *Cm* alone and did not exert additional inhibitory effects when treated together with IFN-γ (Figure 3.2A). Lastly, IL-17C and IL-17E did not show any significant suppressive effects on *Cm* growth in BALB/c MEFs (Figure 3.2B). Instead, IL-17C significantly enhanced *Cm* growth compared to *Cm* alone at 40 hours p.i. (Figure 3.2B).

Murine McCoy fibroblast cells were also used to examine the effects of IL-17A and IFN-γ on *Cm* growth. While IFN-γ once again displayed robust inhibitory effects on *Cm* replication in the McCoy cells, recombinant IL-17A treatments, alone or in combination with IFN-γ, did not exert any inhibitory effect on *Cm* replication (Figure 3.3). Since exogenous IL-17A did not exert any inhibitory effect on *Cm* growth in fibroblast cells, we examined the role of endogenous IL-17A by infecting WT, IL-17RAKO, and IL-17RCKO MEFs with *Cm.* Loss of IL-17RA in MEFs significantly increased *Cm* replication compared to WT and IL-17RCKO MEFs (Figure 3.4). However, IL-17RCKO MEFs also had heightened bacterial burden compared to WT MEFs but was not statistically significant (Figure 3.4).

These results indicated that IL-17A did not suppress *Cm* growth in C57BL/6 or BALB/c MEFs or McCoy cells and was unable to increase the suppressive effect when treated together with IFN-γ. However, endogenous IL-17A/IL-17R-dependent signaling may be required in controlling *Cm* replication in MEFs. Also, although IL-17C and IL-17E also utilize one of the same receptor subunits as IL-17A (154), these cytokines did not suppress *Cm* replication in C57BL/6 or BALB/c MEFs *in vitro.*

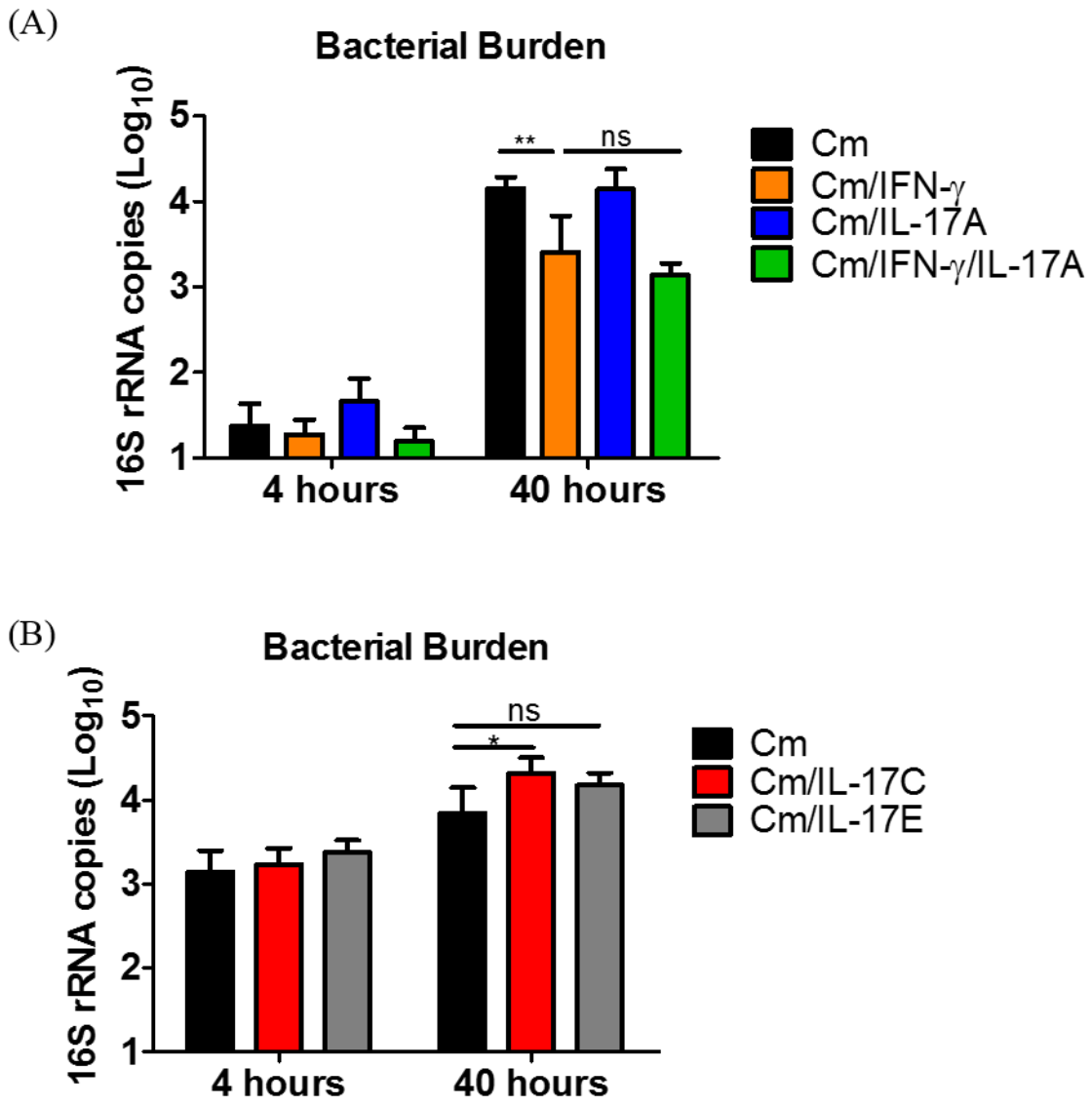

Figure 3.2 IFN-γ, but not IL-17A, IL-17C, or IL-17E, suppress *Cm* growth in BALB/c MEFs *in vitro*. Cultured BALB/c MEFs were infected with *Cm* at MOI of 0.5 and treated with medium alone, IFN-γ (20 ng/ml) and/or IL-17A (10 ng/ml) (A), IL-17C (10 ng/ml), or IL-17E (10 ng/ml) (B). The culture supernatant was collected at 4 and 40 hours post infection for each experiment and gDNA was isolated. The amount of *Cm*-specific gDNA encoding 16s rRNA in each sample was measured by qPCR and the total IFU was calculated and presented as Log_{10} copy number for each condition. For (A), data is shown as representative of two experiments with triplicate samples for all conditions. For (B), data are from 2 pooled experiments with 6 independent samples for *Cm,* and one experiment with triplicate samples for all other conditions. All data are graphed as mean±SD. $p^*<0.05$, $p^{**}<0.01$, $^{***}p<0.001$ using one-way ANOVA per time point.

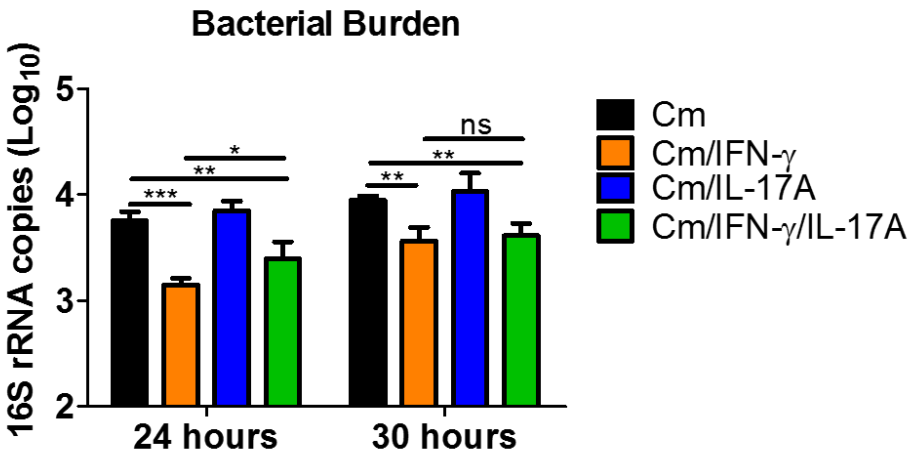

Figure 3.3 IFN-γ, but not IL-17A, suppresses *Cm* growth in McCoy cells *in vitro.* McCoy cells were infected with *Cm* at MOI of 1 and treated with medium alone, IFN-γ (20 ng/ml) and/or IL-17A (10 ng/ml). The culture supernatant was collected at 24 and 30 hours and the gDNA was isolated. The amount of *Cm*-specific gDNA encoding 16s rRNA in each sample was measured by qPCR and the total IFU was calculated and presented as Log_{10} copy number for each condition. Data are from one experiment with triplicate samples for each condition and graphed as the mean±SD. *p<0.05, **p<0.01, ***p<0.001 using one-way ANOVA per time point.

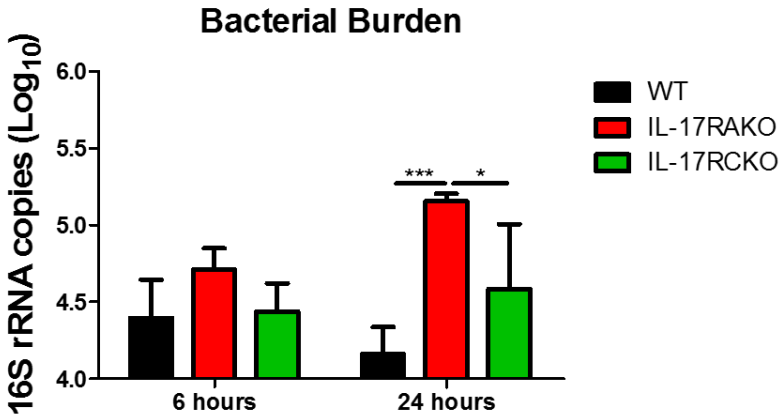

Figure 3.4 Loss of IL-17RA in C57BL/6 MEFs results in heightened bacterial burden upon *Cm* infection *in vitro.* WT (C57BL/6), IL-17RAKO, and IL-17RCKO MEFs were infected with *Cm* at MOI of 0.5. The culture supernatant was collected at 6 and 24 hours and the gDNA was isolated. The amount of *Cm*-specific gDNA encoding 16s rRNA in each sample was measured by qPCR and the total IFU was calculated and presented as Log_{10} copy number. Data are from one experiment with triplicate samples for each strain per time point and graphed as the mean±SD. *p<0.05, ***p<0.001 using one-way ANOVA per time point.

3.2 Characterization of cytokines and chemokines induced in MEFs during *Cm* infection *in vitro*

3.2.1 *Cm* induces a large spectrum of cytokine/chemokine production in C57BL/6 WT MEFs

To further characterize the tissue structure cell response to *Cm*, we examined a panel of chemokines and cytokines in culture supernatants collected from primary C57BL/6 MEFs with and without *Cm* infection using a Luminex assay. Although *Cm* infection induced CXCL1, CXCL2, and IL-6 from MEFs, the induced measurements were above the upper limit of quantitation of the standard curve for the assay. Also, the measurements for IL-31, IL-23, IL-12p70, and IL-18 were under the lower limit of quantitation of the standard curves. Although detected at low levels, IL-2, IL-17E, IL-13, IL-27, IFN-γ, IL-17A, IL-7, IL-9, IL-21, IL-15/IL-15R, IL-1α, and IL-1β were significantly induced by *Cm* infection in MEFs (Figure 3.5A and C). Some cytokines and chemokines were also significantly induced by *Cm* infection in MEFs that were detected at a higher level than cytokines and chemokines from Figure 3.4A, including IL-10, IL-22, CCL3, and GM-CSF (Figure 3.5B). Lastly, some cytokines were induced by *Cm* infection in MEFs in a dose-dependent manner which included IL-15/IL-15R, IL-1α, IL-1β, TSLP (Figure 3.5C). Collectively, these results demonstrate that *Cm* infection in C57BL/6 MEFs induces potent cytokine and chemokine responses which could influence innate and adaptive immune responses at the infection site.

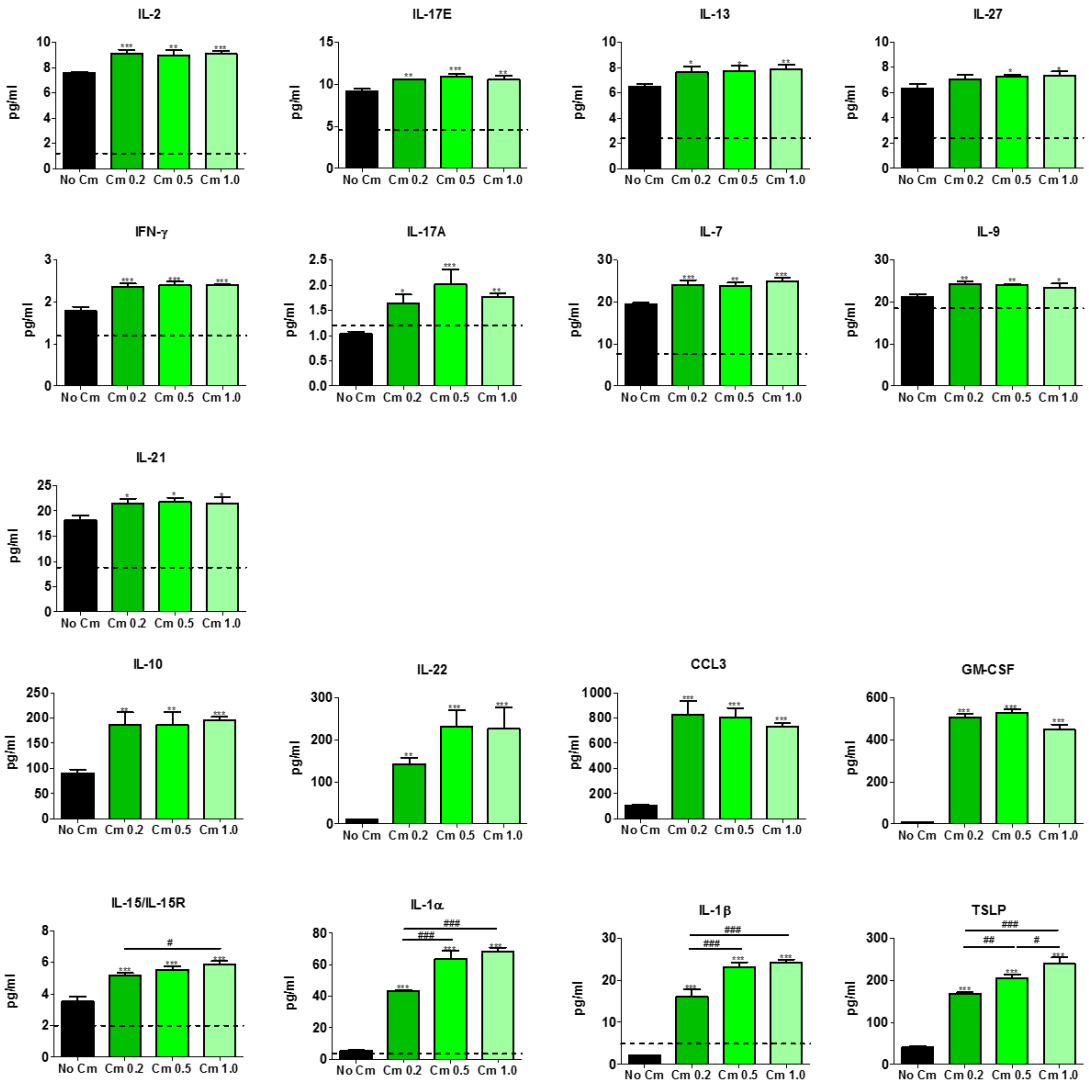

Figure 3.5 Chemotactic and inflammatory cytokines are induced in C57BL/6 MEFs upon *Cm* infection. Culture supernatant from non-infected or *Cm*-infected C57BL/6 MEFs at MOI of 0.2, 0.5, or 1.0 at 40 hours post infection were collected. The cytokine levels were measured by using a Luminex assay and graphed in concentration of pg/ml. Cytokines and chemokines induced by *Cm* at a low level are shown (A). Mediators that were markedly induced by *Cm* (B) and induced in a dose-dependent manner of *Cm* are also shown (C). Numbers beside "*Cm*" are the MOI used. Data are from one experiment with triplicate samples for each condition and graphed as mean±SD. The dashed line represents the lower limit of detection for the particular cytokine/chemokine. Stars above *Cm* stimulated bars indicate significance compared to No *Cm*. **p*<0.05, ***p*<0.01, ****p*<0.001 using one-way ANOVA. Comparison between infection doses as indicated with #*p*<0.05, ##*p*<0.01, ###*p*<0.001 using one-way ANOVA.

3.2.2 *Cm* triggers an altered cytokine/chemokine profile in IL-17RAKO and IL-17RCKO MEFs

Given that the potent cytokine responses are induced by *Cm* infection in primary MEFs, we characterized the cytokine profile from IL-17RAKO and IL-17RCKO MEFs. CXCL1, TNF, and IL-6, and IL-1β were measured in the supernatants of non-infected or *Cm*-infected WT (C57BL/6), IL-17RAKO, and IL-17RCKO MEFs as these are some of the proinflammatory cytokines and chemokines that are induced by IL-17A (158, 162). However, there was no detectable level of IL-1β in the culture supernatants. At an MOI of 0.5 (Figure 3.6A) or 2 (Figure 3.6B), *Cm* induced significantly higher levels of CXCL1, TNF, and IL-6 in IL-17RAKO MEFs compared to WT MEFs at 24 and 48 hours p.i. *Cm* also induced significantly higher levels of CXCL1 and IL-6, albeit to a lesser extent, in IL-17RCKO MEFs compared to WT MEFs at some time points or doses of *Cm* (Figure 3.6A and B). Due to inconsistent trends of cytokine production at different doses of *Cm*, the experiment needs to be reproduced to confirm the results. Taken together, these data suggests that a heightened proinflammatory profile was induced by *Cm* in IL-17RAKO, and IL-17RCKO MEFs to a lesser extent, compared to WT MEFs. However, it remains unclear whether the heightened immune responses in tissue structure cells can enhance host resistance against bacterial infection and/or aggravate infection-induced tissue damage *in vivo*.

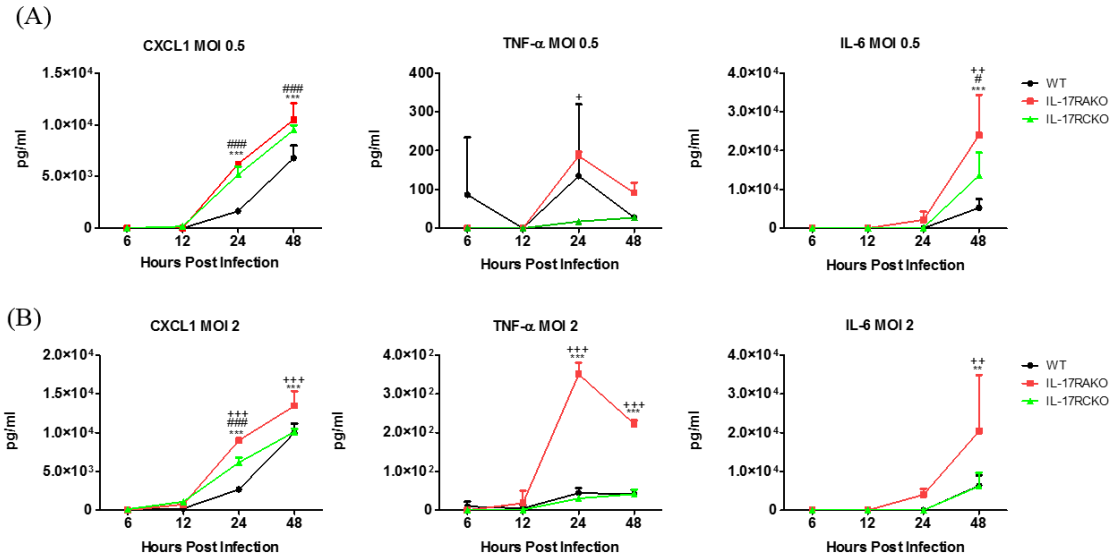

Figure 3.6 Proinflammatory cytokines are heightened in IL-17RAKO and IL-17RCKO MEFs, but not WT MEFs, during *Cm* infection. MEFs from WT (C57BL/6), IL-17RAKO, and IL-17RCKO mice were obtained and then infected with *Cm* at an MOI of 0.5 or 2 and the culture supernatant was collected at 6, 12, 24, 48 hours. The cytokine levels in the culture supernatant were measured by ELISA and graphed in concentration of pg/ml. Levels of CXCL1, TNF-α, and IL-6 were measured from infected cells at MOI of 0.5 (A) and MOI of 2 (B). Data are from one experiment with triplicate samples for each strain per time point and graphed as mean±SD. Comparison between WT and IL-17RAKO, *p<0.05, **p<0.01, ***p<0.001 using two-way ANOVA. Comparison between WT and IL-17RCKO, #p<0.05, ###p<0.001 using two-way ANOVA. Comparison between IL-17RAKO and IL-17RCKO, +p<0.05, ++p<0.01, +++p<0.001 using one-way ANOVA per time point.

3.3 IL-17RA and IL-17RC in the tissue stromal cells are critically required in host defense against *Cm* infection *in vivo*

3.3.1 Loss of IL-17RA and IL-17RC in the tissue stromal cells causes greater clinical disease in mice with respiratory *Cm* infection

An intranasal *Cm* infection was established in WT-BMC, IL-17RAKO-BMC, and IL-17RCKO-BMC mice to examine the role of IL-17RA and IL-17RC in tissue stromal cells during *Cm* infection *in vivo*. WT (non-chimeric) mice were included in some experiments to examine any potential impact of γ-irradiation in altering immune responses to *Cm* infection. Indeed, WT and WT-BMC mice did not show significant differences in body weight changes, and both groups of mice had transient body weight loss (peaking at day 7 p.i.) and then rebounded afterwards. In comparison, IL-17RAKO-BMC and IL-17RCKO-BMC mice progressively lost their body weight by day 11 p.i. and, although not statistically different, had a greater percentage of body weight loss compared to WT-BMC mice (Figure 3.7A). Overall, these observations suggest that IL-17RA and IL-17RC in the tissue structure cells have an important role in controlling respiratory *Cm* infection and the severity of clinical disease *in vivo*.

3.3.2 Loss of IL-17RA and IL-17RC in the tissue stromal cells results in heightened bacterial burden in the lungs upon respiratory *Cm* infection *in vivo*

Given that a greater body weight loss was observed in *Cm*-infected IL-17RAKO-BMC and IL-17RCKO-BMC mice compared to WT-BMC mice, we wondered whether this correlated with a greater profile of bacterial burden in the lung. Indeed, *Cm* replication was significantly increased in the lung samples collected from IL-17RAKO-BMC and IL-17RCKO-BMC mice compared to WT-BMC mice at days 3, 5, and 11 p.i. (Figure 3.7B).

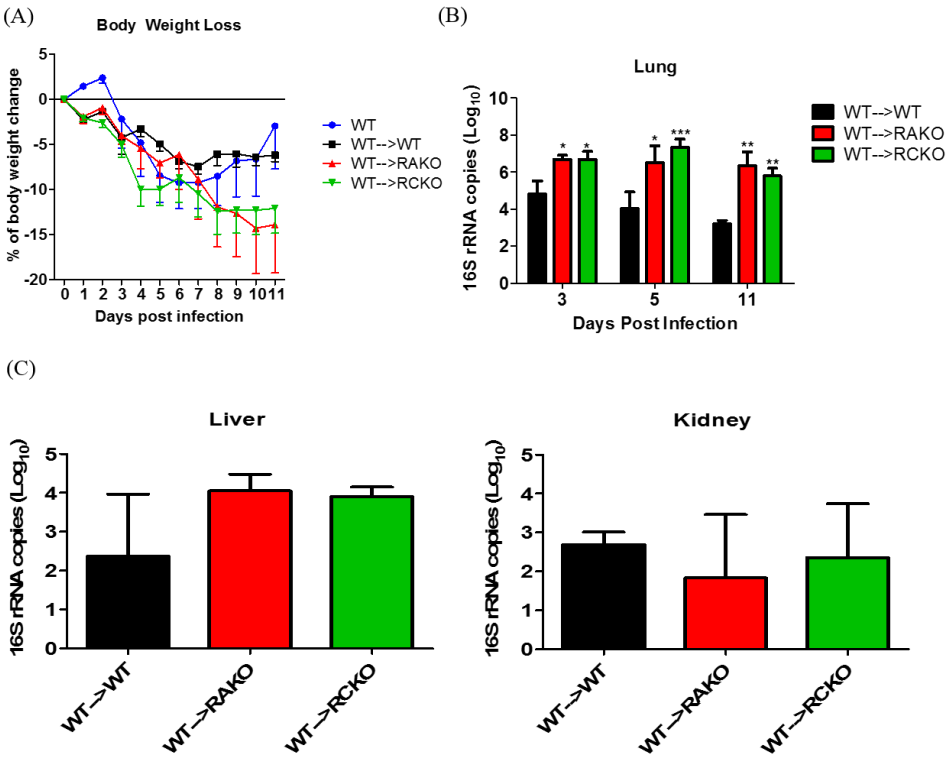

Figure 3.7 Loss of IL-17RA and IL-17RC in the tissue stromal cells causes greater clinical disease and bacterial burden during respiratory *Cm* infection. The body weight was measured for each strain of mouse daily after respiratory *Cm* infection and the percent of body weight change was calculated based on their original weight at Day 0. The average body weight change (A) for each strain of mice were graphed up to day 11 post infection. The mice which lost 20% of original body weight or greater were included and were kept at the same weight from the day of sacrifice to day 11 post infection. Data for WT are from one experiment with n=6 mice. Data for WT-BMC are from 4 pooled experiments with mice numbers of n=18 to day 2, n=13 to day 3, n=10 to day 5, n=5 to day 11. Data for IL-17RAKO-BMC are from 4 pooled experiments with mice numbers of n=17 to day 2, n=13 to day 3, n=9 to day 5, n=5 to day 11. Data for IL-17RCKO-BMC are from 4 pooled experiments with mice numbers of n=26 to day 2, n=21 to day 3, n=19 to day 5, n=12 to day 11. The left lobe of the lung, and a section of kidney and liver were dissected and gDNA was isolated. qPCR was performed on the samples to measure the *Chlamydia*-specific 16S rRNA and the data was graphed in Log_{10} value (B-C). For the lung, data are shown from 2 pooled experiments for all strains at day 3 with WT-BMC and IL-17RAKO-BMC n=8 mice and RCKO-BMC n=7 mice, one experiment for all strains at day 5 with WT-BMC and IL-17RAKO-BMC n=4 mice and IL-17RCKO-BMC n=7, one experiment for WT-BMC n=5 and IL-17RAKO-BMC n=4 at day 11, 2 pooled experiments for IL-17RCKO-BMC n=10 at day 11. For the kidney/liver, data are from one experiment with WT-BMC n=4, IL-17RAKO-BMC n=3, IL-17RCKO-BMC n=6. Body weight loss and lung bacterial burden data are graphed as mean±SEM and liver/kidney bacterial burden data are graphed as mean±SD with one-way ANOVA statistical analysis. *p<0.05, **p<0.01, ***p<0.001 using one-way ANOVA performed for body weight loss and lung bacterial burden (compared to WT-BMC) per time point.

Bacterial burden in IL-17RAKO-BMC and IL-17RCKO-BMC mice were not significantly different from each other (Figure 3.7B).

Previously, *Cm* infection in the genital tract has been reported to disseminate to other organs of the mouse particularly to the spleen, kidneys, and the liver (203). Therefore, we checked whether the *Cm* dissemination may also occur in our model. While low levels of *Cm* dissemination were detected in the liver and kidney, no statistical differences were observed between the strains. However there was a trend towards higher levels in the liver samples collected from IL-17RAKO-BMC and IL-17RCKO-BMC mice compared to WT-BMC mice (Figure. 3.7C). This data suggests an important role for IL-17RA and IL-17RC in the tissue stromal cells of the lung to control respiratory *Cm* infection *in vivo*. However, IL-17RA and IL-17RC does not have a significant effect on disseminated *Cm* growth in the kidney and liver tissue.

3.3.3 Loss of IL-17RA and IL-17RC signaling in the tissue stromal cells results in heightened cellular infiltration upon respiratory *Cm* infection

We next examined the pathology of the lung in *Cm*-infected WT-BMC, IL-17RAKO-BMC, and IL-17RCKO-BMC mice by histological staining of the lung. *Cm*-infected IL-17RAKO-BMC and IL-17RCKO-BMC mice had observably greater cellular infiltration and reduced alveolar space at 3 days and 5 days p.i. compared to WT-BMC mice (Figure 3.8A). By day 11 p.i., the inflammatory infiltration was observably reduced in all mouse strains although a small area of cellular infiltration was still evident in IL-17RAKO-BMC mice. Despite the apparent differences in the intensity of inflammation in different groups, the majority of the cells infiltrating the tissue were mononuclear cells as shown in Figure 3.8B and were in clusters surrounding blood vessels. This data is consistent

Figure 3.8 Respiratory *Cm* infection leads to heightened cellular infiltration in the lungs of IL-17RAKO-BMC and IL-17RCKO-BMC mice. The lower right lobe of the lung was dissected from *Cm*-infected or non-infected mice at the indicated time points and stored in 10% buffered formalin. The lung tissue was then prepared for H & E staining to look at the lung pathology and cellular infiltration between the strains. Representative H & E stained lung tissue from WT-BMC, IL-17RAKO-BMC, and IL-17RCKO-BMC mice at 3, 5, and 11 days post infection with *Cm* are shown (A). Lungs from mice that were euthanized prior to the end point due to a weight loss of >20% were also stained with H & E (B). Black boxes indicate the area of view for the corresponding images below each image. H & E stained lung tissue from WT at 11 days post infection was used as a comparison for the WT-BMC mice and stained tissue from naïve WT-BMC mice was used as a non-irradiated control (C). (Magnification; 50x and 400X).

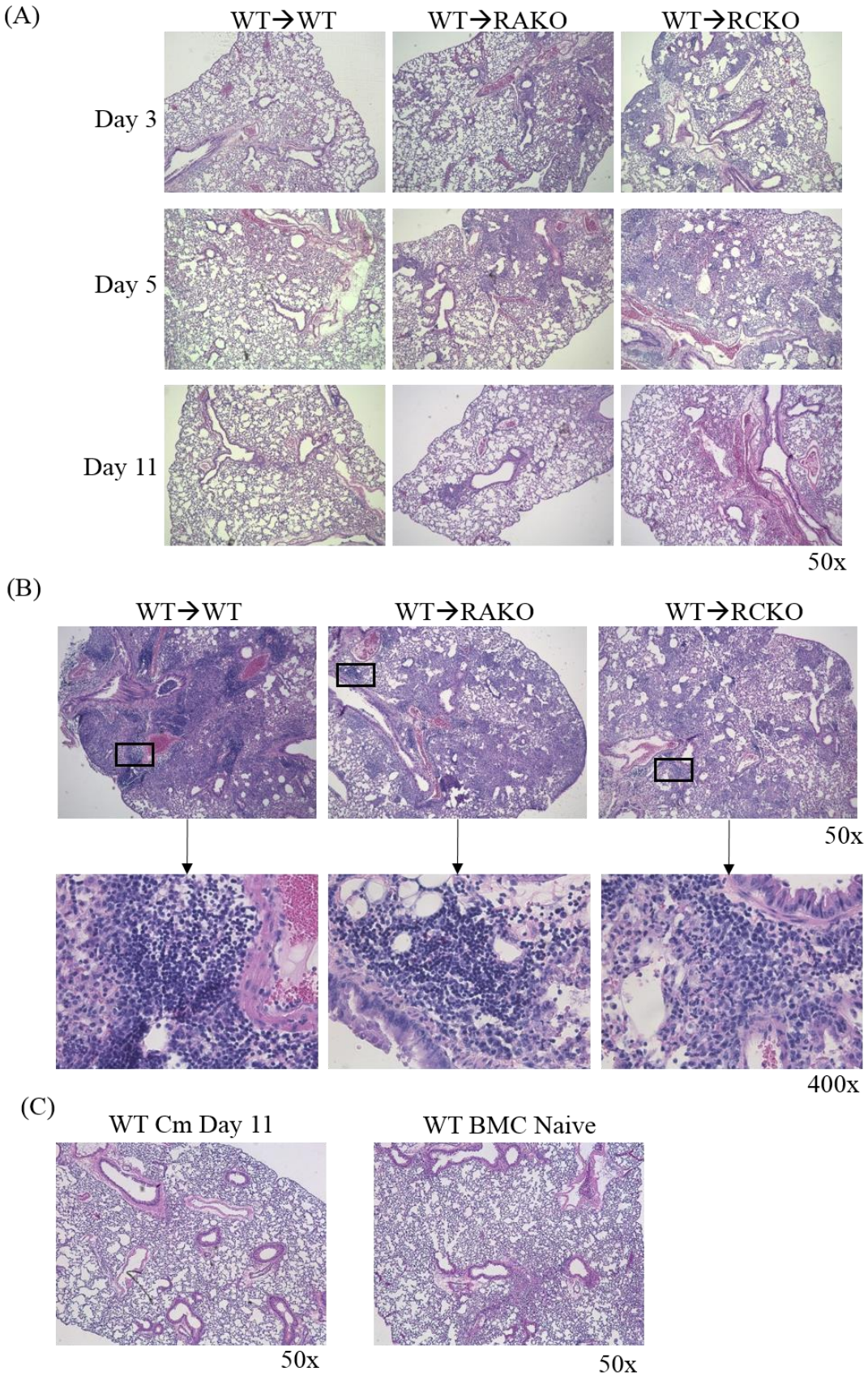
(A)
WT→WT
WT→RAKO
WT→RCKO
Day 3
Day 5
Day 11
50x
(B)
WT→WT
WT→RAKO
WT→RCKO
50x
400x
(C)
WT Cm Day 11
WT BMC Naive
50x
50x

with our *in vitro* observation that IL-17RAKO and IL-17RCKO MEFs produced more proinflammatory cytokine and chemokines. Instead of being proinflammatory, our data suggests an important anti-inflammatory role of IL-17RA and IL-17RC in tissue stromal cells via controlling bacterial replication and infection-induced cytokine and chemokine production.

3.3.4 Loss of IL-17RC in the tissue stromal cells heightens apoptosis in the lung upon respiratory *Cm* infection *in vivo*

Because *Chlamydia* modulates cell death pathways in infected host cells (68), we performed fluorescent TUNEL staining to examine the level of apoptosis in infected lungs. Lung tissue was counter-stained with DAPI to distinguish TUNEL-positive apoptotic bodies from apparent unknown non-specific TUNEL staining (Figure 3.9A). Interestingly, the non-specific TUNEL staining seemed to be heightened in the IL-17RAKO-BMC and IL-17RCKO-BMC mice lung tissue samples compared to WT-BMC mice samples (Figure 3.9A). IL-17RCKO-BMC, but not IL-17RAKO-BMC mice, had significantly higher levels of apoptosis compared to WT-BMC mice at 3 and 5 days p.i. (Figure 3.9B). Therefore, these results showed that loss of IL-17RC in the tissue stromal cells leads to elevated apoptosis in the lung upon respiratory *Cm* infection, and IL-17RA and IL-17RC appear to have a differential impact on the outcome of apoptosis.

Figure 3.9 Loss of IL-17RA and IL-17RC in the tissue stromal cells results in heightened apoptosis after early respiratory *Cm* infection. Fluorescent TUNEL staining (red; TUNEL, blue; DAPI nuclear counterstain) was performed to label fragmented DNA in the lung tissues of the mice. (A) The representative images from the lung tissue at day 5 post infection are shown and the white arrows show cell-associated TUNEL+ staining which represent apoptosis. (B) For each sample, five fields were chosen that had the highest observable amount of TUNEL staining. The average was taken for all strains per time point and graphed as mean±SD. Data are from of one experiment with mouse numbers of WT-BMC n=5 for all time points, IL-17RAKO BMC n=4 for all time points, IL-17RCKO BMC n=5 for day 3, n=7 for day 5, n=3 for day 11. *$p<0.05$ using one-way ANOVA per time point. (Magnification 630X).

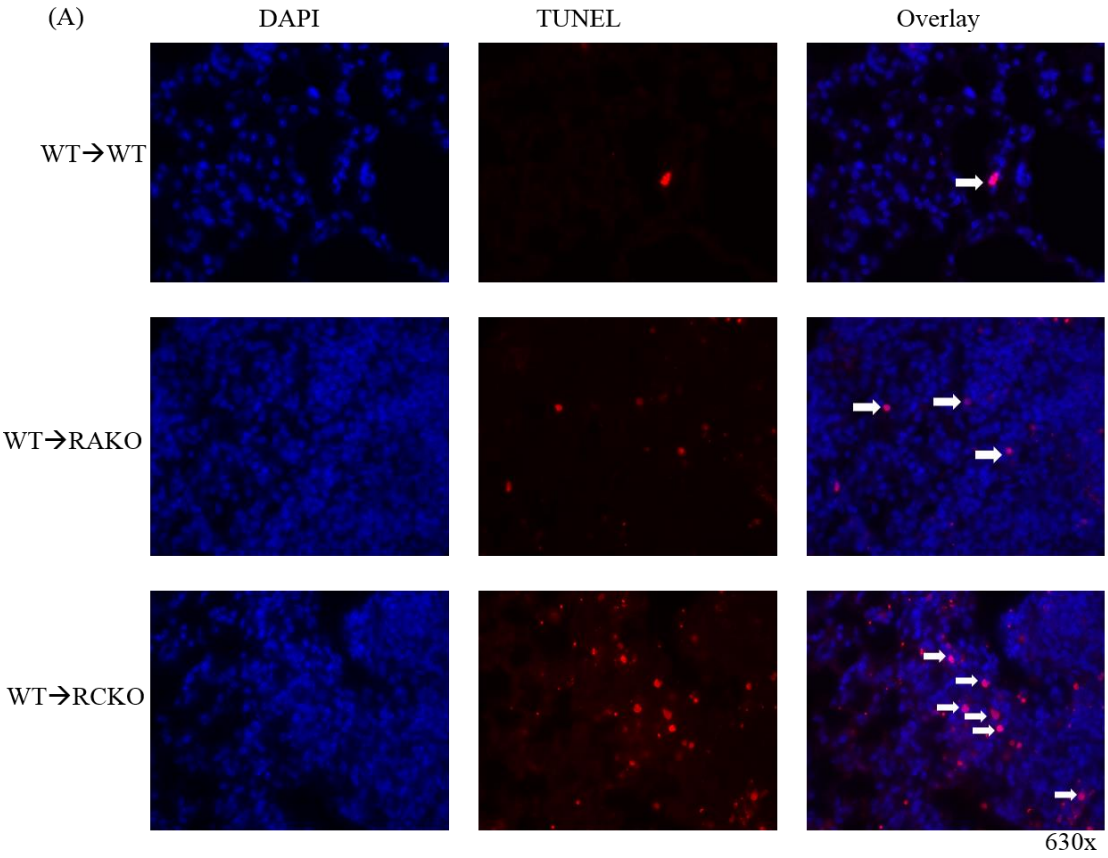
(A)
DAPI
TUNEL
Overlay
WT→WT
WT→RAKO
WT→RCKO
630x

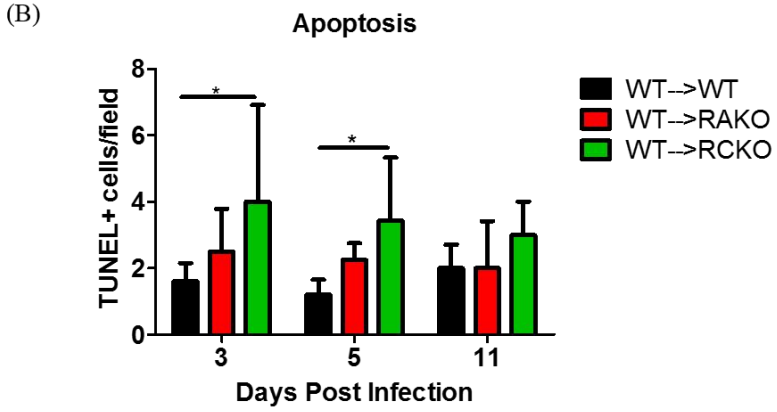
(B)
Apoptosis
TUNEL+ cells/field
0
2
4
6
8
*
*
3
5
11
Days Post Infection
WT-->WT
WT-->RAKO
WT-->RCKO

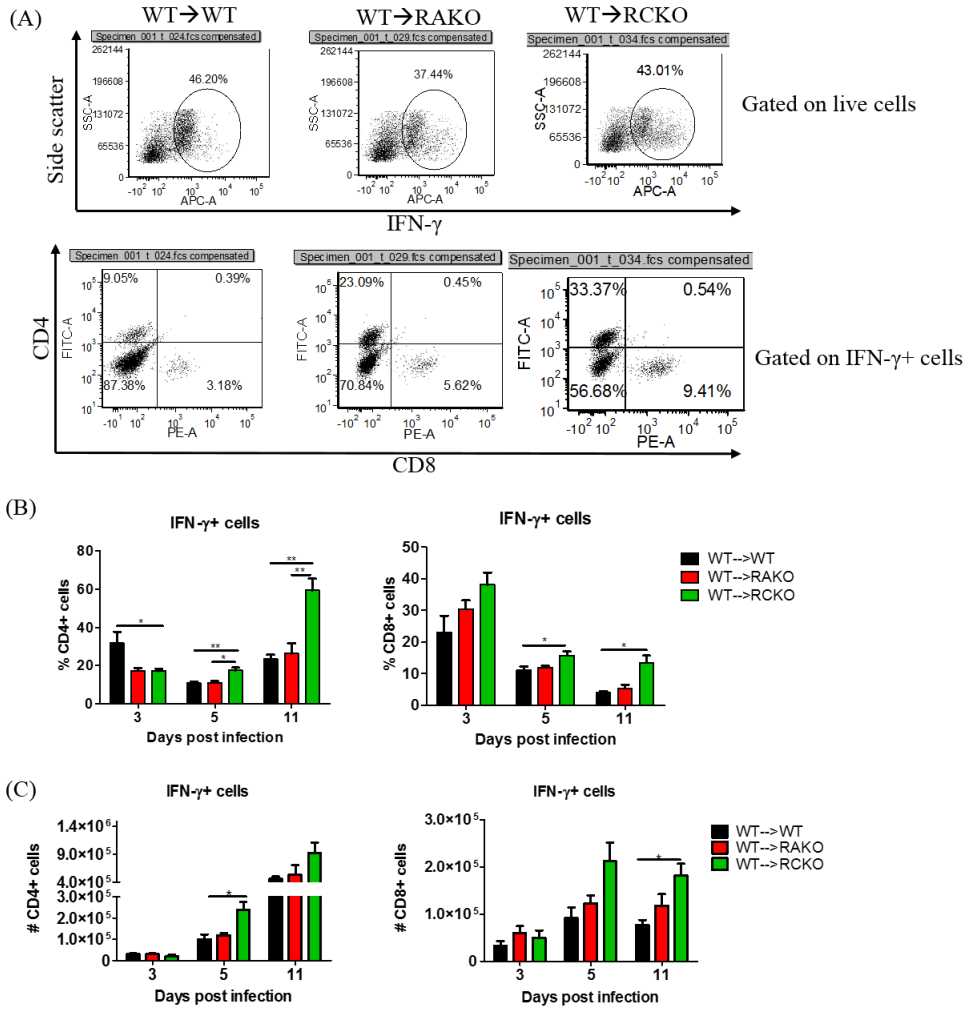

Figure 3.10 IL-17RCKO-BMC, but not IL-17RAKO-BMC, induced type 1 responses in the lung upon *Cm* infection. WT-BMC, IL-17RAKO-BMC, or IL-17RCKO-BMC mice were infected intranasally with 4,000 IFU of *C. muridarum.* The lung was dissected from all of the mice, processed for cell isolation and then performed ICCS for IFN-γ and surface stained for CD4 and CD8 T cell markers. (A) The representative FACS plots and gating strategy for day 11 post infection are shown for WT-BMC, IL-17RAKO-BMC, and IL-17RCKO lung cells. The frequency (B) and total (C) CD4+ and CD8+ IFN-γ-producing cells are shown for each time point. Data are from two pooled experiments for all strains at day 3 with WT-BMC n=8, IL-17RAKO-BMC n=7, and IL-17RCKO-BMC n=7, one experiment for all strains at day 5 with WT-BMC n=5, IL-17RAKO-BMC n=4, IL-17RCKO-BMC n=7, and one experiment for WT-BMC n= 5 and IL-17RAKO-BMC n=4 at day 11 and 4 pooled experiments for IL-17RCKO-BMC at day 11 with n=10 mice. Data are graphed as mean±SEM. **p*<0.05, ***p*<0.01 using one-way ANOVA for each time point.

3.4 IL-17RA and IL-17RC in the tissue stromal cells are differentially required in shaping host immune responses against *Cm* infection *in vivo*

3.4.1 *Cm* infection induces distinct type 1 and type 17 immune responses in the lung of IL-17RCKO-BMC and IL-17RAKO-BMC mice respectively

We next sought to examine whether the loss of IL-17RA or IL-17RC in the tissue stromal cells altered immune responses, particularly adaptive immune responses *in vivo*. To differentiate between IFN-γ production by CD4+ (Th1) and CD8+ (Tc1) cells, we performed intracellular cytokine staining (ICCS) for IFN-γ (Figure 3.10A). WT-BMC and IL-17RAKO-BMC mice had comparable levels of IFN-γ-producing CD4+ and CD8+ T cells in the lung at 3, 5, and 11 days p.i. (Figure 3.10B and C). At day 3 p.i., the frequency of IFN-γ-producing CD4+ T cells was elevated in WT-BMC mice compared to IL-17RCKO-BMC mice (Figure 3.10B). In contrast, the frequency of IFN-γ-producing CD4+ T cells was significantly elevated in IL-17RCKO-BMC mice compared to IL-17RAKO-BMC and WT-BMC mice at day 5 and 11 p.i (Figure 3.10B). However, the number of IFN-γ-producing CD4+ T cells was elevated in IL-17RCKO-BMC mice compared to WT-BMC mice only at day 5 p.i. (Figure 3.10C). IL-17RCKO-BMC mice also had an elevated frequency of IFN-γ-producing CD8+ T cells compared to IL-17RAKO-BMC and WT-BMC mice at day 5 and 11 p.i. (Figure 3.10B). However, the number of IFN-γ-producing CD8+ T cells was elevated in IL-17RCKO-BMC compared to IL-17RAKO-BMC and WT-BMC only at 11 p.i. (Figure 3.10C).

Since IL-17A is produced by multiple innate and adaptive immune subsets (154, 168), ICCS for IL-17A was performed on lung cells to distinguish between IL-17A-producing B cells, CD4+ and CD8+, T cell receptor (TCR) γδ+, and TCRβ+ T cells. At 3 days p.i., the frequency and total number of IL-17A-producing CD4+ T cells (conventional

Figure 3.11 Loss of IL-17RA, but not loss of IL-17RC, in the tissue stromal cells enhances early type 17 responses in the lung during *Cm* infection WT-BMC, IL-17RAKO-BMC, or IL-17RCKOBMC mice were infected intranasally with 4,000 IFU of *Cm*. Frequency and total number of IL-17A+ cells among CD4+ and CD4- cells in the lung was determined by ICCS. (A) Representative FACS plots are shown depicting live cells with CD4 on the y-axis and IL-17A on the x-axis. (B) For each time point, the frequency and total number of CD4+IL-17A+ and CD4-IL-17A+ cells are shown. Data are from 2 pooled experiments for day 3 with WT-BMC n=8, IL-17RAKO-BMC n=8, IL-17RCKO-BMC n=7, one experiment for day 5 with WT-BMC n=5, IL-17RAKO-BMC n=4, IL-17RCKO-BMC n=7, one experiment for day 11 for WT-BMC and IL-17RAKO-BMC n=5 and n=4 respectively, and 4 pooled experiments for day 11 for IL-17RCKO-BMC n=10. Data are presented as mean±SEM. $*p<0.05$, $**p<0.01$, $***p<0.001$ using one-way ANOVA for each time point. (C) Lung cells from naïve WT, IL-17RAKO, IL-17RCKO, and WT-BMC mice are shown with total number of CD4+ and CD4- producing IL-17A cells. Data are from one experiment with n=2 mice per strain. Data are presented as mean±SD.

(A)

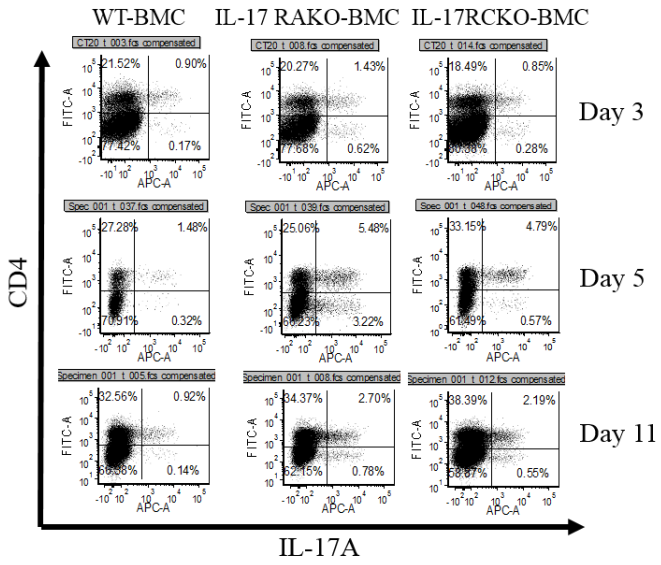
WT-BMC
IL-17 RAKO-BMC
IL-17RCKO-BMC
Day 3
Day 5
Day 11
CD4
IL-17A
FITC-A
APC-A
21.52%
0.90%
7.42%
0.17%
20.27%
1.43%
7.66%
0.62%
18.49%
0.85%
0.28%
27.28%
1.48%
0.32%
25.06%
5.48%
3.22%
33.15%
4.79%
0.57%
32.56%
0.92%
0.14%
34.37%
2.70%
0.78%
38.39%
2.19%
0.55%

(B)

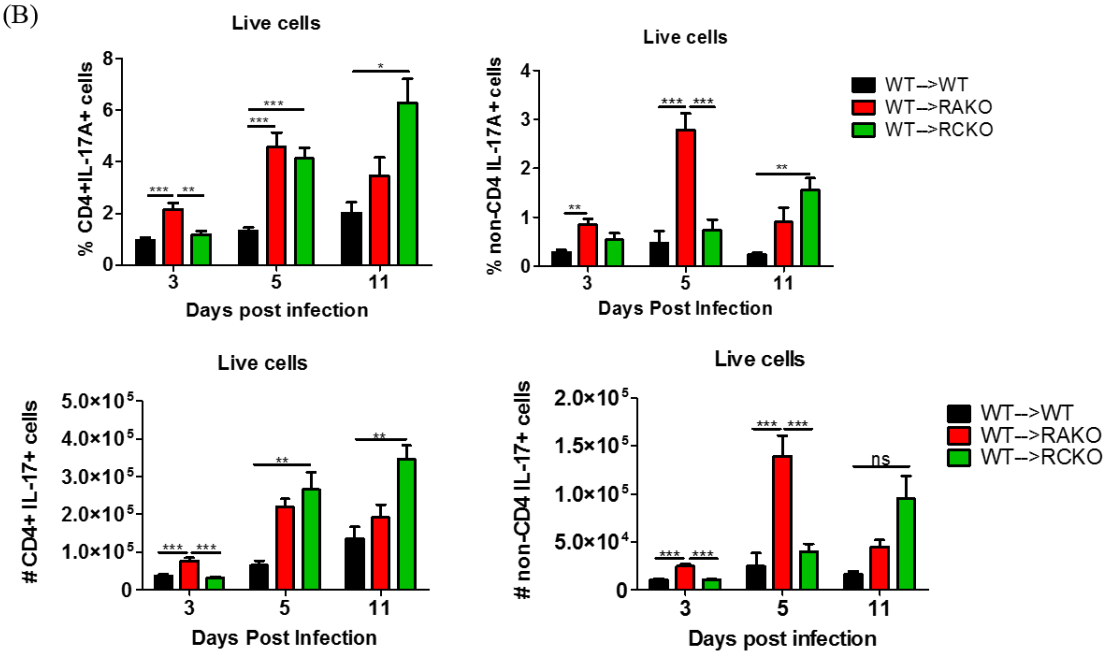
Live cells
% CD4+IL-17A+ cells
Days post infection
% non-CD4 IL-17A+ cells
Days Post Infection
WT-->WT
WT-->RAKO
WT-->RCKO
CD4+ IL-17+ cells
Days Post Infection
non-CD4 IL-17+ cells
Days post infection
ns

(C)

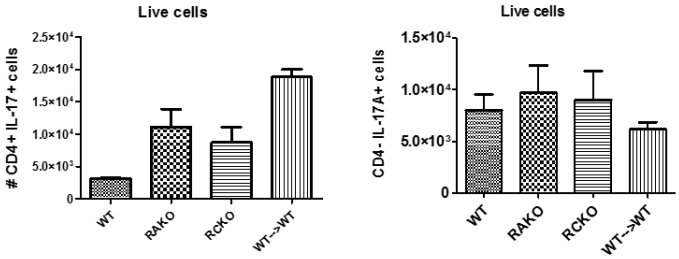
Live cells
CD4+ IL-17+ cells
CD4- IL-17A+ cells
WT
RAKO
RCKO
WT->WT

Th17 cells) was significantly heightened in IL-17RAKO-BMC mice compared to WT-BMC and IL-17RCKO-BMC mice (Figure 3.11A and B). *Cm* infection significantly increased the frequency of IL-17A-producing Th17 cells in both IL-17RAKO-BMC and IL-17RCKO-BMC mice compared to WT-BMC mice at 5 and 11 days p.i. (Figure 3.11A and B). Interestingly, a population of IL-17A-producing non-CD4 cells was significantly increased in IL-17RAKO-BMC mice compared to WT-BMC and IL-17RCKO-BMC mice upon *Cm* infection at 3 and 5 days p.i. (Figure 3.11A and B). The frequency of the IL-17A-producing non-CD4 population was significantly increased in IL-17RCKO-BMC mice compared to WT-BMC at day 11 p.i. (Figure 3.11B). Although the basal level of IL-17A-producing CD4+ cells varied among naïve WT, IL-17RAKO, IL-17RCKO (intact knockouts) and naïve WT-BMC mice, the basal level production of the IL-17A-producing non-CD4 cells were comparable (Figure 3.11C), suggesting that the IL-17A-producing non-CD4 cells are induced by *Cm* infection. Further analysis of the IL-17A-producing non-CD4 cells showed that they were not B cells or TCRβ+. Additionally, these IL-17A-producing non-CD4 cells contained a small number of CD8+ T cells and γδ T cells and a large fraction of non T cells with unknown characteristics (Figure 3.12). Collectively, our results indicate that IL-17RA and IL-17RC in tissue stromal cells have a differential role in shaping type 1 and type 17 responses in the lung that appear to be independent of *Chlamydia* replication.

3.4.2 Loss of IL-17RA and IL-17RC in the tissue stromal cells markedly promotes accumulation of novel ILC17s in the lung upon respiratory *Cm* infection

We next wondered whether the IL-17A-producing non T cells, preferentially induced in IL-17RAKO-BMC mice during *Cm* infection, could potentially be IL-17A-

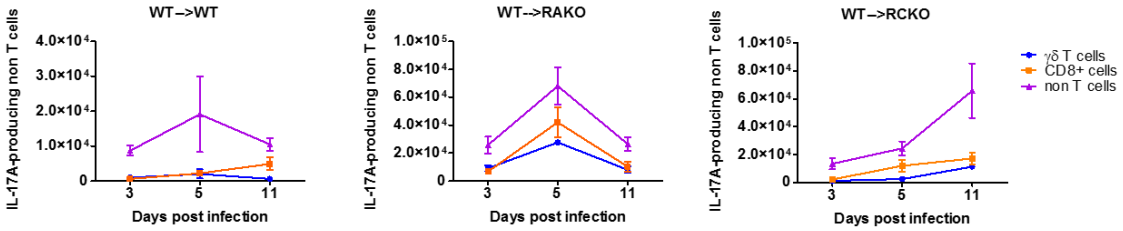

Figure 3.12 The majority of IL-17A-producing non-CD4 cells induced in the lung upon *Cm* respiratory infection were non-CD8+ or non-γδ T cells. WT-BMC, IL-17RAKO-BMC, or IL-17RCKO-BMC mice were infected intranasally with 4,000 IFU of *C. muridarum*. The total number of IL-17A-producing non CD4 cells in the lung was determined by ICCS. The number of γδ T cells, CD8+ and non T cells were determined among the CD4- IL-17A+ population. Data are from 2 pooled experiments for day 3 with WT-BMC n=8, IL-17RAKO-BMC n=8, IL-17RCKO-BMC n=7, one experiment for day 5 with WT-BMC n=5, IL-17RAKO-BMC n=4, IL-17RCKO-BMC n=7, one experiment for day 11 for WT-BMC and IL-17RAKO-BMC n=5 and n=4 respectively, and 4 pooled experiments for day 11 for IL-17RCKO-BMC n=10. Data are presented as mean±SEM.

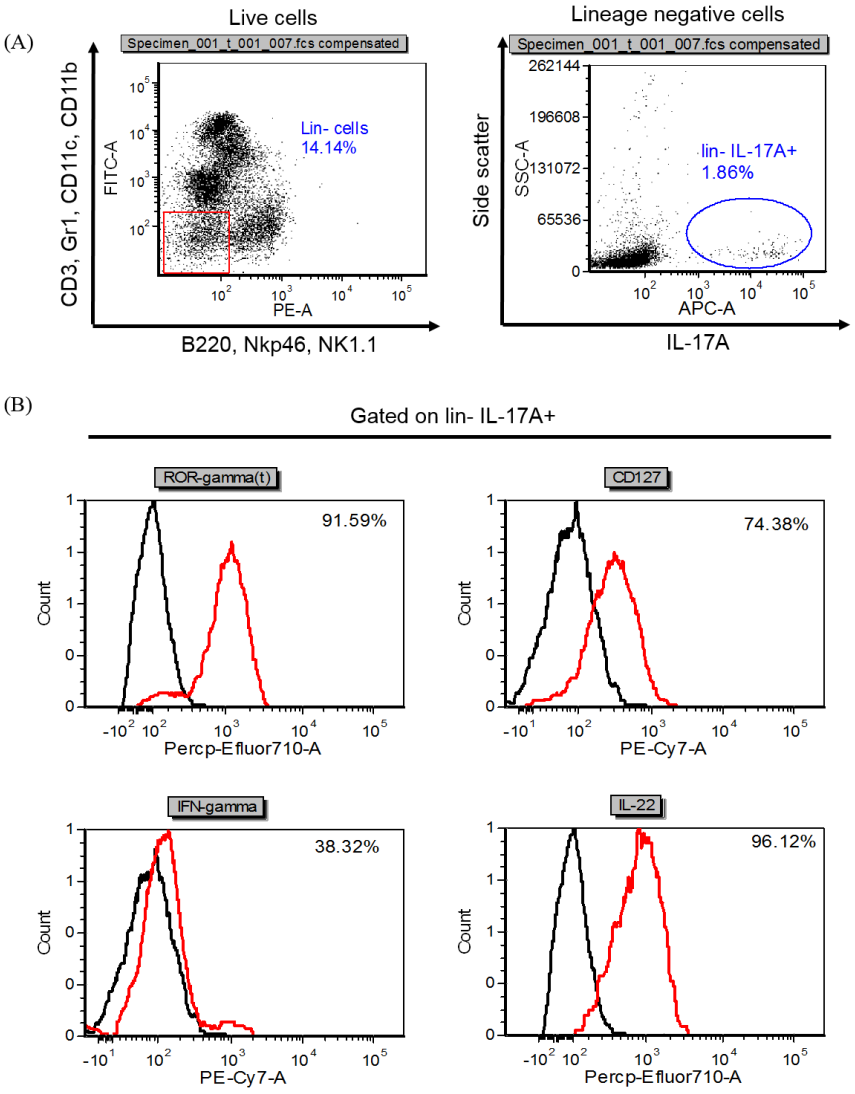

Figure 3.13 The IL-17A-producing non-CD4 cells induced in the lung during respiratory *Cm* infection are ILC17s. IL-17RCKO mice were infected intranasally with 4,000 IFU of *Cm* and euthanized at 5 days post infection. Lung cells from the mice were analyzed by ICCS by FACS staining and lineage negative (lin-) (negative for CD3, Gr1, CD11c, CD11b, B220, Nkp46, NK1.1) IL-17A+ cells (A) were analyzed for RORγt, CD127, IFN-γ, and IL-22 expression (B). The black line indicates the negative fluorescence control and the red line indicates stained lung cells with the indicated cytokine or transcription factor. The percentage in each FACS plot represents the frequency of positive live cells compared to the negative control. FACS plots are representative of 4 pooled mice for each strain and are from one experiment.

producing ILC3s. ILC3s express the transcription factor RORγt and a subtype of these cells are able to produce IL-17A (91). To this end, we performed ICCS to examine the phenotype of these IL-17A-producing non T cells in the lung of *Cm*-infected WT and IL-17RCKO mice at 5 days post infection. Antibodies that recognize B220, CD11b, CD11c, CD3, NK1.1, NKp46, and Gr1 were used to exclude various lineage cells (Figure 3.13A). We found that the lymphoid lineage negative (Lin-) IL-17A+ population indeed expressed RORγt and CD127 (also known as IL-7 receptor) (Figure 3.13B) and were indicative of ILC3s. Additionally, the Lin- IL-17A+ population highly co-expressed IL-22 but not IFN-γ (Figure 3.13B). As such, these IL-17A-producing ILC3s can be categorized as ILC17s, a subset of ILC3s that produce IL-17A/IL-22 (93).

We further examined the relationship between the *Cm*-induced ILC17s and body weight change of respiratory *Cm*-infected mice. The results showed that induced ILC17s negatively correlated with the body weight change of *Cm*-infected mice at 3 days p.i. (Figure 3.14A and B). Taken together, these data revealed a subset of ILC3s, called ILC17s, which were induced in the lung upon early *Cm* infection *in vivo* which negatively correlate with the percentage of body weight loss in *Cm*-infected mice.

3.4.3 Loss of IL-17RA and IL-17RC in the tissue stromal cells results in a differential cytokine profile in splenocyte cultures following *Cm* antigen re-stimulation *ex vivo*

We next sought to characterize the antigen-specific memory responses in the splenocyte cultures with or without HK-*Cm* stimulation. The overall immune responses, including IL-17A, IFN-γ, and IL-13, were significantly higher in IL-17RAKO-BMC and IL-17RCKO-BMC cells compared to WT-BMC cells at day 5 p.i. (Figure 3.15). However, distinct immune responses were observed between IL-17RAKO-BMC and IL-17RCKO-

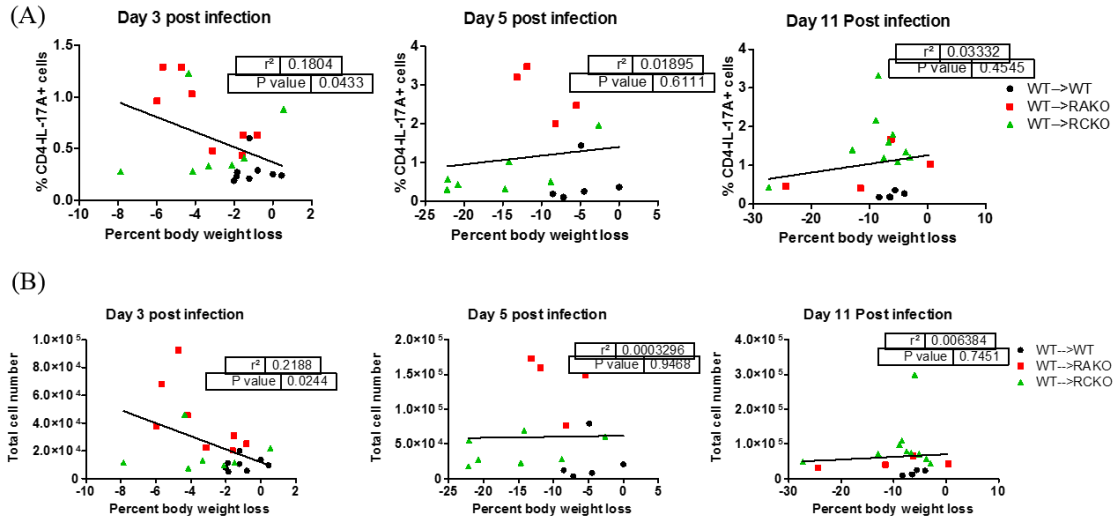

Figure 3.14 ILC17s induced in the lung during respiratory *Cm* infection negatively correlates with the percentage of body weight change. WT-BMC, IL-17RAKO-BMC, and IL-17RCKO-BMC mice were infected intranasally with 4,000 IFU of *Cm*. Frequency and total number of IL-17A+ cells among CD4+ and CD4- cells from the lung was determined by ICCS. Data are from 2 pooled experiments for day 3 (n=7-8 per group), one experiment for day 5 (n=4-7 per group), and 2 pooled experiments for day 11 (n=4-10 per group) post infection. The percentage (A) and total cell number (B) was plotted against the body weight change of individual mice. Each dot corresponds to one mouse and the different colors correspond to the different chimeras. A *p* value of less than 0.05 was considered as a significantly non-zero slope.

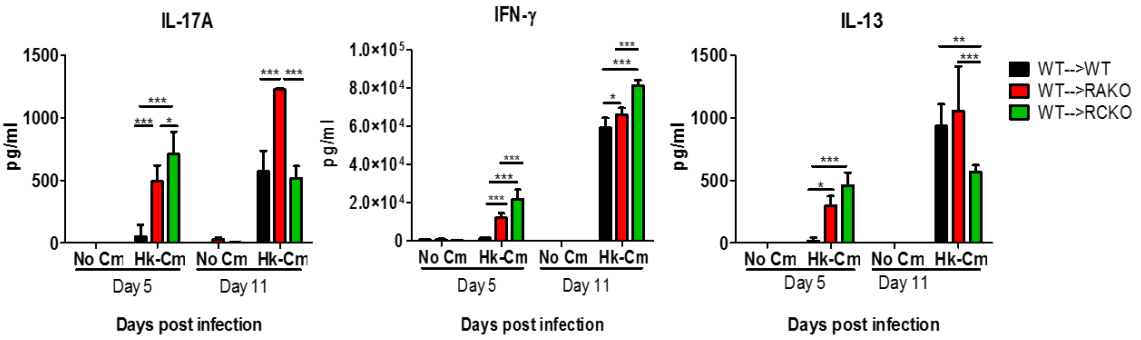

Figure 3.15 A differential *in vitro* antigen-stimulated Th17/Th1 response was induced in IL-17RAKO-BMC and IL-17RCKO-BMC spleen cells. Splenocytes were isolated from the WT-BMC, IL-17RAKO-BMC, and IL-17RCKO-BMC mice at day 5 or 11 post infection and stimulated with heat killed *Cm* or medium only (No *Cm*), cultured for 72 hours, and the supernatant was collected for cytokine measurement. Data are from one experiment of triplicate samples for each strain per time point and are graphed as mean±SD. **p*<0.05, ***p*<0.01, ****p*<0.001 using one-way ANOVA per time point.

BMC mice at day 11 post infection. Similar to the early immune responses in the lung, HK-*Cm* stimulation induced robust IL-17A production in IL-17RAKO-BMC splenocyte cultures (Figure 3.15). However, this data did not reflect the heightened type 17 response also seen in the IL-17RCKO-BMC mice from CD4+ cells at day 5 and 11 p.i. (Figure 3.11B). HK-*Cm* stimulation induced the highest IFN-γ production in IL-17RCKO-BMC splenocyte cultures compared to WT-BMC and IL-17RAKO-BMC splenocytes. Furthermore, HK-*Cm* induced the lowest IL-13 production in IL-17RCKO-BMC cultures compared to the other two strains (Figure 3.15).

Taken together, immune profiles collected from the lung and splenocyte cultures clearly indicate that IL-17RA and IL-17RC in tissue structure cells have differential impacts on shaping adaptive immune responses, although both receptors are required for host defense against *Cm* replication.

3.4.4 Loss of IL-17RA and IL-17RC in the tissue stromal cells results in a differential cytokine profile in the lungs upon respiratory *Cm* infection *in vivo*

We speculated that the cytokine response from the tissue stromal cells may be responsible for the differential host responses in IL-17RAKO-BMC and IL-17RCKO-BMC mice. Therefore, we measured a panel of cytokine and chemokines in the BAL samples by a Luminex assay. Although many cytokines and chemokines were induced by respiratory *Cm* infection at 3 days post infection (Figure 3.16A-C), some mediators were not detected in the assay. Mediators with undetectable levels were IL-10, IL-21, IL-1α, IL-25, IL-9, IL-13, IL-23, GM-CSF, IL-15, TSLP, IL-7, and IL-31. In the IL-17RCKO-BMC mice, CCL3 and CXCL2 were significantly heightened in the BAL compared to WT-BMC mice along with IL-2 although not significantly (Figure 3.16A). In the IL-17RAKO-BMC

Figure 3.16 Loss of IL-17RA and IL-17RC in the tissue stromal cells causes a skewed cytokine profile in the lungs upon respiratory *Cm* infection. The BAL was obtained from the *Cm*-infected mice at 3 and 5 days post infection and the cytokine and chemokines levels were measured by a Luminex assay. Mediators that were not detectable in the assay are not shown. The cytokines or chemokines that showed an elevated trend in IL-17RCKO-BMC mice at day 5 post infection (A), elevated trend in IL-17RAKO-BMC mice at day 5 post infection (B) or elevated trend in both IL-17-RAKO-BMC and IL-17RCKO-BMC mice at day 5 post infection (C) are shown. The measurement for non-infected WT BMC mice BAL sample is not shown due to undetectable levels. Data are from 2 pooled experiments for day 3 with WT-BMC n=8, IL-17RAKO-BMC n=8, and IL-17RCKO-BMC n=7 mice, one experiment for day 5 with WT-BMC n=5, IL-17RAKO-BMC n=4, and IL-17RCKO-BMC n=7 mice. Data are graphed as mean±SEM. *$p<0.05$, **$p<0.01$ using one-way ANOVA per time point.

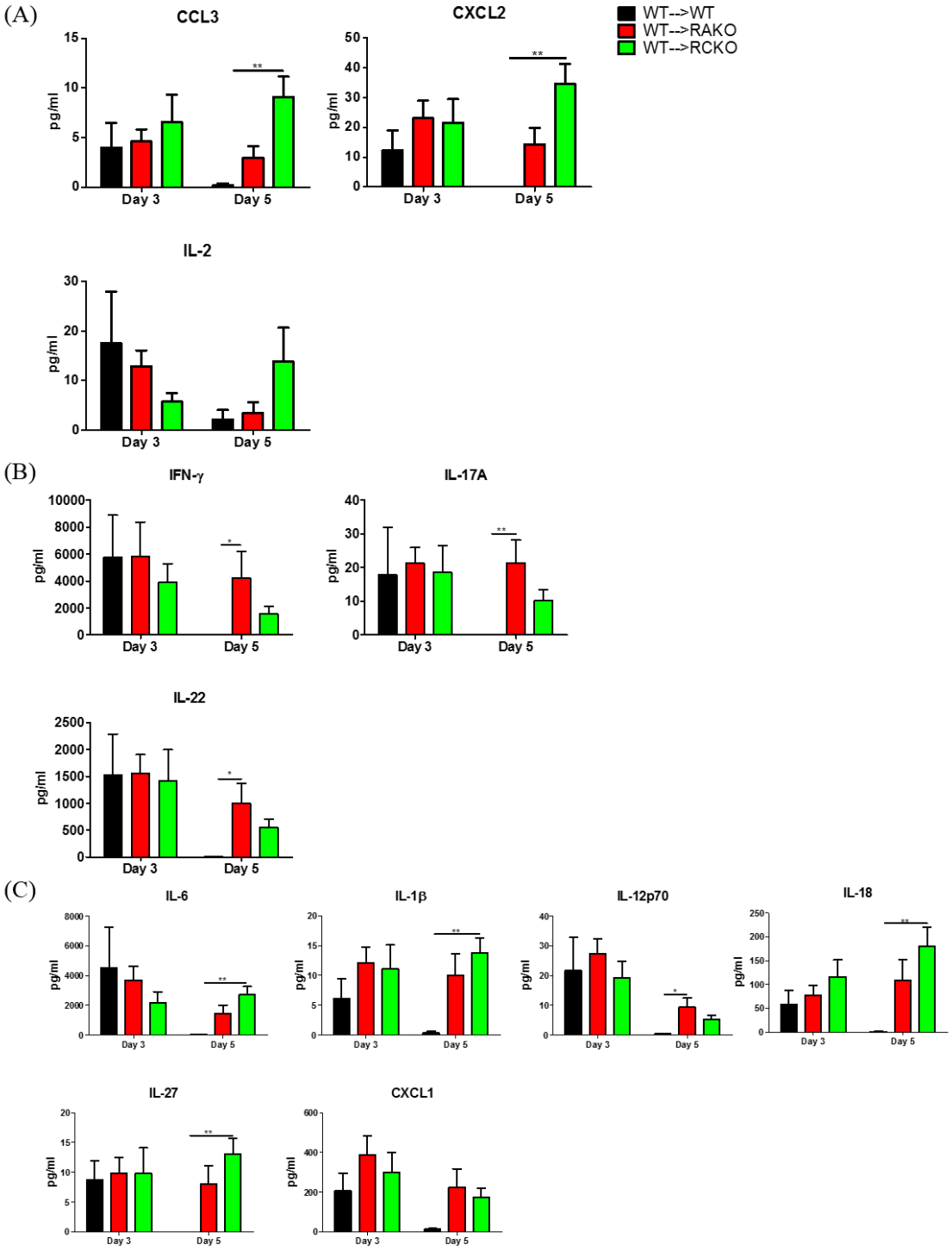
(A)
CCL3
CXCL2
WT-->WT
WT-->RAKO
WT-->RCKO
pg/ml
Day 3
Day 5
IL-2
(B)
IFN-γ
IL-17A
IL-22
(C)
IL-6
IL-1β
IL-12p70
IL-18
IL-27
CXCL1

mice, IL-22, IL-17A, and IFN-γ were significantly heightened in the BAL compared to WT-BMC mice (Figure 3.16B). The cytokines and chemokines in the lungs that appeared to be comparable between IL-17RAKO-BMC and IL-17RCKO-BMC mice were IL-1β, IL-12p70, IL-27, IL-18, IL-6, and CXCL1 (Figure 3.16C). Notably, the cytokine and chemokine levels in the BAL were not significantly different between IL-17RAKO-BMC and IL-17RCKO-BMC mice (Figure 3.16A-C).

Next we wondered whether the expression of IL-17C and IL-17E and their corresponding receptor subunits were altered in the lung during *Cm* infection to drive the differential immune responses. Lung expression of IL-17C mRNA was reduced in *Cm*-infected IL-17RCKO mice but expression levels of IL-17E, IL-17RB, and IL-17RE were comparable to the WT mice (Figure 3.17). Overall, these data indicate that loss of IL-17RA and IL-17RC in the tissue structure cells causes a differential cytokine/chemokine response in the lung upon respiratory *Cm* infection. However, the immune mechanisms whereby differential adaptive immune responses are triggered in IL-17RAKO-BMC and IL-17RCKO-BMC mice remain unclear.

3.4.5 Type 17, but not type 1, immune responses in the draining lymph node of WT-BMC, IL-17RAKO-BMC, and IL-17RCKO-BMC mice were comparable

Next, we checked whether loss of IL-17RA or IL-17RC in the tissue stromal cells would alter the type 1 responses in the local draining lymph node during respiratory *Cm* infection. ICCS for IFN-γ was performed on MLN cells to distinguish between IFN-γ-producing CD4+ and CD8+ T cells. The frequency of IFN-γ-producing CD4+ and CD8+ T cells in the lymph node were not different between WT-BMC, IL-17RAKO-BMC, and IL-17RCKO-BMC mice except for the heightened frequency of IFN-γ-producing CD8+

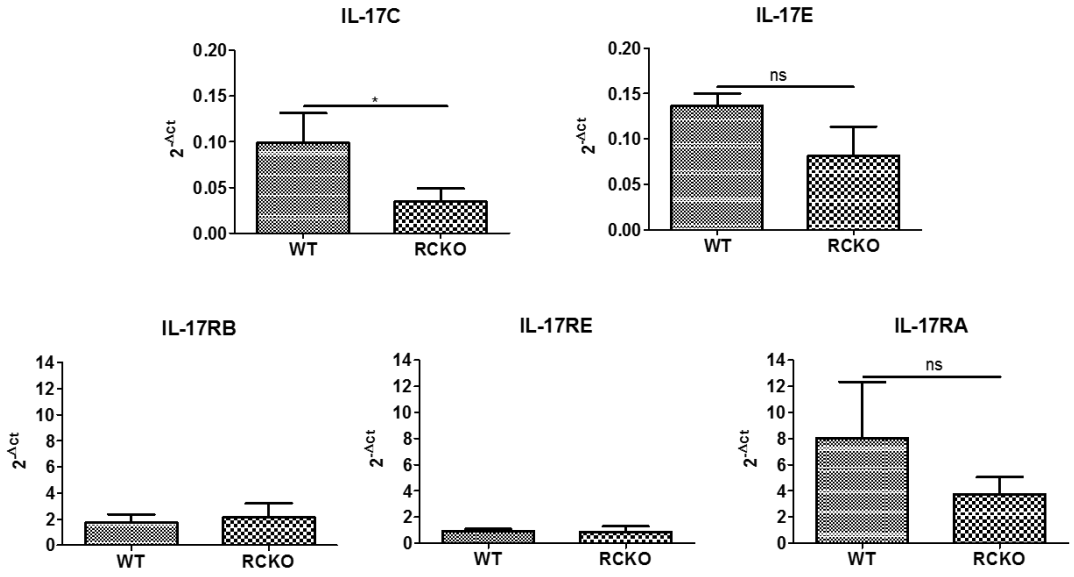

Figure 3.17 IL-17C expression in the lung is reduced in IL-17RCKO mice during *Cm* infection. The lung was extracted from intranasal *Cm*-infected (4,000 IFU) WT and IL-17RC knockout mice at 5 days post infection and then processed for mRNA extraction. The lung tissue was placed in tissue lysis buffer and then homogenized to break up the tissue. mRNA was extracted from the sample and subsequent RT-PCR and qPCR was performed to measure the expression level of IL-17C, IL-17E, IL-17RB, IL-17RE, and IL-17RA calculated from the Ct value of the GAPDH housekeeping gene ($2^{-\Delta Ct}$). Data are from one experiment with n=3 mice for each strain and graphed as mean±SD. *$p<0.05$ using two-tailed Student's *t* test.

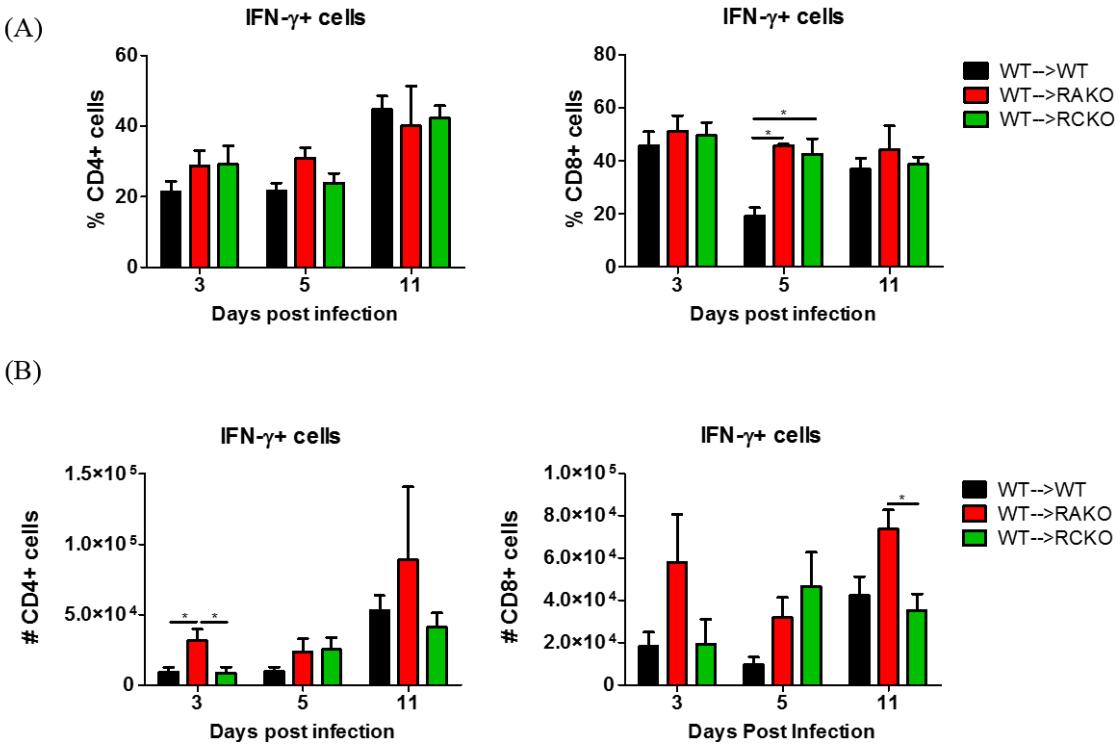

Figure 3.18 The type 1 response in the local draining lymph node is heightened in IL-17RAKO-BMC mice at some time points during *Cm* infection. WT-BMC, IL-17RAKO-BMC, or IL-17RCKO-BMC mice were infected intranasally with 4,000 IFU of *Cm*. The mediastinal lymph node was dissected from all of the mice and then processed for cell isolation. The cells were stained by ICCS for IFN-γ and surface stained for CD4 and CD8 T cell markers. The frequency (A) and total number (B) of CD4+ and CD8+ IFN-γ-producing cells are shown for each time point. Data are from 2 pooled experiments for day 3 with WT-BMC n=7, IL-17RAKO-BMC n=5, IL-17RCKO-BMC n=6 mice, one experiment for day 5 with WT-BMC n=5, IL-17RAKO-BMC n=3, IL-17RCKO-BMC n=7 mice, one experiment for day 11 with WT-BMC n=5, IL-17RAKO-BMC n=3, IL-17RCKO-BMC n=5 mice. Data are graphed as mean±SEM. *$p<0.05$ using one-way ANOVA per time point.

cells at day 5 p.i. in both KO-BMC mice compared to WT-BMC mice (Figure 3.18A). Also, the number of IFN-γ-producing CD4+ and CD8+ T cells in the lymph node were not different between all strains of chimeric mice except at day 3 and 11 p.i. (Figure 3.18B). IL-17RAKO-BMC mice had a significantly higher number of IFN-γ-producing CD4+ T cells compared to WT-BMC and IL-17RCKO-BMC mice at day 3 p.i. (Figure 3.18B). Also, IL-17RAKO-BMC mice had significantly higher number of IFN-γ-producing CD8+ cells compared to WT-BMC mice at day 11 p.i. (Figure 3.18B). This data suggests that loss of IL-17RA in the tissue stromal cells do not alter the Th1 or Tc1 responses in the local draining lymph node to a large extent upon respiratory *Cm* infection but may have an effect at some time points during infection.

Furthermore, we checked whether loss of IL-17RA or IL-17RC in the tissue stromal cells would alter the type 17 responses in the local draining lymph node during respiratory *Cm* infection. ICCS for IL-17A was performed on mediastinal lymph node cells to distinguish between IL-17A-producing CD4+ or CD4- cells. The frequency and number of IL-17A-producing CD4+ and CD4- cells in the lymph node was comparable between WT-BMC, IL-17RAKO-BMC, IL-17RCKO-BMC mice (Figure 3.19A and B). However, there was a trend towards a heightened number of IL-17A-producing CD4+ and CD4- cells at day 3 p.i. (Figure 3.19B). These data showed that loss of IL-17RA or IL-17RC in the tissue stromal cells results in comparable type 17 responses to WT-BMC mice in the local draining lymph node upon respiratory *Cm* infection.

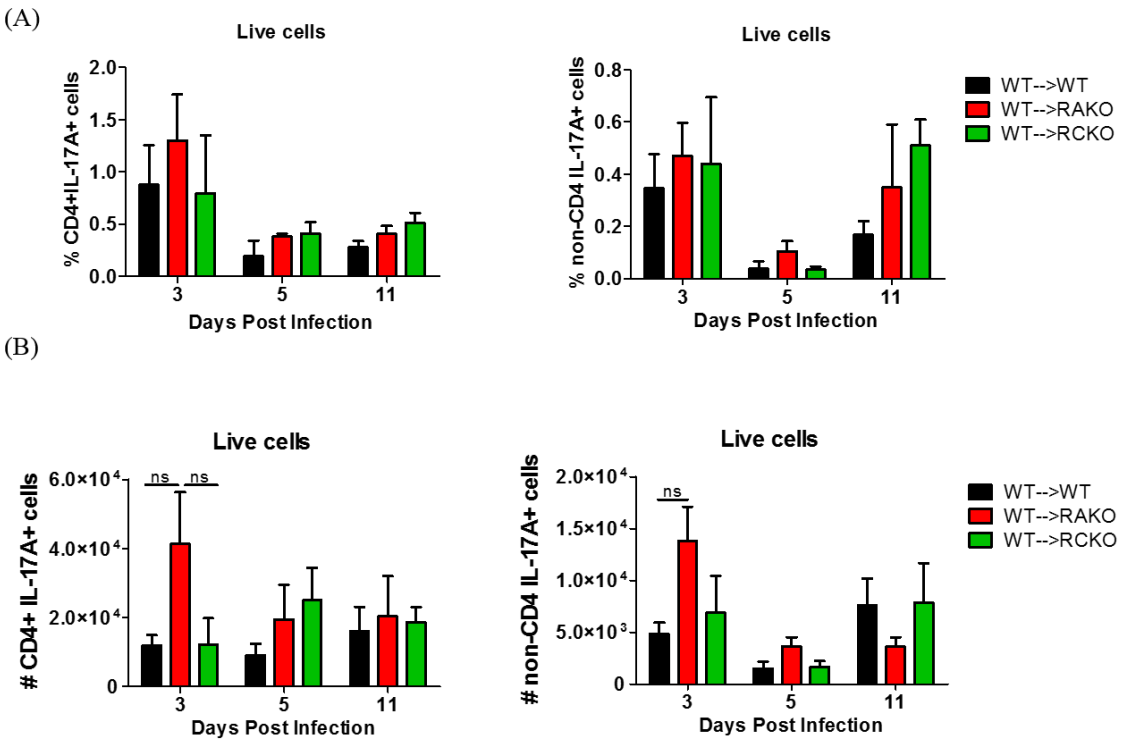

Figure 3.19 The type 17 response in the local draining lymph node is comparable between WT-BMC, IL-17RAKO-BMC, and IL-17RCKO-BMC mice at during *Cm* infection. WT-BMC, IL-17RAKO-BMC, or IL-17RCKO-BMC mice were infected intranasally with 4,000 IFU of *Cm*. Frequency and total number of IL-17A+ cells among CD4+ and CD4- mediastinal lymph node cells was determined by ICCS. For each time point, the frequency (A) and total number (B) of CD4+IL-17A+ and CD4-IL-17A+ cells are shown. Data are from 2 pooled experiments for day 3 with WT-BMC n=7, IL-17RAKO-BMC n=5, IL-17RCKO-BMC n=6 mice, one experiment for day 5 with WT-BMC n=5, IL-17RAKO-BMC n=3, IL-17RCKO-BMC n=7 mice, one experiment for day 11 with WT-BMC n=5, IL-17RAKO-BMC n=3, IL-17RCKO-BMC n=5 mice. Data are graphed as mean±SEM with one-way ANOVA statistical analysis per time point.

Figure 3.20 Characterization of clinical disease, type 1, and type 17 response to *Cm* infection in IL-17RA and IL-17RC whole knockout mice. WT, IL-17RAKO, and IL-17RCKO mice were infected with intranasal *Cm (*4,000 IFU) and the body weight of the mice were measured daily to calculate the body weight change post infection relative to day 0 up to day 6 and 12 (A). Body weight change graphs are from 2 experiments with n=5-6 for each strain per time point. Data are graphed as mean±SEM. *$p<0.05$ compared to WT using two-way ANOVA. The lung was obtained and processed for cell isolation and ICCS for IFN-γ and surface marker staining of CD4 and CD8 (B) or IL-17A with CD4 (C). FACS data are from one experiment with 3-4 mice per strain per time point. Data are graphed as mean±SD. *$p\leq0.05$ using one-way ANOVA per time point.

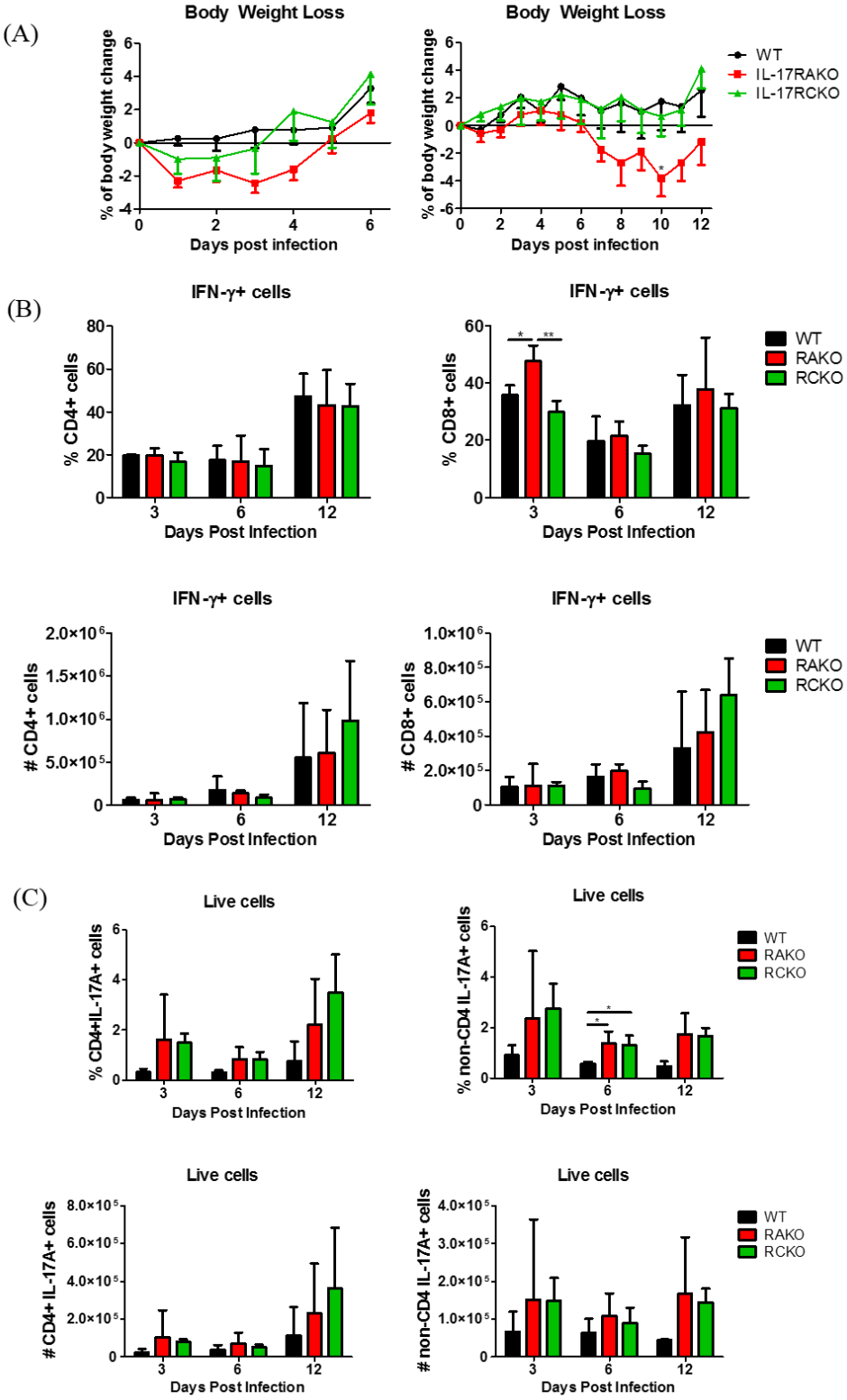
(A)
Body Weight Loss
% of body weight change
Days post infection
WT
IL-17RAKO
IL-17RCKO
(B)
IFN-γ+ cells
% CD4+ cells
% CD8+ cells
# CD4+ cells
# CD8+ cells
Days Post Infection
WT
RAKO
RCKO
(C)
Live cells
% CD4+IL-17A+ cells
% non-CD4 IL-17A+ cells
# CD4+ IL-17A+ cells
# non-CD4 IL-17A+ cells
Days Post Infection
WT
RAKO
RCKO

3.5 Characterization of clinical disease, type 1, and type 17 responses to *Cm* infection in IL-17RA and IL-17RC knockout mice

During my study, I also examined the outcome of respiratory *Cm* infection in IL-17RAKO and IL-17RCKO mice. Upon respiratory *Cm* infection, IL-17RAKO displayed the greatest weight loss trend compared to WT and IL-17RCKO mice up to 6 and 12 days post infection (Figure 3.20A). Intriguingly, the body weight loss trend was comparable between the WT and IL-17RCKO upon *Cm* infection (Figure 3.20A). Though only significant at day 10 p.i., IL-17RAKO mice had greater body weight loss trend compared to WT mice (Figure 3.20A). In addition, the overall weight loss of all mice in these experiments was approximately -2% of the original weight. In comparison, *Cm*-infected BMC mice that survived up to day 11 p.i. had approximately lost 5-10% of their original weight (Figure 3.7A). Overall, the body weight loss trends in these experiments were different than the trends in Figure 3.7A, with BMC-mice. This observation may be due to a different batch of *Cm* that was utilized for the earlier experiments in Figure 3.20. However, a difference in body weight loss in WT, IL-17RAKO, and IL-17RCKO mice was still observed upon respiratory *Cm* infection.

The type 1 response in the lungs of these mice was examined by ICCS for IFN-γ. The percentage and total cell number of IFN-γ-producing Th1 cells and Tc1 cells were not significantly different between WT, IL-17RAKO, and IL-17RCKO mice except for day 3 p.i. where the frequency of IFN-γ-producing CD8+ cells was heightened in IL-17RAKO mice compared to WT and IL-17RCKO (Figure 3.20B).

The IL-17A-producing cell profile was also examined by ICCS. The frequency and total cell number of IL-17A-producing CD4+ T cells and non CD4 cells were not significantly different between WT, IL-17RAKO, and IL-17RCKO mice except for day 5

p.i. where the frequency of IL-17A-producing non-CD4 cells were heightened in IL-17RAKO and IL-17RCKO mice compared to WT mice (Figure 3.20C). Overall, the IL-17RAKO and IL-17RCKO mice had a heightened trend towards type 17 responses compared to WT mice (Figure 3.20C). These results collectively show a contrasting immune profile of the IL-17RA and IL-17RC knockout mice compared to the immune profiles of the IL-17RAKO-BMC and IL-17RCKO-BMC mice during respiratory *Cm* infection.

CHAPTER 4 DISCUSSION

4.1 IL-17A does not directly reduce *Cm* growth in C57BL/6 or BALB/c MEFs or McCoy cells and does not have an additive inhibitory effect with IFN-γ

The objective of this study was to examine the role of IL-17RA and IL-17RC in the tissue stromal cells in the host defense against *Cm* infection. We hypothesized that IL-17RA and IL-17RC in tissue stromal cells may have differential roles in controlling *Cm* infection and subsequently shaping the host immune responses. The IL-17A signaling pathway is of interest because of the importance of IL-17A/IL-17R in protective and immunopathological host responses in *Chlamydia* infection (81, 82, 198, 204).

Regulation of epithelial immunity has been shown to be executed by IL-17 family cytokine members (166). In particular, IL-17A can directly target epithelial cells to induce various antimicrobial responses against pathogens (166). IL-17A has been shown to have no direct effect on *Cm* growth *in vitro* and instead enhances the production of proinflammatory cytokines and chemokines suggestive of indirect anti-chlamydial effects (32). The authors found that *Cm* growth in a mouse L929 cell line and mouse primary lung fibroblasts were not affected by exogenous IL-17A stimulation by measuring *Cm* levels with the IFU assay (32). In the current study, we found that IL-17A had no inhibitory effect on *Cm* growth in C57BL/6 or BALB MEFs or McCoy cells, by measuring *Cm* levels in the culture supernatants via qPCR. Although IL-17A production in the lung is greater in BALB/c mice compared to C57BL/7 mice upon respiratory *Cm* infection (81), the expression level of the IL-17A receptor is not known in BALB/c and C57BL/6 MEFs and needs to be confirmed.

In contrast to the studies by Zhang *et al.* (32), IL-17A has recently been shown to suppress growth of *Cm in vitro* by synergizing with IFN-γ to upregulate iNOS and NO in

the murine lung epithelial and macrophage cell lines TC-1 and RAW264.7, respectively (129). The results in our studies showed that IL-17A did not exert further inhibitory effects on *Cm* growth with the addition of IFN-γ to C57BL/6 and BALB/c primary MEFs and McCoy cells even though mouse fibroblasts upregulate iNOS (205). These results are in contrast to the study by Zhang *et al.* (129) which showed an important inhibitory role of IL-17A/IFN-γ on chlamydial growth *in vitro* (129). Our data reveal that IFN-γ alone had inhibitory effects on *Cm* growth in C57BL/6 or BALB/c MEFs when the identical concentration of IFN-γ (20 ng/ml) as the previous study was used (129). MEFs have been shown to undergo L-arginine/glycolysis-dependent cell death by treatment with low doses of IFN-γ (10 U/ml) in combination with LPS (206). However, in the current study, *Cm* infection alone enhanced morphological structure changes in the cells while MEFs with *Cm* infection and IFN-γ treatment retained their original cell structure. Another study has shown that *Cm* growth was less inhibited by IFN-γ in cultured *ex vivo* macrophages from C3H/HeN mice compared to C57BL/6 mice (207). McCoy cells which are a type of mouse fibroblast cell line, has been used to propagate different strains of *Chlamydia* as it is susceptible to growth of the bacteria (201). Confirming the inhibitory role of IFN-γ in *Cm*-infected C57BL/6 and BALB/c MEFs, IFN-γ stimulation of *Cm*-infected parental McCoy cells significantly reduced *Cm* growth. Also, IL-17A treatment of *Cm*-infected WT McCoy cells did not affect bacterial growth compared to *Cm* infection alone (Figure 3.3B). This data, together with the MEF results, confirm that exogenous IL-17A does not have a direct suppressive effect on *Cm* growth and does not have an effect on the inhibitory effect IFN-γ in multiple strains of primary MEFs and a fibroblast cell line. However, *Cm*-infected IL-17RAKO MEFs had significantly greater bacterial burden than *Cm*-infected WT MEFs. IL-17RCKO MEFs also had heightened *Cm* growth compared to *Cm*-infected WT MEFs

though this was not significant. This suggests that although exogenous IL-17A has no effect on *Cm* growth in fibroblasts, endogenous IL-17A and basal level IL-17A signaling is required in controlling *Cm* replication.

Similar to IL-17A, IL-17C directly targets epithelial cells to induce various responses against pathogens by the induction of similar cytokines, chemokines, and antimicrobial peptides (208). In contrast, IL-17E mainly acts on leukocytes and induces type 2 immunity for the protection against parasites (166). Even though different immune responses are induced, IL-17C and IL-17E both utilize IL-17RA and therefore share the same receptor subunit as IL-17A (154). Although, the role of IL-17A on the growth of *Chlamydia* has been studied, the role of IL-17C or IL-17E in *Chlamydia* infection is unclear. There are studies demonstrating induction of IL-17E from lung epithelial cells during *Cm* and *C. pneumoniae* lung infection (209, 210) particularly in high amounts during re-infection with *Cm* (210). In the current study, we found that IL-17C and IL-17E did not inhibit *Cm* growth in C57BL/6 or BALB/c MEFs.

With a closer examination at the cytokines and chemokine profile of *Cm*-infected WT C57BL/6 MEFs, we showed a significant induction of IL-17A from the infected cells and some cytokines, particularly IL-15/IL-15R, IL-1α, IL-1β, TSLP, and IL-18, which were induced by *Cm* in a dose-dependent manner (Figure 3.5C). Although IL-17A was significantly induced in *Cm*-infected MEFs compared to non-infected MEFs, the level of IL-17A was very low. This indicates that *Cm*-infected MEFs are not a particularly major producer of IL-17A *in vitro*. Additionally, these results showed that *Cm* induces specific cytokine/chemokine responses to potentially modulate the innate and adaptive immune responses in the tissue structure cells. Given that potent cytokine and chemokine production was observed in primary MEFs upon *Cm* infection, we hypothesized that there could be a

skewed cytokine profile in *Cm*-infected IL-17RAKO and IL-17RCKO MEFs. Indeed, we observed significantly higher levels of CXCL1, TNF, and IL-6 in IL-17RAKO MEFs, and to a lesser extent in IL-17RCKO MEFs, compared to WT MEFs. Normally, IL-6 and CXCL1 are proinflammatory mediators that are highly produced upon IL-17A signaling (166), whereas TNF is cytokine that is able to synergize with IL-17A to amplify proinflammatory responses from tissue structure cells (166, 211, 212). We have shown that without IL-17RA or IL-17RC in MEFs, the proinflammatory response to *Cm* is heightened compared to *Cm*-infected WT MEFs. A possible mechanism for this outcome could be reduced feedback inhibitory pathways due to decreased IL-17A signaling, therefore leading to heightened inflammatory pathways (213). A loss of the IL-17A receptors in MEFs heightens the proinflammatory cytokine response upon *Cm* infection suggesting an anti-inflammatory role of IL-17RA and IL-17RC. However, whether this heightened immune response in tissue stromal cells could enhance the host resistance against *Cm* infection or promote detrimental responses needed further investigation.

4.2 IL-17RA and IL-17RC in the tissue stromal cells control respiratory *Cm* infection *in vivo*

To investigate the role of IL-17RA and IL-17RC in tissue stromal cells in the response against *Cm* infection *in vivo,* we established an intranasal *Cm* infection in WT-BMC, IL-17RAKO-BMC, and IL-17RCKO-BMC mice. Loss of IL-17RA or IL-17RC in non-hematopoietic cells resulted in heightened bacterial replication in the lungs. At the earliest time point of day 3 p.i., *Cm* amounts were significantly greater in IL-17RAKO-BMC and IL-17RCKO-BMC mice compared to WT-BMC mice indicating that there was increased bacterial burden during early infection in the KO-BMC mice. A shorter time

point of day 1 or 2 p.i. would confirm this result. Also, it appears that IL-17RAKO-BMC and IL-17RCKO-BMC mice had impaired bacterial clearance by day 11 p.i. while WT-BMC mice were able to reduce their bacterial load from day 3 to 11 p.i., although not significantly (Figure 3.7B). A longer time point of *Cm* infection would confirm if the KO chimeric mice have impaired bacterial clearance compared to WT-BMC mice.

A previous report with *C. trachomatis* genital tract infection in mice found dissemination of bacteria to the local draining lymph nodes, peritoneal cavity, spleen, liver, kidneys, and lungs (203). Another study with *C. pneumoniae* infection showed detection of bacteria in the thymus, spleen, and lymph nodes (214). Interestingly, we found some dissemination in the liver and kidney but no differences between the strains of mice. A longer time point of *Cm* infection may be required to confirm if there are differences in bacterial burden in these organs between the strains of chimeric mice. Genital tract *Cm* infection of WT C57BL/6 mice showed minimal dissemination to other organs from day 10 to 50 p.i. whereas IFN-γ KO or C57BL/6 severe combined immunodeficiency (SCID) mice had greater bacterial dissemination peaking at day 23 to 38 p.i. (203).

In our respiratory *Cm* infection model, IL-17RAKO-BMC and IL-17RCKO-BMC mice had progressively greater loss in body weight compared to WT-BMC mice by day 11 p.i. (Figure 3.7A). We observed a correlation between greater body weight loss in the mice, heightened cellular infiltration, and reduced alveolar space in the lungs during respiratory *Cm* infection. IL-17RAKO-BMC and IL-17RCKO-BMC mice displayed heightened intensity of inflammation in the lung with the majority of the infiltrating cells being mononuclear cells. Although neutrophils have a prominent role in the immunopathology of the lung during infection with intracellular *Cm* (81, 82), we observed minimal neutrophil infiltration in the lung of IL-17RAKO-BMC and IL-17RCKO-BMC mice. However, this

observation was based on H & E staining of the lung and would need to be confirmed with FACS staining for neutrophils especially during early infection. Early differences in the neutrophil recruitment and activity in the IL-17RAKO-BMC and IL-17RCKO-BMC mice could lead to the subsequent adaptive immune responses. With a trend of greater CXCL1 production in the BAL of the KO-BMC mice (Figure 3.16C) and heightened Th17 responses (Figure 3.11), we would expect greater neutrophils in the lung of these mice during early *Cm* infection. Nonetheless, the overall observations are consistent with the *in vitro* results whereby IL-17RAKO and IL-17RCKO MEFs produced more proinflammatory mediators after *Cm* infection. Our results suggest a role of IL-17RA and IL-17RC in tissue stromal cells in controlling and clearing *Cm* and the subsequent proinflammatory response at the site of infection.

There have been many reports associating *Chlamydia* infection with apoptosis and other forms of cell death as an innate response to infection (72). As a counter-response, *Chlamydia* have developed mechanisms to overcome this form of immunity by dysregulating the cell death responses which in turn can enhance in persistence of infection and heighten the pathology (68, 215, 216). In the current study, we showed that IL-17RCKO-BMC, but not IL-17RAKO-BMC mice, had greater apoptosis compared to WT-BMC mice. A previous study showed that specific overexpression of IL-17RC protects prostate cancer cells lines from TNF-induced apoptosis (217). Therefore, IL-17RC may interact with the apoptosis pathway and suggests an anti-apoptotic role for IL-17RC signaling which warrants further investigation during *Chlamydia* infection. With greater apoptosis in IL-17RCKO-BMC mice, heightened secondary necrosis in these mice was also possible due to reduced apoptotic body clearance. The identification of apoptotic secondary necrosis is characterized by the co-existence of apoptotic changes like nuclear

fragmentation and/or chromatin condensation and necrotic changes like damaged cytoplasmic membrane (218). Also, cells undergoing secondary necrosis, unlike primary necrotic cells, release activated caspase-3 (219). Therefore, it is important to distinguish if there are any differences in primary necrosis, apoptosis, or secondary necrosis between the KO-BMC mice compared to WT-BMC mice after *Cm* infection.

Necrosis and apoptosis are known to have immune modulatory roles in both innate and adaptive immunity. For example, macrophages are able to engulf apoptotic cells by phagocytosis and this process actively inhibits the production of proinflammatory cytokines like IL-1β and TNF (220). Also, DCs can capture apoptotic cells and cross-present antigen derived from the internalized dying cell to CD8+ T cells (221, 222). There is a study showing that necrotic, but not apoptotic death allows passive release of HSPs that are inflammatory and stimulate macrophages to secrete cytokines (223). In turn, the HSPs induce expression of antigen-presenting and co-stimulatory molecules on DCs and activate the NFκB pathway (223). Therefore, apoptosis and necrosis pathways may be important in shaping the host immune responses and need to be further elucidated in our current *Cm* infection model. In the current study, the results suggest that loss of IL-17RA and IL-17RC in the tissue stromal cells have a differential role in the control of apoptosis or clearance in apoptotic bodies in the lung during respiratory *Cm* infection.

With fluorescent TUNEL/DAPI staining alone, it was unclear whether the cells undergoing apoptosis were also infected with *Cm*. To achieve chlamydial-infected cell death readouts, one could utilize the *C. trachomatis* strain transformed with a plasmid encoding the green fluorescent protein (GFP) (224) in which the EBs can be detected by anti-GFP antibody. This strain of *Chlamydia* could then be also stained for fluorescent TUNEL and analyzed for chlamydial cell death.

Collectively, these results show a crucial role for IL-17RA and IL-17RC in the tissue stromal cells in controlling *Cm* replication leading to subsequent anti-inflammatory responses at the infected tissue site. Respiratory *Cm* infection in IL-17RAKO-BMC and IL-17RCKO-BMC mice resulted in greater body weight loss, heightened bacterial burden in the lungs, higher levels of cellular infiltration in the infected tissue, and increased apoptosis in the lung.

4.3 IL-17RC and IL-17RA in the tissue stromal cells shape the type 1 and type 17 responses, respectively, in the lung during respiratory *Cm* infection *in vivo*

We next hypothesized that loss of IL-17RA or IL-17RC in the tissue stromal cells would modulate the adaptive immune responses *in vivo* upon respiratory *Cm* infection. It is very well established that the Th1 response is crucial in resolving *Chlamydia* infection (198, 225–227). We sought to examine the type 1 responses in IL-17RAKO-BMC and IL-17RCKO-BMC mice compared to WT-BMC mice during *Cm* infection. With a loss of IL-17RC in the tissue structure cells, mice had markedly higher Th1 and Tc1 responses in the lung compared to WT-BMC and IL-17RAKO-BMC mice. However, even with a heightened type 1 response, bacterial burden in the lung of IL-17RCKO-BMC mice were not reduced and was comparable to IL-17RAKO-BMC mice. Notably, the lower Th1 and Tc1 responses in the lung of WT-BMC mice could be the result of reduced initial chlamydial levels in the lung compared to IL-17RAKO-BMC and IL-17RCKO-BMC mice. In contrast, with heightened bacterial levels in the lung of IL-17RCKO-BMC mice, a type 1 adaptive immune response was induced. Therefore, these results show that IL-17RC in the tissue stromal cells is not required to induce a type 1 response in the lung during *Cm* infection. Intriguingly, IL-17RAKO-BMC mice, which had comparable levels of *Cm* in the

lung to IL-17RCKO-BMC mice, were not able to induce a type 1 response to the same extent. Although IL-17RCKO-BMC mice displayed a heightened type 1 response in the lung, *Cm* was not cleared and the mice did not seem to show reduced clinical disease. These observations could be the result of other host immune responses, like heightened Th17 responses or greater apoptosis, which were exacerbated and could be detrimental to the host. It was unclear whether the heightened Th1 and Tc1 response in the lung would be protective for the IL-17RCKO-BMC mice over a longer course of infection. Excessive IL-12 and IFN-γ contributes to poor memory CD8+ T cell development during *C. trachomatis* infection of mice (228). Since CD8+ T cells are also an important adaptive component (228, 229) it appears that excessive IFN-γ could potentially be detrimental during *Chlamydia* infection in that this may dysregulate subsequent memory T cell responses. Regardless, *Cm* levels in the IL-17RAKO-BMC and IL-17RCKO-BMC mice were comparable in our study despite having differential type 1 responses in the lung. Also, the IFN-γ responses in the local draining lymph node were comparable among all strains of mice except for the heightened frequency or number of IFN-γ-producing CD4+ or CD8+ cells at some time points. This indicates that loss of IL-17RA or IL-17RC in the tissue stromal cells has no effect on induction of type 1 responses in the lymph node. To determine whether the T cells in the lung and lymph node were antigen-specific or accumulated due to bystander recruitment, these results can be compared to the basal level of these T cells in naïve mice.

With the importance of IL-17/Th17 responses in *Chlamydia* infection (82, 198), it was imperative that we examined the type 17 responses in *Cm*-infected IL-17RAKO-BMC and IL-17RCKO-BMC mice. Previous reports have showed that IL-17RA-deficient mice displayed exacerbated Th17 responses (189, 230). A recent study showed that conditional

deletion of IL-17RA in the enteric epithelium resulted in dysregulated segmented filamentous bacterial growth and uncontrolled Th17 responses (231). In agreement with the previous study, we observed that IL-17A production from conventional Th17 cells was elevated in IL-17RAKO-BMC and IL-17RCKO-BMC mice compared to WT-BMC mice at 5 and 11 days p.i. In contrast, during earlier stages of infection, IL-17RAKO-BMC mice had greater amounts of IL-17A-producing Th17 cells and also IL-17A-producing non-CD4 cells. The authors in the previous study showed that expansion of Th17 cells in IL-17RA-deficient mice were not T cell intrinsic and instead were expanded due to commensal dysbiosis (231). Depletion of gram-positive bacteria, including segmented filamentous bacteria, by oral vancomycin in IL-17RA-deficient mice reduced the amount of Th17 cells (231). Also in agreement with our results, intestinal-epithelial-specific expression of IL-17RA or IL-17RC regulated bacterial colonization in the intestine (231). However, the recent study did not investigate additional immune responses, especially ILC3s, which may be expanded due to loss of IL-17RA. In our study, we observed that the frequency of IL-17A-producing non-CD4 cells was comparable between naïve WT, IL-17RAKO, and IL-17RCKO mice, suggesting that these cells were induced after *Cm* infection. Only a minor population of IL-17A-producing non CD4 T cells were CD8+ or γδ T cells. Additionally, IL-17RAKO-BMC mice displayed a heightened number of IL-17A production of CD4+ and CD4- cells in the local draining lymph compared to WT-BMC and IL-17RCKO-BMC mice at day 3 p.i. This result shows that loss of IL-17RA in the tissue stroma results in greater type 17 responses in the draining lymph node, which is in line with the host responses in the lung. In addition to the finding that tissue stromal IL-17RA and IL-17RC regulates bacterial replication and subsequently constrains Th17 responses, our results also suggest that constrain of type 1 responses and ILC17s are also important in the *Cm* infection

model. The authors in the recent study showed that IL-17RA in the intestine control segmented filamentous bacterial growth by regulating expression of α-defensins (231). Therefore, it would be worthwhile to investigate whether IL-17RA or IL-17RC have a role in regulating expression of antimicrobial peptides in the lung.

In line with the immune responses in the lung, HK-*Cm* stimulation induced IL-17A and IFN-γ production in IL-17RAKO-BMC and IL-17RCKO-BMC splenocyte antigen-recall cultures respectively. However, re-stimulated splenocytes from IL-17RCKO-BMC mice produced comparable levels of IL-17A to WT-BMC cells. In the lung, IL-17A-producing CD4+ cells were heightened in IL-17RCKO-BMC mice compared to WT-BMC mice. It is not known what specific cells from the spleen were being stimulated by *Cm*. Splenocytes from naïve mice could be stimulated with HK-*Cm* to investigate whether the cells in our experiments were responding to HK-*Cm* via TCR or a PRR. In naïve splenocytes, we would expect to observe a response via PRR instead of via the TCR. Additionally, HK-*Cm* induced the lowest IL-13 production in IL-17RCKO-BMC splenocyte cultures compared to IL-17RAKO-BMC and WT-BMC cells. Collectively, the immune profiles in the lung and splenocytes show that IL-17RA and IL-17RC in tissue stromal cells have differential impacts on shaping the adaptive immune responses.

In addition to some discrepancies observed in the immune response from lung, spleen, and lymph node, the cytokine pattern was different in the BAL samples and from MEF *in vitro* cultures upon *Cm* infection. Differences in the cytokine and chemokine production in these two systems were not surprising. Fibroblasts are unlikely to be the main cells that are infected with *Cm in vivo* whereas epithelial cells are likely to be the first cells to be infected in mice. One benefit for analyzing the cytokine/chemokine profile from *Cm*-infected MEFs is that the mediators produced are strictly coming from one isolated cell

type without mediators that may be produced from recruited cells *in vivo*. It is important to expand our *in vitro Cm* experiments to mouse lung epithelial cell lines to confirm our MEF results. In a previous study, proinflammatory cytokine induction was analyzed in *Cm*-infected mouse oviduct epithelial cells (232). *Cm*-infection-associated induction of TNF, IL-6, IFN-β, IL-12p35, IL-12p40, IL-1α, IFN-α, CXCL2, and CCL1 were shown (232). *Cm*-infection-associated upregulation of IL-7, IL-15, IL-3, CCL5, CXCL10, and CCL2 were shown as well (232). In our BAL data, we saw some cytokines that remained elevated in the IL-17RCKO-BMC mice compared to WT-BMC mice including CXCL2, although IL-1β was elevated in our results and was not shown in the previous study. Additionally, IL-12p70 remained heightened in the IL-17RAKO-BMC mice compare to WT-BMC mice which was induced in epithelial cells in the previous study. Intriguingly, it was surprising to see that IFN-γ, IL-17A, and IL-22 remained heightened in IL-17RAKO-BMC mice compared to WT-BMC. This suggests that the cytokines produced in the lung airway were not cleared despite a heightened type 17, and not type 1, responses in the IL-17RAKO-BMC mice. IL-17C mRNA, but not IL-17RE mRNA, expression in the lung of intranasal *Cm*-infected IL-17RCKO mice was reduced compared to WT mice at day 5 p.i. In a previous study, it has been shown that IL-17C promotes Th17 responses via IL-17RE in an experimental autoimmune encephalomyelitis model (233). However, we did not observe dysregulated Th17 responses in the intact IL-17RCKO mice compared to WT mice (Figure 3.20C). Therefore, these experiments need to be reproduced in the chimeric mice, especially in IL-17RAKO-BMC mice, to confirm if IL-17C has a role in Th17 responses during *Cm* infection *in vivo*. We would expect to observe a greater impact on IL-17C expression with greater Th17 responses in tissue stroma-specific knockdown of IL-17RA due to the important role of IL-17C in these tissues (177).

Together, these results show that despite having comparable chlamydial replication in the lungs, IL-17RAKO-BMC and IL-17RCKO-BMC mice displayed differential host responses upon respiratory *Cm* infection. This observation suggests that IL-17RA and IL-17RC in the tissue stromal cells have a differential role in modulating the type 1 and type 17 responses in the lung and is independent on *Cm* replication. With the apoptosis and cytokine/chemokine profile data and the differences observed in the IL-17RAKO-BMC and IL-17RCKO-BMC mice, a potential mechanism for the differential adaptive immune responses could be driven by cell death mechanisms and the cytokine environment induced in the lung.

4.4 Respiratory *Cm* infection *in vivo* induces ILC17s in the lung

We hypothesized that the IL-17A-producing non-CD4 cells were possibly innate lymphoid cells, specifically a type of ILC3 that produce IL-17A. We were able to confirm that this population of cells express the transcription factor RORγt, indicative of the RORγt+ ILC, or ILC3s. There are multiple different sub-populations of ILC3s (Figure 1.2) categorized by their cytokine production and phenotypic surface expression markers. Due to overlap between these cells and incompletely defined methods to fully distinguish subpopulations of ILCs, it has proven difficult to characterize these cells. Non-cytotoxic ILCs are known to lack surface expression markers for T cells (CD3), B cells (B220), NK cells (NK1.1 and NKp46), neutrophils (Gr1), macrophages (CD11b), and DCs (CD11c) (99). Additionally, the Lin- population of lung cells were further confirmed to be ILCs with the positive expression of CD127 (α chain of IL-7 receptor). Further, intracellular cytokine staining was performed for IFN-γ and IL-22. Our results showed that the Lin- IL-17A+ cells did not highly express IFN-γ, but strikingly, the majority of Lin- IL-17A+ cells also

express IL-22. This study was the first to identify induction of Lin- IL-17A+IL-22+, or ILC17s, in the lung during respiratory *Cm* infection.

In a *S. pneumoniae* infection model, IL-17A and IL-22 production by ILC3s was also enhanced (99). It has been shown that among total lung ILCs, about 20% are ILC3 with about 10,000 total ILC and 2000 ILC3 at steady state in C57BL/6 mice (99). This is a striking difference to what we observed in our naïve C57BL/6 mice, where approximately 7000-8000 IL-17A-producing non-CD4 cells were present (Figure 3.11C). Future experiments to confirm if these IL-17A-producing non-CD4 cells are ILC3s at basal conditions will be important. Previous studies which examined the presence and function of ILC3 in the lung have been unclear. ILC3 production of IL-22 has been identified in the lung in an experimental model of asthma in mice and has been shown to limit airway inflammation and tissue damage (234). On the other hand, it has also been shown that Lin- cells in the lung that are stimulated by IL-23 do not produce IL-22 so it was unclear whether these are the same population of cells described in the previous study (235). In another study, ILC3s seem to be absent in the lungs of healthy mice (236), which is in contrast to the previous study with *S. pneumoniae* infection (99), but are expanded in a mouse model of obesity-induced asthma in response to NLRP3-dependent production of IL-1β by macrophages (236). In a recent study, ILC3s were shown to promote T-cell-mediated immune responses (237). The authors in this previous study showed that IL-1β stimulation of NCR− ILC3s induced expression of MHC class II and costimulatory molecules (237). These NCR− ILC3s became bona fide APCs as these cells were able to promote OVA-specific CD4+ T cell proliferation *in vivo* (237). Also, T-cell priming, in the presence of antigen, led to a prolonged activation of ILC3s which suggests that upon inflammation, the

interaction of ILC3s and CD4+ T cells contributes to adaptive immunity (237). Taken together, ILC3s and CD4+ T cells may have an important role in linking the innate and adaptive immune responses.

In the current study, it is the first time IL-17RA has been linked to the control of ILC17s in a *Chlamydia* infection model. Together, with previous studies, it is suggested that ILC3s could be expanded in different types of infection and play an important pathogenic role in the airways. Since ILCs can exacerbate inflammation in the tissues and be detrimental to the host (238), we hypothesized that the number of ILC17s in the lung could negatively correlate with the body weight change in infected mice. Indeed, the percentage and number of ILC17s negatively correlated with the body weight change at day 3 p.i. in mice. However, we need to confirm whether the induction of ILC17s have a direct role in causing body weight loss upon *Cm* respiratory infection *in vivo,* or whether the body weight loss was due to other confounding factors upon infection with a coincidental increase of ILC17s. To expand on these experiments, depletion of ILC3s could be achieved in mice upon respiratory *Cm* infection by anti-CD90 in mice, utilizing *Ahr-/-* mice, or reconstitution of bone marrow cells in the recipient chimeric mice with donor cells from RORγt-/- mice. This may suggest whether ILC17s have a crucial impact on disease outcome although it might be difficult to target ILC3s specifically. Interestingly, ILC3s have been shown to be protective in some infection models. During fungal infection with *C. albicans,* antibody depletion of IL-17A-producing-ILCs in recombination-activation gene (RAG)1-deficient mice or ILC deficiency in RORc-/- mice resulted in uncontrolled infection (239).

Loss of IL-17RA during early *Cm* infection caused increased induction of the number of ILC17s in the local draining lymph node although not significantly (Figure 3.19B). It has been shown that T-bet− NKp46− RORγ+ ILCs express MHC class II and can present antigen but act to limit commensal bacteria-specific CD4+ T-cell responses instead of inducing T-cell proliferation (240). Also, the regulation of adaptive immune responses were not dependent on IL-17A, IL-22, or IL-23 (240). The results from this previous study identified RORγt+ ILCs as regulators of intestinal homeostasis via MHC class II interactions with CD4+ T cells which subsequently controlled pathological adaptive immune responses to commensal bacteria (240). Expanding on this previous study, a more recent report showed that RORγt+ ILCs are able to migrate from the intestine to the draining mesenteric lymph node (241). Additionally, the trafficking of RORγ+ ILCs to the lymph node was dependent on CCR7 and created a unique microenvironment within interfollicular spaces of the mucosal draining lymph node (241). However, the RORγt+ ILCs in these previous studies were suggestive of LTi cells and did not distinguish the other subsets of ILC3s. Therefore, further studies on the MLN ILC17s observed in our model might suggest whether these cells trafficked from the lung and whether they were antigen-specific.

We hypothesized that the cytokine response from the tissue stromal cells could be responsible for driving the differential immune responses in IL-17RAKO-BMC mice and IL-17RCKO-BMC mice. Therefore, we assayed an array of cytokines and chemokines in the BAL samples from the lung. In response to pathogens, DCs secrete IL-23 and IL-1β to induce production of IL-17A and IL-22 from ILC3s (242). Surprisingly, IL-1β, but not IL-23, was elevated in the IL-17RAKO-BMC and IL-17RCKO-BMC BAL samples in our

study. IL-23 and IL-7, which are also important cytokines in driving ILC3 activation (243), were also not detected in the BAL. Although these ILC3-activating cytokines were not detected, IL-1β, which also drive the activation of ILC3s (243), was increased in the lung of IL-17RAKO-BMC and IL-17RCKO-BMC mice compared to WT-BMC mice. Due to the induction of other inflammatory cytokines and chemokines, like IL-6, CXCL2, CCL3, CXCL1 (although not significant) indicates an overall proinflammatory response when there is a loss of IL-17RA or IL-17RC expression in the tissue stromal cells. IL-17A and IL-22 were heightened in the IL-17RAKO-BMC compared to WT-BMC and IL-17RCKO-BMC which correlates to a higher type 17 response. Inducers of IFN-γ production, IL-12 and IL-27, were also elevated in the IL-17RAKO-BMC and IL-17RCKO-BMC mice respectively, compared to WT-BMC. CCL3 and CXCL2 were elevated in the lung of chimeric mice but to a greater extent in the IL-17RCKO-BMC mice. Interestingly, it has been reported that the expression of CXCL2 is related to persistent *C. trachomatis* infection while CCL3 and IL-2 are upregulated over time during infection (244). Also, IL-17RCKO-BMC mice had heightened active IL-1β and IL-18 production compared to WT-BMC mice. Inactive precursors of IL-1β and IL-18 are cleaved into bioactive cytokines when inflammasomes activate intracellular caspase-1 (245). IL-18 is important for the induction of Th1 responses, characterized by the production of IFN-γ (245). IL-1β is important for the differentiation of Th17 responses and is amplified in the presence of IL-23 (246). However, IFN-γ and IL-23 were not significantly heightened in the BAL of IL-17RCKO-BMC mice which did not agree with the elevated type 1 responses observed in the lung by ICCS. These results suggest that the production of IFN-γ in the cells was elevated, detected by ICCS after PMA stimulation, but release of IFN-γ from the cells was detected at lower levels in the IL-17RCKO-BMC mice. Therefore, future experiments measuring the

cytokine levels in the lung homogenate from the chimeric mice are important. Together, these results show that loss of IL-17RA and IL-17RC in the tissue stromal cells results in differential cytokine and chemokine responses in the lung during respiratory *Cm* infection. However, with these results, it is still unclear what may be the specific mechanism triggering the induction of ILC17s and differential immune responses in the lung of *Cm*-infected IL-17RAKO-BMC and IL-17RCKO-BMC mice. A change in the cytokine environment in the lung may be the driving factor for induction of ILC17s which warrant a closer examination of the cytokine production in the lung tissue. Also, T cells can regulate the population size and function of ILC3s in the intestine (240) and therefore, examination of this mechanism in the lung may be important in our model.

4.5 Conclusions

Currently, there needs to be a safe and effective vaccine for *Chlamydia* species to address the gradual rise in *Chlamydia* infections worldwide despite the availability of antibiotics and improved screening for sexually transmitted infections. To develop a vaccine, extensive research on the immunobiology, and protective versus detrimental immune responses to *Chlamydia* infection, are essential. Although there has been research to develop a vaccine, it has proven difficult due to the incomplete understanding of the immune mechanisms involved in host resistance and immunopathology during infection.

Many reports have shown that the balance in IL-17A/Th17 responses in *Chlamydia* infection are crucial due to immunopathology that can occur through heightened Th17 responses (81, 82, 149, 204). Currently, there have been no studies dissecting the role of IL-17RA and IL-17RC in the tissue stromal cells in shaping the adaptive immune response

during *Chlamydia* infection. We hypothesized that IL-17RA and IL-17RC are important in controlling *Cm* infection and may differentially shape the host immune responses.

When there was a loss in IL-17RC in the tissue stromal cells, a type 1 response through production of IFN-γ and Th17 response was enhanced. In contrast, loss of IL-17RA resulted in heightened type 17 responses with IL-17A production coming from Th17 cells and ILC17s, but no increase in Th1. This is a novel finding whereby IL-17RA not only controls the typical IL-17A responses from CD4+ T cells, but also of an under described group of innate lymphoid cells in the lung. There have been few reports on ILC3s in the lung of mice and humans (99, 247), but they have never been associated with IL-17RA in the during *Chlamydia* infection. Suboptimal IL-17RA or IL-17RC function in the tissue stromal cells resulted in differential adaptive immune responses which could be induced by different soluble mediators or forms of cell death (Figure 4.1). IL-17RA and IL-17RC is required in the tissue stromal cells to control differential forms of subsequent immunopathology. This is indicative that the immune response to *Chlamydia* infection is shaped by individual IL-17RA and IL-17RC roles in the tissue stromal cells which is independent on *Chlamydia* replication.

Investigation and elucidation of the specific roles of IL-17RA and IL-17RC in non-hematopoietic cells provides insights into additional pathways and mediators that are important in *Chlamydia* infection and potentially other intracellular bacterial infections. The data generated in this study have important implications for the control of *Chlamydia* infections and may give indications on how to design vaccines strategically to control the balance between protective and non-protective immune responses. With the knowledge that ILC3s can direct adaptive immune responses, specifically the CD4+ T cell responses, we

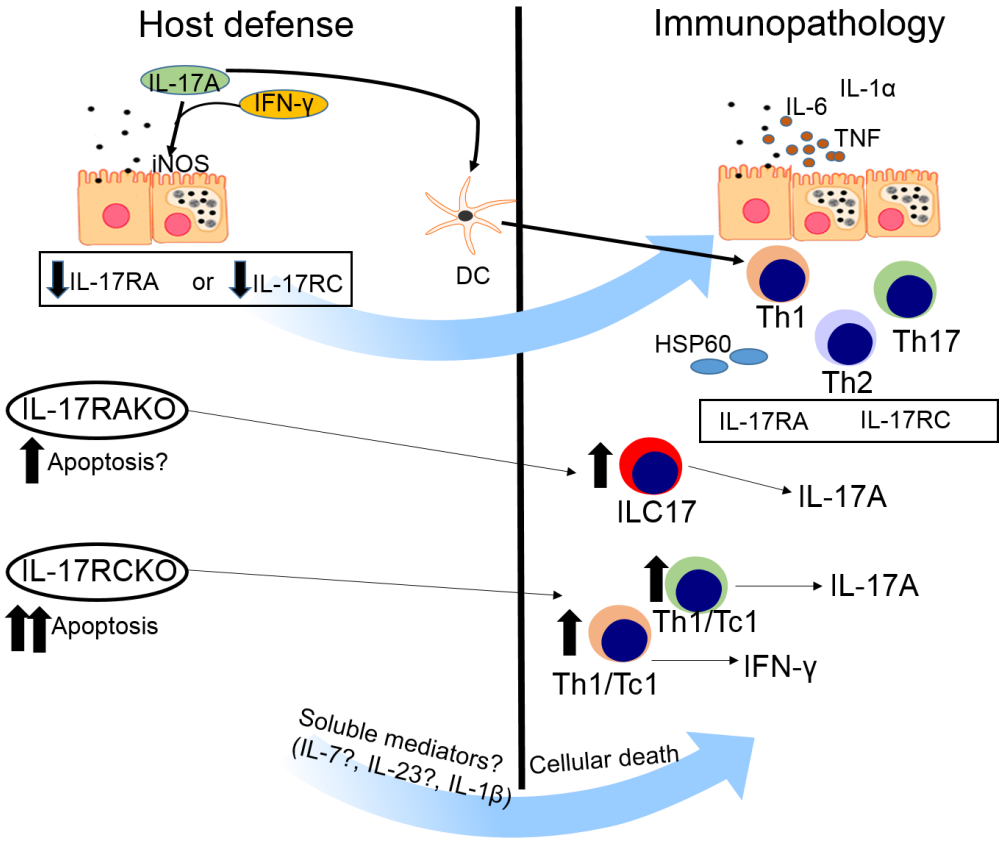

Figure 4.1 Model of *Cm* infection in non-hematopoietic cells and IL-17A/IL-17R immunity. The role of IL-17A in *Chlamydia* infection has been inconsistent. IL-17A has no direct effect on chlamydial replication and instead enhances proinflammatory cytokines. IL-17A is important in inducing protective Th1 responses by modulating dendritic cells to indirectly control *Chlamydia* replication. Alternatively, IL-17A directly inhibits *Chlamydia* growth by synergizing with IFN-γ to induce iNOS. A heightened Th17 response and subsequent IL-17A production during *Chlamydia* infection is detrimental, causing immunopathology. The host defence against *Chlamydia* infection and its impact on the immunopathology and vice versa is unclear. The current study focused on creating a suboptimum initial host defence against *Chlamydia* infection via IL-17RA and IL-17RC knockout mice and investigating how this affects the adaptive immune response leading to subsequent immunopathology. Loss of IL-17RA and IL-17RC signaling in the tissue structure cells resulted in higher bacterial burden, driving immunopathology. Further, suboptimal IL-17RA or IL-17RC function in the tissue stromal cells resulted in differential adaptive immune responses which could be a result of induction of different soluble mediators and forms of cell death. IL-17RA and IL-17RC is required in the tissue stromal cells to control differential forms of subsequent immunopathology. This is indicative that the immune response to *Chlamydia* infection is shaped by individual IL-17RA and IL-17RC roles in the tissue stromal cells which is independent on *Chlamydia* replication. HSP60, heat shock protein 60; IFN-γ, interferon-γ; IL, interleukin; IL-17RAKO, interleukin-17 receptor A knockout; IL-17RCKO, interleukin-17 receptor C knockout; ILC, innate lymphoid cell; iNOS, inducible nitric oxide; Tc, T cytotoxic; Th, T helper; TNF, tumor necrosis factor (32, 129, 198).

predict that targeting ILC3s might provide early regulation of immune responses in therapeutic strategies against pathogens. Since ILCs are important immune cells prior to the development of the adaptive immune response, this provides a new avenue for immunotherapies. In our model, ILC3 cells were exacerbated with a loss of IL-17RA in the tissue stromal cells and worsened overall *Cm* infection in mice. Therefore, ILC3s can potentially be a therapeutic target in our current model of *Chlamydia* infection. However, the specific activators for ILCs are not fully understood. Some of the activators for ILC subsets also induce T cells (91) and therefore, cytokine therapies would need to be provided or blocked locally and time-dependently to avoid detrimental systemic immune responses. Alternatively, specific receptors on ILC3s may be targeted or blocked as a form of immunotherapy but these receptors are also not clearly understood. Overall, the results from the current study indicate that IL-17RA and IL-17RC in the tissue stromal cells are important during *Cm* infection and may serve as an important therapeutic target for regulating the type 1 and type 17 responses to ensure the balance of these adaptive immune responses are sufficient for controlling the infection.

Having a better understanding of the role of IL-17A/IL-17AR during *Chlamydia* infection could guide us to an improved formulation of a *Chlamydia* vaccine that will shape the most ideal immune response against the infection. This is the first study in the *Chlamydia* research field that provides in-depth immune characterization of this novel animal model of respiratory *Chlamydia* infection.

4.6 Future directions

For further characterization of *in vitro* results in my study, *Cm* infection of primary epithelial cells from WT, IL-17RAKO, and IL-17RCKO mice could be performed with or without IL-17A and/or IFN-γ stimulation. Since epithelial cells are the first responders to *Chlamydia* infection, results from experiments performed on these cells would be more characteristic of observations *in vivo*. Additionally, *Cm*-infected IL-17RAKO and IL-17RCKO epithelial cells could also be stimulated with IL-17A and/or IFN-γ. Results from these experiments would provide a complete characterization of the effects of IL-17A on chlamydial growth and any facilitation of the inhibitory effects of IFN-γ across many tissue stromal cells *in vitro*.

To further characterize the *in vivo* results in my study, neutralizing antibody against IL-17C and/or IL-17E could be administered to *Cm*-infected IL-17RCKO-BMC mice, which would still have IL-17RA intact in the tissue structure cells. Results from this model could confirm whether IL-17C and IL-17E indeed do not contribute to the control of chlamydial infection *in vivo*. Additionally, the respiratory *Cm* infection model that was established in the current study could be used as a mouse model for a persistent *Chlamydia* infection model. IL-17RAKO-BMC and IL-17RCKO-BMC mice had elevated bacterial burden at day 11 p.i. whereas WT-BMC mice seemed to reduce their bacterial levels by this time point. Longer time points of *Cm* infection in our model may indicate whether the *Cm* in the IL-17RAKO-BMC and IL-17RCKO-BMC mice could become persistent. If persistent infection is established in these mice, this may suggest a role for IL-17RA or IL-17RC and possible immune responses involved in persistent *Cm* infection.

REFERENCES

1. Hafner, L., K. Beagley, and P. Timms. 2008. *Chlamydia trachomatis* infection: host immune responses and potential vaccines. *Mucosal Immunol.* 1: 116–30.

2. Brunham, R. C., and J. Rey-Ladino. 2005. Immunology of *Chlamydia* infection: implications for a *Chlamydia trachomatis* vaccine. *Nat. Rev. Immunol.* 5: 149–61.

3. Newman, L., J. Rowley, S. Vander Hoorn, N. S. Wijesooriya, M. Unemo, N. Low, G. Stevens, S. Gottlieb, J. Kiarie, and M. Temmerman. 2015. Global estimates of the prevalence and incidence of four curable sexually transmitted infections in 2012 based on systematic review and global reporting. *PLoS One* 10: e0143304.

4. Peipert, J. F. 2003. Genital chlamydial infections. *N. Engl. J. Med.* 349: 2424–30.

5. Cecil, J. A., M. R. Howell, J. J. Tawes, J. C. Gaydos, K. T. McKee Jr, T. C. Quinn, and C. A. Gaydos. 2001. Features of *Chlamydia trachomatis* and *Neisseria gonorrhoeae* infection in male army recruits. *Source J. Infect. Dis.* 1841737287: 1216–9.

6. Bastidas, R. J., C. A Elwell, J. N. Engel, and R. H. Valdivia. 2013. Chlamydial intracellular survival strategies. *Cold Spring Harb. Perspect. Med.* 3: a010256.

7. Marrazzo, J., and R. Suchland. 2014. Recent advances in understanding and managing *Chlamydia trachomatis* infections. *F1000Prime Rep.* 6: 120.

8. Numazaki, K., H. Asanuma, and Y. Niida. 2003. *Chlamydia trachomatis* infection in early neonatal period. *BMC Infect. Dis.* 3: 2.

9. Colarizi, P., C. Chiesa, L. Pacifico, E. Adorisiol, N. Rossi, A. Ranucci, L. S. Annicchiarico, and A. Panero. 1996. *Chlamydia trachomatis*-associated respiratory disease in the very early neonatal period. *Acta Paediatr.* 85: 991–4.

10. Rosenman, M. B., B. E. Mahon, S. M. Downs, and M. B. Kleiman. 2003. Oral erythromycin prophylaxis vs watchful waiting in caring for newborns exposed to *Chlamydia trachomatis*. *Arch. Pediatr. Adolesc. Med.* 157: 565.

11. Mishra, K. N., P. Bhardwaj, A. Mishra, and A. Kaushik. 2011. Acute *Chlamydia trachomatis* respiratory infection in infants. *J. Glob. Infect. Dis.* 3: 216–20.

12. Yang, C., T. Starr, L. Song, J. H. Carlson, G. L. Sturdevant, P. a Beare, W. M. Whitmire, and H. D. Caldwell. 2015. Chlamydial lytic exit from host cells is plasmid regulated. *MBio* 6: e01648–15.

13. Ceovic, R., and S. J. Gulin. 2015. Lymphogranuloma venereum: diagnostic and treatment challenges. *Infect. Drug Resist.* 8: 39–47.

14. Chen, J. C.-R., and R. S. Stephens. 1994. Trachoma and LGV biovars of *Chlamydia trachomatis* share the same glycosaminoglycan-dependent mechanism for infection of eukaryotic cells. *Mol. Microbiol.* 11: 501–7.

15. Falsey, A. R., and E. E. Walsh. 1993. Transmission of *Chlamydia pneumoniae*. *J. Infect. Dis.* 168: 493–6.

16. Hammerschlag, M. R. M. 2000. The role of *Chlamydia* in upper respiratory tract infections. *Curr. Infect. Dis. Rep.* 2: 115–20.

17. Grayston, J. T., L. A. Campbell, C. Kuo, C. H. Mordhorst, P. Saikku, D. H. Thom, and S.-P. Wang. 1990. A new respiratory tract pathogen : *Chlamydia pneumoniae* strain TWAR. *J. Infect. Dis.* 161: 618–25.

18. Webley, W. C., Y. Tilahun, K. Lay, K. Patel, E. S. Stuart, C. Andrzejewski, and P. S. Salva. 2009. Occurrence of *Chlamydia trachomatis* and *Chlamydia pneumoniae* in paediatric respiratory infections. *Eur. Respir. J.* 33: 360–7.

19. Campbell, L. A., and C. Kuo. 2004. *Chlamydia pneumoniae* — an infectious risk factor for atherosclerosis? *Nat. Rev. Microbiol.* 2: 23–32.

20. Hahn, D. L. 1999. *Chlamydia pneumoniae*, asthma, and COPD: what is the evidence? *Ann. Allergy, Asthma Immunol.* 83: 271–92.

21. Saikku, P., K. Mattila, M. S. Nieminen, J. K. Huttunen, M. Leinonen, M. R. Ekman, P. H. Makela, and V. Valtonen. 1988. Serological evidence of an association of novel *Chlamydia*, TWAR, with chronic coronary heart disease and acute myocardial infarction. *Lancet* 332: 983–6.

22. Yang, Z., C. Kuo, and J. T. Grayston. 1995. Systemic dissemination of *Chlamydia pneumoniae* following intranasal inoculation in mice. *J. Infect. Dis.* 171: 736–8.

23. Krüll, M., A. C. Klucken, F. N. Wuppermann, O. Fuhrmann, C. Magerl, J. Seybold, S. Hippenstiel, J. H. Hegemann, C. A. Jantos, and N. Suttorp. 1999. Signal transduction pathways activated in endothelial cells following infection with *Chlamydia pneumoniae*. *J. Immunol.* 162: 4834–41.

24. Smieja, M., R. Leigh, A. Petrich, S. Chong, D. Kamada, F. E. Hargreave, C. H. Goldsmith, M. Chernesky, and J. B. Mahony. 2002. Smoking, season, and detection of *Chlamydia pneumoniae* DNA in clinically stable COPD patients. *BMC Infect. Dis.* 2: 12.

25. Harkinezhad, T., T. Geens, and D. Vanrompay. 2009. *Chlamydophila psittaci* infections in birds: A review with emphasis on zoonotic consequences. *Vet. Microbiol.* 135: 68–77.

26. Bachmann, N. L., T. A. Fraser, C. Bertelli, M. Jelocnik, A. Gillett, O. Funnell, C. Flanagan, G. S. A. Myers, P. Timms, and A. Polkinghorne. 2014. Comparative genomics of koala, cattle and sheep strains of *Chlamydia pecorum*. *BMC Genomics* 15: 667.

27. Donati, M., H. Huot-Creasy, M. Humphrys, M. Di Paolo, A. Di Francesco, and G. S. A. Myers. 2014. Genome sequence of *Chlamydia suis* MD56, Isolated from the conjunctiva of a weaned piglet. *Genome Announc.* 2: e00425–14.

28. Ramsey, K. H., I. M. Sigar, J. H. Schripsema, C. J. Denman, A. K. Bowlin, G. A. S. Myers, and R. G. Rank. 2009. Strain and virulence diversity in the mouse pathogen *Chlamydia muridarum*. *Infect. Immun.* 77: 3284–93.

29. Nigg, C. 1942. An unidentified virus which produces pneumonia and systemic infection in mice. *Science* 95: 49–50.

30. Barron, A. L., H. J. White, R. G. Rank, B. L. Soloff, E. B. Moses, S. The, I. Diseases, N. Jan, A. L. Barron, H. J. White, R. G. Rank, B. L. Soloff, and E. B. Moses. 1981. A new animal model for the study of *Chlamydia trachomatis* genital infections: infection of mice with the agent of mouse pneumonitis. *J. Infect. Dis.* 143: 63–6.

31. Peng, Y., X. Gao, J. Yang, S. Shekhar, S. Wang, Y. Fan, and X. Yang. 2015. Chlamydial lung infection induces transient IL-9 production which is redundant for host defense against primary infection. *PLoS One* 10: e0115195.

32. Zhang, X., L. Gao, L. Lei, Y. Zhong, P. Dube, M. T. Berton, B. Arulanandam, J. Zhang, and G. Zhong. 2009. A MyD88-dependent early IL-17 production protects mice against airway infection with the obligate intracellular pathogen *Chlamydia muridarum*. *J. Immunol.* 183: 1291–300.

33. Asquith, K. L., J. C. Horvat, G. E. Kaiko, A. J. Carey, K. W. Beagley, P. M. Hansbro, and P. S. Foster. 2011. Interleukin-13 promotes susceptibility to chlamydial infection of the respiratory and genital tracts. *PLoS Pathog.* 7: e1001339.

34. Campbell, S., J. Larsen, S. T. Knight, N. R. Glicksman, and P. B. Wyrick. 1998. Chlamydial elementary bodies are translocated on the surface of epithelial cells. *Am. J. Pathol.* 152: 1167–70.

35. AbdelRahman, Y. M., and R. J. Belland. 2005. The chlamydial developmental cycle. *FEMS Microbiol. Rev.* 29: 949–59.

36. Hogan, R. J., S. A. Mathews, S. Mukhopadhyay, J. T. Summersgill, and P. Timms. 2004. Chlamydial persistence: beyond the biphasic paradigm. *Infect. Immun.* 72: 1843–55.

37. Hackstadt, T. 2000. Redirection of host vesicle trafficking pathways by intracellular parasites. *Traffic* 1: 93–9.

38. Moulder, J. W. 1991. Interaction of *Chlamydia*e and host cells in vitro. *Microbiol. Rev.* 55: 143–90.

39. Beatty, W. L., R. P. Morrison, and G. I. Byrne. 1994. Persistent *Chlamydia*e: from cell culture to a paradigm for chlamydial pathogenesis. *Microbiol. Rev.* 58: 686–99.

40. Beatty, W. L., R. P. Morrison, and G. I. Byrne. 1994. Immunoelectron-microscopic quantitation of differential levels of chlamydial proteins in a cell culture model of persistent *Chlamydia trachomatis* infection. *Infect. Immun.* 62: 4059–62.

41. Airenne, S., H. M. Surcel, H. Alakärppä, K. Laitinen, J. Paavonen, P. Saikku, and A. Laurila. 1999. *Chlamydia pneumoniae* infection in human monocytes. *Infect. Immun.* 67: 1445–9.

42. Officer, J. E., and A. Brown. 1961. Serial changes in virus and cells in cultures chronically infected with psittacosis virus. *Virology* 14: 88–99.

43. Hsia, R., H. Ohayon, P. Gounon, A. Dautry-Varsat, and P. M. Bavoil. 2000. Phage infection of the obligate intracellular bacterium, *Chlamydia psittaci* strain guinea pig inclusion conjunctivitis. *Microbes Infect.* 2: 761–72.

44. Kutlin, A., C. Flegg, D. Stenzel, T. Reznik, P. M. Roblin, S. Mathews, P. Timms, and M. R. Hammerschlag. 2001. Ultrastructural study of *Chlamydia pneumoniae* in a continuous-infection model. *J. Clin. Microbiol.* 39: 3721–3.

45. Lee, C. K. 1981. Factors affecting the rate as which a trachoma strain of *Chlamydia trachomatis* establishes persistent infections in mouse fibroblasts (McCoy cells). *Infect. Immun.* 33: 954–7.

46. Moulder, J. W., N. J. Levy, and L. P. Schulman. 1980. Persistent infection of mouse fibroblasts (L cells) with *Chlamydia psittaci*: evidence for a cryptic chlamydial form. *Infect. Immun.* 30: 874–83.

47. Nanagara, R., F. Li, A. Beutler, A. Hudson, and H. R. Schumacher. 1995. Alteration of *Chlamydia trachomatis* biologic behavior in synovial membranes. Suppression of surface antigen production in reactive arthritis and Reiter's syndrome. *Arthritis Rheum.* 38: 1410–7.

48. Thygeson, P. 1963. Epidemiologic observations on trachoma in the United States. *Invest. Ophthalmol. Vis. Sci.* 2: 482–9.

49. Yang, X., and R. Brunham. 1998. T lymphocyte immunity in host defence against *Chlamydia trachomatis* and its implication for vaccine development. *Can. J. Infect. Dis.* 9: 99–108.

50. Geisler, W. M. 2010. Duration of untreated, uncomplicated *Chlamydia trachomatis* genital infection and factors associated with *Chlamydia* resolution: a review of human studies. *J. Infect. Dis.* 201: 104–13.

51. McGhee, J. R., J. Mestecky, M. T. Dertzbaugh, J. H. Eldridge, M. Hirasawa, and H. Kiyono. 1992. The mucosal immune system: from fundamental concepts to vaccine development. *Vaccine* 10: 75–88.

52. Nandi, D., and J. P. Allison. 1993. Characterization of neutrophils and T lymphocytes associated with the murine vaginal epithelium. *Reg. Immunol.* 5: 332–8.

53. Tlaskalová-Hogenová, H., R. Štěpánková, T. Hudcovic, L. Tučková, B. Cukrowska, R. Lodinová-Žádníková, H. Kozáková, P. Rossmann, J. Bártová, D. Sokol, D. P. Funda, D. Borovská, Z. Řeháková, J. Šinkora, J. Hofman, P. Drastich, and A. Kokešová. 2004. Commensal bacteria (normal microflora), mucosal immunity and chronic inflammatory and autoimmune diseases. *Immunol. Lett.* 93: 97–108.

54. Rasmussen, S. J., L. Eckmann, a J. Quayle, L. Shen, Y. X. Zhang, D. J. Anderson, J. Fierer, R. S. Stephens, and M. F. Kagnoff. 1997. Secretion of proinflammatory cytokines by epithelial cells in response to *Chlamydia* infection suggests a central role for epithelial cells in chlamydial pathogenesis. *J. Clin. Invest.* 99: 77–87.

55. Beckett, E. L., S. Phipps, M. R. Starkey, J. C. Horvat, K. W. Beagley, P. S. Foster, and P. M. Hansbro. 2012. TLR2, but not TLR4, is required for effective host defence against *Chlamydia* respiratory tract infection in early life. *PLoS One* 7: e39460.

56. Whitsett, J. A., and T. Alenghat. 2015. Respiratory epithelial cells orchestrate pulmonary innate immunity. *Nat. Immunol.* 16: 27–35.

57. Schwandner, R., R. Dziarski, H. Wesche, M. Rothe, and C. J. Kirschning. 1999. Peptidoglycan- and lipoteichoic acid-induced cell activation is mediated by toll-like receptor 2. *J. Biol. Chem.* 274: 17406–9.

58. Wyrick, P. B., J. Choong, C. H. Davis, S. T. Knight, M. O. Royal, A. S. Maslow, and C. R. Bagnell. 1989. Entry of genital *Chlamydia trachomatis* into polarized human epithelial cells. *Infect. Immun.* 57: 2378–89.

59. Tang, L., J. Chen, Z. Zhou, P. Yu, Z. Yang, and G. Zhong. 2015. *Chlamydia*-secreted protease CPAF degrades host antimicrobial peptides. *Microbes Infect.* 17: 402–8.

60. Porter, E., H. Yang, S. Yavagal, G. C. Preza, O. Murillo, H. Lima, S. Greene, L. Mahoozi, M. Klein-Patel, G. Diamond, S. Gulati, T. Ganz, P. A. Rice, and A. J. Quayle. 2005. Distinct defensin profiles in *Neisseria gonorrhoeae* and *Chlamydia trachomatis* urethritis reveal novel epithelial cell-neutrophil interactions. *Infect. Immun.* 73: 4823–33.

61. Shimada, K., T. R. Crother, and M. Arditi. 2012. Innate immune responses to *Chlamydia pneumoniae* infection: role of TLRs, NLRs, and the inflammasome. *Microbes Infect.* 14: 1301–7.

62. Kumar, H., T. Kawai, and S. Akira. 2011. Pathogen recognition by the innate immune system. *Int. Rev. Immunol.* 30: 16–34.

63. Welter-Stahl, L., D. M. Ojcius, J. Viala, S. Girardin, W. Liu, C. Delarbre, D. Philpott, K. A. Kelly, and T. Darville. 2006. Stimulation of the cytosolic receptor for peptidoglycan, Nod1, by infection with *Chlamydia trachomatis* or *Chlamydia muridarum*. *Cell. Microbiol.* 8: 1047–57.

64. Yasir, M., N. D. Pachikara, X. Bao, Z. Pan, and H. Fan. 2011. Regulation of chlamydial infection by host autophagy and vacuolar ATPase-bearing organelles. *Infect. Immun.* 79: 4019–28.

65. Maxion, H. K., and K. A. Kelly. 2002. Chemokine expression patterns differ within anatomically distinct regions of the genital tract during *Chlamydia trachomatis* infection. *Infect. Immun.* 70: 1538–46.

66. Johnson, R. M. 2004. Murine oviduct epithelial cell cytokine responses to *Chlamydia muridarum* infection include interleukin-12-p70 secretion. *Infect. Immun.* 72: 3951–60.

67. Sharma, M., and T. Rudel. 2009. Apoptosis resistance in *Chlamydia*-infected cells: a fate worse than death? *FEMS Immunol. Med. Microbiol.* 55: 154–61.

68. Byrne, G. I., and D. M. Ojcius. 2004. *Chlamydia* and apoptosis: life and death decisions of an intracellular pathogen. *Nat. Rev. Microbiol.* 2: 802–8.

69. Olivares-Zavaleta, N., A. Carmody, R. Messer, W. M. Whitmire, and H. D. Caldwell. 2011. *Chlamydia pneumoniae* inhibits activated human T lymphocyte proliferation by the induction of apoptotic and pyroptotic pathways. *J. Immunol.* 186: 7120–6.

70. Tait, S. W. G., G. Ichim, and D. Green. 2014. Die another way - non-apoptotic mechanisms of cell death. *J. Cell Sci.* 127: 2135–44.

71. Fink, S. L., and B. T. Cookson. 2005. Apoptosis, pyroptosis, and necrosis: mechanistic description of dead and dying eukaryotic cells. *Infect. Immun.* 73: 1907–16.

72. Ying, S., S. F. Fischer, M. Pettengill, D. Conte, S. A. Paschen, D. M. Ojcius, and G. Häcker. 2006. Characterization of host cell death induced by *Chlamydia trachomatis*. *Infect. Immun.* 74: 6057–66.

73. Nazzal, D., A.-V. Cantero, N. Therville, B. Segui, A. Negre-Salvayre, M. Thomsen, and H. Benoist. 2006. *Chlamydia pneumoniae* alters mildly oxidized low-density lipoprotein-induced cell death in human endothelial cells, leading to necrosis rather than apoptosis. *J. Infect. Dis.* 193: 136–45.

74. Jungas, T., P. Verbeke, T. Darville, and D. M. Ojcius. 2004. Cell death, BAX activation, and HMGB1 release during infection with *Chlamydia*. *Microbes Infect.* 6: 1145–55.

75. Nathan, C. 2006. Neutrophils and immunity: challenges and opportunities. *Nat. Rev. Immunol.* 6: 173–182.

76. Lacy, H. M., A. K. Bowlin, L. Hennings, A. M. Scurlock, U. M. Nagarajan, and R. G. Rank. 2011. Essential role for neutrophils in pathogenesis and adaptive immunity in *Chlamydia caviae* ocular infections. *Infect. Immun.* 79: 1889–97.

77. Fridlender, Z. G., J. Sun, S. Kim, V. Kapoor, G. Cheng, L. Ling, G. S. Worthen, and S. M. Albelda. 2009. Polarization of Tumor-Associated Neutrophil (TAN) Phenotype by TGF-β: "N1" versus "N2" TAN. *Cancer Cell* 16: 183–94.

78. Brinkmann, V., U. Reichard, C. Goosmann, B. Fauler, Y. Uhlemann, D. S. Weiss, Y. Weinrauch, and A. Zychlinsky. 2004. Neutrophil extracellular traps kill bacteria. *Science* 303: 1532–5.

79. Tecchio, C., A. Micheletti, and M. A. Cassatella. 2014. Neutrophil-derived cytokines: facts beyond expression. *Front. Immunol.* 5: 508.

80. Cassatella, M. A. 1999. Neutrophil-derived proteins: selling cytokines by the pound. *Adv. Immunol.* 73: 369–509.

81. Jiang, X., C. Shen, H. Yu, K. P. Karunakaran, and R. C. Brunham. 2010. Differences in innate immune responses correlate with differences in murine susceptibility to *Chlamydia muridarum* pulmonary infection. *Immunology* 129: 556–66.

82. Zhou, X., Q. Chen, J. Moore, J. K. Kolls, S. Halperin, and J. Wang. 2009. Critical role of the interleukin-17/interleukin-17 receptor axis in regulating host susceptibility to respiratory infection with *Chlamydia* species. *Infect. Immun.* 77: 5059–70.

83. Horvat, J. C., K. W. Beagley, M. A. Wade, J. A. Preston, N. G. Hansbro, D. K. Hickey, G. E. Kaiko, P. G. Gibson, P. S. Foster, and P. M. Hansbro. 2007. Neonatal chlamydial infection induces mixed T-cell responses that drive allergic airway disease. *Am. J. Respir. Crit. Care Med.* 176: 556–64.

84. Shekhar, S., Y. Peng, X. Gao, A. G. Joyee, S. Wang, H. Bai, L. Zhao, J. Yang, and X. Yang. 2015. NK cells modulate the lung dendritic cell-mediated Th1/Th17 immunity during intracellular bacterial infection. *Eur. J. Immunol.* 45: 2810–20.

85. Sato, K., and S. Fujita. 2007. Dendritic cells-nature and classification. *Allergol. Int.* 56: 183–91.

86. Guilliams, M., F. Ginhoux, C. Jakubzick, S. H. Naik, N. Onai, B. U. Schraml, E. Segura, R. Tussiwand, and S. Yona. 2014. Dendritic cells, monocytes and macrophages: a unified nomenclature based on ontogeny. *Nat. Rev. Immunol.* 14: 571–8.

87. Steinman, R. M. 2007. Dendritic cells: understanding immunogenicity. *Eur. J. Immunol.* 37: S53–S60.

88. Joyee, A. G., and X. Yang. 2013. Plasmacytoid dendritic cells mediate the regulation of inflammatory type T cell response for optimal immunity against respiratory *Chlamydia pneumoniae* infection. *PLoS One* 8: e83463.

89. Guilliams, M., B. N. Lambrecht, and H. Hammad. 2013. Division of labor between lung dendritic cells and macrophages in the defense against pulmonary infections. *Mucosal Immunol.* 6: 464–73.

90. Lagranderie, M., M.-A. Nahori, A.-M. Balazuc, H. Kiefer-Biasizzo, J.-R. Lapa e Silva, G. Milon, G. Marchal, and B. B. Vargaftig. 2003. Dendritic cells recruited to the lung shortly after intranasal delivery of Mycobacterium bovis BCG drive the primary immune response towards a type 1 cytokine production. *Immunology* 108: 352–64.

91. Artis, D., and H. Spits. 2015. The biology of innate lymphoid cells. *Nature* 517: 1–9.

92. Spits, H., D. Artis, M. Colonna, A. Diefenbach, J. P. Di Santo, G. Eberl, S. Koyasu, R. M. Locksley, A. N. J. McKenzie, R. E. Mebius, F. Powrie, and E. Vivier. 2013. Innate lymphoid cells-a proposal for uniform nomenclature. *Nat. Rev. Immunol.* 13: 145–9.

93. Marashian, S., E. Mortaz, H. Jamaati, M. Alavi-Moghaddam, A. Kiani, A. Abedini, J. Garssen, I. M Adcock, and A. Velayati. 2015. Role of innate lymphoid cells in lung disease. *Iran. J. Allergy. Asthma. Immunol.* 14: 346–60.

94. Culley, F. J. 2009. Natural killer cells in infection and inflammation of the lung. *Immunology* 128: 151–63.

95. Tseng, C. T. K., and R. G. Rank. 1998. Role of NK cells in early host response to chlamydial genital infection. *Infect. Immun.* 66: 5867–75.

96. Eberl, G., J. P. Di Santo, and E. Vivier. 2014. The brave new world of innate lymphoid cells. *Nat. Immunol.* 16: 1–5.

97. Klose, C. S. N., M. Flach, L. Möhle, L. Rogell, T. Hoyler, K. Ebert, C. Fabiunke, D. Pfeifer, V. Sexl, D. Fonseca-Pereira, R. G. Domingues, H. Veiga-Fernandes, S. J. Arnold, M. Busslinger, I. R. Dunay, Y. Tanriver, and A. Diefenbach. 2014. Differentiation of type 1 ILCs from a common progenitor to all helper-like innate lymphoid cell lineages. *Cell* 157: 340–56.

98. Neill, D. R., S. H. Wong, A. Bellosi, R. J. Flynn, M. Daly, T. K. A. Langford, C. Bucks, C. M. Kane, P. G. Fallon, R. Pannell, H. E. Jolin, and A. N. J. McKenzie. 2010. Nuocytes represent a new innate effector leukocyte that mediates type-2 immunity. *Nature* 464: 1367–70.

99. Van Maele, L., C. Carnoy, D. Cayet, S. Ivanov, R. Porte, E. Deruy, J. A. Chabalgoity, J. C. Renauld, G. Eberl, A. G. Benecke, F. Trottein, C. Faveeuw, and J. C. Sirard. 2014. Activation of type 3 innate lymphoid cells and interleukin 22 secretion in the lungs during streptococcus *pneumoniae* infection. *J. Infect. Dis.* 210: 493–503.

100. Sawa, S., M. Lochner, N. Satoh-Takayama, S. Dulauroy, M. Bérard, M. Kleinschek, D. Cua, J. P. Di Santo, and G. Eberl. 2011. RORγt+ innate lymphoid cells regulate intestinal homeostasis by integrating negative signals from the symbiotic microbiota. *Nat. Immunol.* 12: 320–6.

101. Dumoutier, L., M. de Heusch, C. Orabona, N. Satoh-Takayama, G. Eberl, J. C. Sirard, J. P. Di Santo, and J. C. Renauld. 2011. IL-22 is produced by γC-independent CD25+ CCR6+ innate murine spleen cells upon inflammatory stimuli and contributes to LPS-induced lethality. *Eur. J. Immunol.* 41: 1075–85.

102. Sonnenberg, G. F., L. A. Fouser, and D. Artis. 2010. Functional biology of the IL-22-IL-22R pathway in regulating immunity and inflammation at barrier surfaces. *Adv. Immunol.* 107: 1–29.

103. Pitt, J. M., E. Stavropoulos, P. S. Redford, A. M. Beebe, G. J. Bancroft, D. B. Young, and A. O'Garra. 2012. Blockade of IL-10 signaling during Bacillus Calmette-Guerin vaccination enhances and sustains Th1, Th17, and innate lymphoid IFN-γ and IL-17 responses and increases protection to *Mycobacterium tuberculosis* infection. *J. Immunol.* 189: 4079–87.

104. Sarma, J. V., and P. A. Ward. 2011. The complement system. *Cell Tissue Res.* 343: 227–35.

105. Wu, M. C. L., F. H. Brennan, J. P. L. Lynch, S. Mantovani, S. Phipps, R. A. Wetsel, M. J. Ruitenberg, S. M. Taylor, and T. M. Woodruff. 2013. The receptor for complement component C3a mediates protection from intestinal ischemia-reperfusion injuries by inhibiting neutrophil mobilization. *Proc. Natl. Acad. Sci.* 110: 9439–44.

106. Klos, A., E. Wende, K. J. Wareham, and P. N. Monk. 2013. International Union of Pharmacology. LXXXVII. Complement peptide C5a, C4a, and C3a receptors. *Pharmacol. Rev.* 65: 500–543.

107. Dutow, P., B. Fehlhaber, J. Bode, R. Laudeley, C. Rheinheimer, S. Glage, R. A. Wetsel, O. Pabst, and A. Klos. 2014. The complement C3a receptor is critical in defense against *Chlamydia psittaci* in mouse lung infection and required for antibody and optimal T cell response. *J. Infect. Dis.* 209: 1269–78.

108. Kandasamy, M., P. C. Ying, A. W. S. Ho, H. R. Sumatoh, A. Schlitzer, T. R. Hughes, D. M. Kemeny, B. P. Morgan, F. Ginhoux, and B. Sivasankar. 2013. Complement mediated signaling on pulmonary CD103(+) dendritic cells is critical for their migratory function in response to influenza infection. *PLoS Pathog.* 9: e1003115.

109. Yang, Z., T. Conrad, Z. Zhou, J. Chen, P. Dutow, A. Klos, and G. Zhong. 2014. Complement factor C5 but not C3 contributes significantly to hydrosalpinx development in mice infected with *Chlamydia muridarum*. *Infect. Immun.* 82: 3154–63.

110. Brunham, R. C., C. C. Kuo, L. Cles, and K. K. Holmes. 1983. Correlation of host immune response with quantitative recovery of *Chlamydia trachomatis* from the human endocervix. *Infect. Immun.* 39: 1491–4.

111. Punnonen, R., P. Terho, V. Nikkanen, and O. Meurman. 1979. Chlamydial serology in infertile women by immunofluorescence. *Fertil. Steril.* 31: 656–9.

112. Ramsey, K. H., L. S. Soderberg, and R. G. Rank. 1988. Resolution of chlamydial genital infection in B-cell-deficient mice and immunity to reinfection. *Infect. Immun.* 56: 1320–5.

113. Morrison, S. G., H. Su, H. D. Caldwell, and R. P. Morrison. 2000. Immunity to murine *Chlamydia trachomatis* genital tract reinfection involves B cells and CD4+ T cells but not CD8+ T cells. *Infect. Immun.* 68: 6979–87.

114. Moore, T., G. A. Ananaba, J. Bolier, S. Bowers, T. Belay, F. O. Eko, and J. U. Igietseme. 2002. Fc receptor regulation of protective immunity against *Chlamydia trachomatis*. *Immunology* 105: 213–21.

115. Igietseme, J. U., F. O. Eko, Q. He, and C. M. Black. 2004. Antibody regulation of T-cell immunity: implications for vaccine strategies against intracellular pathogens. *Expert Rev. Vaccines* 3: 23–4.

116. Chen, K., and J. K. Kolls. 2013. T cell-mediated host immune defenses in the lung. *Annu. Rev. Immunol.* 31: 605–33.

117. Jonuleit, H., and E. Schmitt. 2003. The regulatory T cell family: distinct subsets and their interrelations. *J. Immunol.* 171: 6323–6327.

118. Fazilleau, N., L. Mark, L. J. McHeyzer-Williams, and M. G. McHeyzer-Williams. 2009. Follicular helper T cells: lineage and location. *Immunity* 30: 324–35.

119. Curotto de Lafaille, M. A., and J. J. Lafaille. 2009. Natural and adaptive Foxp3+ regulatory T cells: more of the same or a division of labor? *Immunity* 30: 626–35.

120. Veldhoen, M., C. Uyttenhove, J. van Snick, H. Helmby, A. Westendorf, J. Buer, B. Martin, C. Wilhelm, and B. Stockinger. 2008. Transforming growth factor-beta "reprograms" the differentiation of T helper 2 cells and promotes an interleukin 9-producing subset. *Nat. Immunol.* 9: 1341–6.

121. Metzger, D. W., C. S. Bakshi, and G. Kirimanjeswara. 2007. Mucosal immunopathogenesis of *Francisella tularensis*. *Ann. N. Y. Acad. Sci.* 1105: 266–83.

122. Geng, Y., K. Berencsi, Z. Gyulai, T. Valyi-Nagy, E. Gonczol, and G. Trinchieri. 2000. Roles of interleukin-12 and gamma interferon in murine *Chlamydia pneumoniae* infection. *Infect. Immun.* 68: 2245–53.

123. Salgame, P. 2005. Host innate and Th1 responses and the bacterial factors that control *Mycobacterium tuberculosis* infection. *Curr. Opin. Immunol.* 17: 374–80.

124. Xing, Z., A. Zganiacz, J. Wang, M. Divangahi, and F. Nawaz. 2000. IL-12-independent Th1-type immune responses to respiratory viral infection: requirement of IL-18 for IFN-γ release in the lung but not for the differentiation of viral-reactive Th1-type lymphocytes. *J. Immunol.* 164: 2575–84.

125. Morrison, R. P., and H. D. Caldwell. 2002. Immunity to murine chlamydial genital infection. *Infect. Immun.* 70: 2741–51.

126. Beatty, W. L., T. A. Belanger, A. A. Desai, R. P. Morrison, and G. I. Byrne. 1994. Tryptophan depletion as a mechanism of gamma interferon-mediated chlamydial persistence. *Infect. Immun.* 62: 3705–11.

127. Carlin, J. M., E. C. Borden, P. M. Sondel, and G. I. Byrne. 2016. Biologic-response-modifier-induced indoleamine 2,3-dioxygenase activity in human peripheral blood mononuclear cell cultures. *J. Immunol.* 139: 2414-8.

128. Okamoto, T., S. Toné, H. Kanouchi, C. Miyawaki, S. Ono, and Y. Minatogawa. 2007. Transcriptional regulation of indoleamine 2,3-dioxygenase (IDO) by tryptophan and its analogue. *Cytotechnology* 54: 107–13.

129. Zhang, Y., H. Wang, J. Ren, X. Tang, Y. Jing, D. Xing, G. Zhao, Z. Yao, X. Yang, and H. Bai. 2012. IL-17A synergizes with IFN-γ to upregulate iNOS and NO production and inhibit chlamydial growth. *PLoS One* 7: e39214.

130. Wang, S., Y. Fan, R. C. C.Brunham, and X. Yang. 1999. IFN-γ knockout mice show Th2-associated delayed-type hypersensitivity and the inflammatory cells fail to localize and control chlamydial infection. *Eur. J. Immunol.* 29: 3782–92.

131. Penttilä, J. M., M. Anttila, K. Varkila, M. Puolakkainen, M. Sarvas, P. H. Mäkelä, and N. Rautonen. 1999. Depletion of CD8+ cells abolishes memory in acquired immunity against *Chlamydia pneumoniae* in BALB/c mice. *Immunology* 97: 490–6.

132. Wizel, B., J. Nyström-Asklin, C. Cortes, and A. Tvinnereim. 2008. Role of CD8(+)T cells in the host response to *Chlamydia*. *Microbes Infect.* 10: 1420–30.

133. Perry, L. L., K. Feilzer, S. Hughes, and H. D. Caldwell. 1999. Clearance of *Chlamydia trachomatis* from the murine genital mucosa does not require perforin-mediated cytolysis or Fas-mediated apoptosis. *Infect. Immun.* 67: 1379–85.

134. Li, J., X. Dong, L. Zhao, X. Wang, Y. Wang, X. Yang, H. Wang, and W. Zhao. 2016. Natural killer cells regulate Th1/Treg and Th17/Treg balance in chlamydial lung infection. *J. Cell. Mol. Med.* 20: 1339–51.

135. Lampe, M. F., C. B. Wilson, M. J. Bevan, and M. N. Starnbach. 1998. Gamma interferon production by cytotoxic T lymphocytes is required for resolution of *Chlamydia trachomatis* infection. *Infect. Immun.* 66: 5457–61.

136. Buzoni-Gatel, D., L. Guilloteau, F. Bernard, S. Bernard, T. Chardès, and A. Rocca. 1992. Protection against *Chlamydia psittaci* in mice conferred by Lyt-2+ T cells. *Immunology* 77: 284–8.

137. Sieper, J. 2007. Pathogenesis of reactive arthritis. *Psoriatic React. Arthritis A Companion to Rheumatol.* 3: 181–7.

138. Vlcek, K. R., W. Li, S. Manam, B. Zanotti, B. J. Nicholson, K. H. Ramsey, and A. K. Murthy. 2016. The contribution of *Chlamydia*-specific $CD8^+$ T cells to upper genital tract pathology. *Immunol. Cell Biol.* 94: 208–12.

139. Hawkins, R. A., R. G. Rank, and K. A. Kelly. 2002. A *Chlamydia trachomatis*-specific Th2 clone does not provide protection against a genital infection and displays reduced trafficking to the infected genital mucosa. *Infect. Immun.* 70: 5132–9.

140. Agrawal, T., R. Gupta, R. Dutta, P. Srivastava, A. R. Bhengraj, S. Salhan, and A. Mittal. 2009. Protective or pathogenic immune response to genital chlamydial infection in women-A possible role of cytokine secretion profile of cervical mucosal cells. *Clin. Immunol.* 130: 347–54.

141. Zhang, G.-X., B. Gran, S. Yu, J. Li, I. Siglienti, X. Chen, M. Kamoun, and A. Rostami. 2003. Induction of experimental autoimmune encephalomyelitis in IL-12 receptor-2-deficient mice: IL-12 responsiveness is not required in the pathogenesis of inflammatory demyelination in the central nervous system. *J. Immunol.* 170: 2153–60.

142. Peck, A., and E. D. Mellins. 2010. Precarious balance: Th17 cells in host defense. *Infect. Immun.* 78: 32–38.

143. Dardalhon, V., T. Korn, V. K. Kuchroo, and A. C. Anderson. 2008. Role of Th1 and Th17 cells in organ-specific autoimmunity. *J. Autoimmun.* 31: 252–6.

144. O'Connor, W., L. a Zenewicz, and R. a Flavell. 2010. The dual nature of Th17 cells: shifting the focus to function. *Nat. Immunol.* 11: 471–6.

145. Dong, C. 2008. Regulation and pro-inflammatory function of interleukin-17 family cytokines. *Immunol. Rev.* 226: 80–6.

146. Acosta-Rodriguez, E. V, L. Rivino, J. Geginat, D. Jarrossay, M. Gattorno, A. Lanzavecchia, F. Sallusto, and G. Napolitani. 2007. Surface phenotype and antigenic specificity of human interleukin 17-producing T helper memory cells. *Nat. Immunol.* 8: 639–46.

147. Torchinsky, M. B., J. Garaude, A. P. Martin, and J. M. Blander. 2009. Innate immune recognition of infected apoptotic cells directs TH17 cell differentiation. *Nature* 458: 78–82.

148. Andrew, D. W., M. Cochrane, J. H. Schripsema, K. H. Ramsey, S. J. Dando, C. P. O'Meara, P. Timms, and K. W. Beagley. 2013. The duration of *Chlamydia muridarum* genital tract infection and associated chronic pathological changes are reduced in IL-17 knockout mice but protection is not increased further by immunization. *PLoS One* 8: e76664.

149. Moore-Connors, J. M., R. Fraser, S. a Halperin, and J. Wang. 2013. $CD4^+CD25^+Foxp3^+$ regulatory T cells promote Th17 responses and genital tract inflammation upon intracellular *Chlamydia muridarum* infection. *J. Immunol.* 191: 3430–9.

150. Hakimi, H., M. M. Akhondi, M. R. Sadeghi, L. Chamani, M. K. Arababadi, B. N. Ahmadabadi, G. Hassanshahi, and M. S. Fathollahi. 2013. Seminal levels of IL-10, IL-12, and IL-17 in men with asymptomatic *Chlamydia* infection. *Inflammation* 37: 122–6.

151. Iwakura, Y., H. Ishigame, S. Saijo, and S. Nakae. 2011. Functional specialization of interleukin-17 family members. *Immunity* 34: 149–62.

152. Liang, S. C., A. J. Long, F. Bennett, M. J. Whitters, R. Karim, M. Collins, S. J. Goldman, K. Dunussi-Joannopoulos, C. M. M. Williams, J. F. Wright, and L. A. Fouser. 2007. An IL-17F/A heterodimer protein is produced by mouse Th17 cells and induces airway neutrophil recruitment. *J. Immunol.* 179: 7791–9.

153. Wright, J. F., Y. Guo, A. Quazi, D. P. Luxenberg, F. Bennett, J. F. Ross, Y. Qiu, M. J. Whitters, K. N. Tomkinson, K. Dunussi-Joannopoulos, B. M. Carreno, M. Collins, and N. M. Wolfman. 2007. Identification of an interleukin 17F/17A heterodimer in activated human CD4+ T cells. *J. Biol. Chem.* 282: 13447–55.

154. Gaffen, S. 2010. Structure and signalling in the IL-17 receptor superfamily. *Nat. Rev. Immunol.* 9: 556.

155. Song, X., and Y. Qian. 2013. The activation and regulation of IL-17 receptor mediated signaling. *Cytokine* 62: 175–82.

156. Kao, C.-Y., Y. Chen, P. Thai, S. Wachi, F. Huang, C. Kim, R. W. Harper, and R. Wu. 2004. IL-17 markedly up-regulates β-defensin-2 expression in human airway epithelium via JAK and NF-κB signaling pathways. *J. Immunol.* 173: 3482–91.

157. Liang, S. C., X.-Y. Tan, D. P. Luxenberg, R. Karim, K. Dunussi-Joannopoulos, M. Collins, and L. A. Fouser. 2006. Interleukin (IL)-22 and IL-17 are coexpressed by Th17 cells and cooperatively enhance expression of antimicrobial peptides. *J. Exp. Med.* 203: 2271–9.

158. Numasaki, M., Y. Tomioka, H. Takahashi, and H. Sasaki. 2004. IL-17 and IL-17F modulate GM-CSF production by lung microvascular endothelial cells stimulated with IL-1β and/or TNF-α. *Immunol. Lett.* 95: 175–84.

159. Yang, X. O., S. H. Chang, H. Park, R. Nurieva, B. Shah, L. Acero, Y.-H. Wang, K. S. Schluns, R. R. Broaddus, Z. Zhu, and C. Dong. 2008. Regulation of inflammatory responses by IL-17F. *J. Exp. Med.* 205: 1063–75.

160. Yagi, Y., A. Andoh, O. Inatomi, T. Tsujikawa, and Y. Fujiyama. 2007. Inflammatory responses induced by interleukin-17 family members in human colonic subepithelial myofibroblasts. *J. Gastroenterol.* 42: 746–53.

161. Albanesi, C., A. Cavani, and G. Girolomoni. 1999. IL-17 is produced by nickel-specific T lymphocytes and regulates ICAM-1 expression and chemokine production in human keratinocytes: synergistic or antagonist effects with IFN-γ and TNF-α. *J. Immunol.* 162: 494–502.

162. Shalom-Barak, T., J. Quach, and M. Lotz. 1998. Interleukin-17-induced gene expression in articular chondrocytes is associated with activation of mitogen-activated protein kinases and NF-κB. *J. Biol. Chem.* 273: 27467–73.

163. Kotake, S., N. Udagawa, N. Takahashi, K. Matsuzaki, K. Itoh, S. Ishiyama, S. Saito, K. Inoue, N. Kamatani, M. T. Gillespie, T. J. Martin, and T. Suda. 1999. IL-17 in synovial fluids from patients with rheumatoid arthritis is a potent stimulator of osteoclastogenesis. *J. Clin. Invest.* 103: 1345–52.

164. Ishigame, H., S. Kakuta, T. Nagai, M. Kadoki, A. Nambu, Y. Komiyama, N. Fujikado, Y. Tanahashi, A. Akitsu, H. Kotaki, K. Sudo, S. Nakae, C. Sasakawa, and Y. Iwakura. 2009. Differential roles of interleukin-17A and -17F in host defense against mucoepithelial bacterial infection and allergic responses. *Immunity* 30: 108–19.

165. Ishigame, H., S. Kakuta, T. Nagai, M. Kadoki, A. Nambu, Y. Komiyama, N. Fujikado, Y. Tanahashi, A. Akitsu, H. Kotaki, K. Sudo, S. Nakae, C. Sasakawa, and Y. Iwakura. 2009. Differential roles of interleukin-17A and -17F in host defense against mucoepithelial bacterial infection and allergic responses. *Immunity* 30: 108–19.

166. Pappu, R., S. Rutz, and W. Ouyang. 2012. Regulation of epithelial immunity by IL-17 family cytokines. *Trends Immunol.* 33: 343–9.

167. Liu, S.-J., J.-P. Tsai, C.-R. Shen, Y.-P. Sher, C.-L. Hsieh, Y.-C. Yeh, A.-H. Chou, S.-R. Chang, K.-N. Hsiao, F.-W. Yu, and H.-W. Chen. 2007. Induction of a distinct CD8 Tnc17 subset by transforming growth factor-β and interleukin-6. *J. Leukoc. Biol.* 82: 354–60.

168. Sutton, C. E., L. a Mielke, and K. H. G. Mills. 2012. IL-17-producing γδ T cells and innate lymphoid cells. *Eur. J. Immunol.* 42: 2221–31.

169. Ferretti, S., O. Bonneau, G. R. Dubois, C. E. Jones, and A. Trifilieff. 2003. IL-17, produced by lymphocytes and neutrophils, is necessary for lipopolysaccharide-induced airway neutrophilia: IL-15 as a possible trigger. *J. Immunol.* 170: 2106–12.

170. Reynolds, J., P. Angkasekwinai, and C. Dong. 2011. IL-17 family member cytokines: regulation, and function in innate immunity. *Cytokine Growth Factor Rev.* 21: 413–23.

171. Cua, D. J., and C. M. Tato. 2010. Innate IL-17-producing cells: the sentinels of the immune system. *Nat. Rev. Immunol.* 10: 479–89.

172. Hayday, A. C. 2009. γδ T cells and the lymphoid stress-surveillance response. *Immunity* 31: 184–196.

173. Hamada, S., M. Umemura, T. Shiono, K. Tanaka, A. Yahagi, M. D. Begum, K. Oshiro, Y. Okamoto, H. Watanabe, K. Kawakami, C. Roark, W. K. Born, R. O'Brien, K. Ikuta, H. Ishikawa, S. Nakae, Y. Iwakura, T. Ohta, and G. Matsuzaki. 2008. IL-17A produced by γδ T cells plays a critical role in innate immunity against listeria monocytogenes infection in the liver. *J. Immunol.* 181: 3456–63.

174. Lockhart, E., A. M. Green, and J. L. Flynn. 2006. IL-17 production is dominated by γδ T cells rather than CD4 T cells during *Mycobacterium tuberculosis* infection. *J. Immunol.* 177: 4662–9.

175. Kuestner, R. E., D. W. Taft, A. Haran, C. S. Brandt, T. Brender, K. Lum, B. Harder, S. Okada, C. D. Ostrander, J. L. Kreindler, S. J. Aujla, B. Reardon, M. Moore, P. Shea, R. Schreckhise, T. R. Bukowski, S. Presnell, P. Guerra-Lewis, J. Parrish-Novak, J. L. Ellsworth, S. Jaspers, K. E. Lewis, M. Appleby, J. K. Kolls, M. Rixon, J. W. West, Z. Gao, and S. D. Levin. 2007. Identification of the IL-17 receptor related molecule IL-17RC as the receptor for IL-17F. *J. Immunol.* 179: 5462–73.

176. Kramer, J. M., L. Yi, F. Shen, A. Maitra, X. Jiao, T. Jin, and S. L. Gaffen. 2006. Evidence for ligand-independent multimerization of the IL-17 receptor. *J. Immunol.* 176: 711–5.

177. Ramirez-Carrozzi, V., A. Sambandam, E. Luis, Z. Lin, S. Jeet, J. Lesch, J. Hackney, J. Kim, M. Zhou, J. Lai, Z. Modrusan, T. Sai, W. Lee, M. Xu, P. Caplazi, L. Diehl, J. de Voss, M. Balazs, L. Gonzalez, H. Singh, W. Ouyang, and R. Pappu. 2011. IL-17C regulates the innate immune function of epithelial cells in an autocrine manner. *Nat. Immunol.* 12: 1159–66.

178. Monteleone, G., F. Pallone, and T. T. MacDonald. 2010. Interleukin-25: A two-edged sword in the control of immune-inflammatory responses. *Cytokine Growth Factor Rev.* 21: 471–475.

179. Gaffen, S. L. 2009. Structure and signalling in the IL-17 receptor family. *Nat. Rev. Immunol.* 9: 556–67.

180. Angkasekwinai, P., H. Park, Y.-H. Wang, Y.-H. Wang, S. H. Chang, D. B. Corry, Y.-J. Liu, Z. Zhu, and C. Dong. 2007. Interleukin 25 promotes the initiation of proallergic type 2 responses. *J. Exp. Med.* 204: 1509–17.

181. Caruso, R., M. Sarra, C. Stolfi, A. Rizzo, D. Fina, M. C. Fantini, F. Pallone, T. T. MacDonald, and G. Monteleone. 2009. Interleukin-25 inhibits interleukin-12 production and Th1 cell-driven inflammation in the gut. *Gastroenterology* 136: 2270–9.

182. Zaph, C., Y. Du, S. A. Saenz, M. G. Nair, J. G. Perrigoue, B. C. Taylor, A. E. Troy, D. E. Kobuley, R. A. Kastelein, D. J. Cua, Y. Yu, and D. Artis. 2008. Commensal-dependent expression of IL-25 regulates the IL-23-IL-17 axis in the intestine. *J. Exp. Med.* 205: 2191–8.

183. Zambrano-Zaragoza, J. F., E. J. Romo-Martínez, M. D. J. Durán-Avelar, N. García-Magallanes, and N. Vibanco-Pérez. 2014. Th17 cells in autoimmune and infectious diseases. *Int. J. Inflam.* 2014: 651503.

184. Zhu, S., and Y. Qian. 2012. IL-17/IL-17 receptor system in autoimmune disease: mechanisms and therapeutic potential. *Clin. Sci.* 122: 487–511.

185. Wang, A., M. Al-Kuhlani, S. C. Johnston, D. M. Ojcius, J. Chou, and D. Dean. 2013. Transcription factor complex AP-1 mediates inflammation initiated by *Chlamydia pneumoniae* infection. *Cell. Microbiol.* 15: 779–94.

186. Zepp, J., L. Wu, and X. Li. 2011. IL-17 receptor signaling and T helper 17-mediated autoimmune demyelinating disease. *Trends Immunol.* 32: 232–9.

187. Ruddy, M. J., G. C. Wong, X. K. Liu, H. Yamamoto, S. Kasayama, K. L. Kirkwood, and S. L. Gaffen. 2004. Functional cooperation between interleukin-17 and tumor necrosis factor-α is mediated by CCAAT-enhancer-binding protein family members. *J. Biol. Chem.* 279: 2559–67.

188. Curtis, M. M., and S. S. Way. 2009. Interleukin-17 in host defence against bacterial, mycobacterial and fungal pathogens. *Immunology* 126: 177–85.

189. Ye, P., F. H. Rodriguez, S. Kanaly, K. L. Stocking, J. Schurr, P. Schwarzenberger, P. Oliver, W. Huang, P. Zhang, J. Zhang, J. E. Shellito, G. J. Bagby, S. Nelson, K. Charrier, J. J. Peschon, and J. K. Kolls. 2001. Requirement of interleukin 17 receptor signaling for lung CXC chemokine and granulocyte colony-stimulating factor expression, neutrophil recruitment, and host defense. *J. Exp. Med.* 194: 519–27.

190. Happel, K. I., P. J. Dubin, M. Zheng, N. Ghilardi, C. Lockhart, L. J. Quinton, A. R. Odden, J. E. Shellito, G. J. Bagby, S. Nelson, and J. K. Kolls. 2005. Divergent roles of IL-23 and IL-12 in host defense against *Klebsiella pneumoniae*. *J. Exp. Med.* 202: 761–9.

191. Yu, J. J., M. J. Ruddy, H. R. Conti, K. Boonanantanasarn, and S. L. Gaffen. 2008. The interleukin-17 receptor plays a gender-dependent role in host protection against *Porphyromonas gingivalis*-induced periodontal bone loss. *Infect. Immun.* 76: 4206–13.

192. Zelante, T., A. De Luca, C. D'Angelo, S. Moretti, and L. Romani. 2009. IL-17/Th17 in anti-fungal immunity: What's new? *Eur. J. Immunol.* 39: 645–8.

193. Huang, W., L. Na, P. L. Fidel, and P. Schwarzenberger. 2004. Requirement of interleukin-17A for systemic anti–Candida albicans host defense in mice. *J. Infect. Dis.* 190: 624–31.

194. Zelante, T., A. De Luca, P. Bonifazi, C. Montagnoli, S. Bozza, S. Moretti, M. L. Belladonna, C. Vacca, C. Conte, P. Mosci, F. Bistoni, P. Puccetti, R. A. Kastelein, M. Kopf, and L. Romani. 2007. IL-23 and the Th17 pathway promote inflammation and impair antifungal immune resistance. *Eur. J. Immunol.* 37: 2695–706.

195. Ling, Y., S. Cypowyj, C. Aytekin, M. Galicchio, Y. Camcioglu, S. Nepesov, A. Ikinciogullari, F. Dogu, A. Belkadi, R. Levy, M. Migaud, B. Boisson, A. Bolze, Y. Itan, N. Goudin, J. Cottineau, C. Picard, L. Abel, J. Bustamante, J.-L. Casanova, and A. Puel. 2015. Inherited IL-17RC deficiency in patients with chronic mucocutaneous candidiasis. *J. Exp. Med.* 212: 619–31.

196. Schulz, S. M., G. Köhler, C. Holscher, Y. Iwakura, and G. Alber. 2008. IL-17A is produced by Th17, γδ T cells and other CD4- lymphocytes during infection with *Salmonella enterica* serovar Enteritidis and has a mild effect in bacterial clearance. *Int. Immunol.* 20: 1129–38.

197. Freches, D., H. Korf, O. Denis, X. Havaux, K. Huygen, and M. Romano. 2013. Mice genetically inactivated in interleukin-17A receptor are defective in long-term control of *Mycobacterium tuberculosis* infection. *Immunology* 140: 220–31.

198. Bai, H., J. Cheng, X. Gao, A. G. Joyee, Y. Fan, S. Wang, L. Jiao, Z. Yao, and X. Yang. 2009. IL-17/Th17 promotes type 1 T cell immunity against pulmonary intracellular bacterial infection through modulating dendritic cell function. *J. Immunol.* 183: 5886–95.

199. Wolf, K., G. V. Plano, and K. a. Fields. 2009. A protein secreted by the respiratory pathogen *Chlamydia pneumoniae* impairs IL-17 signalling via interaction with human Act1. *Cell. Microbiol.* 11: 769–79.

200. Wolf, K., and K. A. Fields. 2013. *Chlamydia pneumoniae* impairs the innate immune response in infected epithelial cells by targeting TRAF3. *J. Immunol.* 190: 1695–701.

201. Li, D., A. Vaglenov, T. Kim, C. Wang, D. Gao, and B. Kaltenboeck. 2005. High-yield culture and purification of *Chlamydia*ceae bacteria. *J. Microbiol. Methods* 61: 17–24.

202. Elder, J., and C. Brown. 1999. Review of techniques for the diagnosis of *Chlamydia psittaci* infection in psittacine birds. *J Vet Diagn Invest* 11: 539–41.

203. Cotter, T. W., K. H. Ramsey, G. S. Miranpuri, C. E. Poulsen, and G. I. Byrne. 1997. Dissemination of *Chlamydia trachomatis* chronic genital tract infection in gamma interferon gene knockout mice. *Infect. Immun.* 65: 2145–52.

204. O'Meara, C. P., C. W. Armitage, M. C. G. Harvie, D. W. Andrew, P. Timms, N. Y. Lycke, and K. W. Beagley. 2014. Immunity against a *Chlamydia* infection and disease may be determined by a balance of IL-17 signaling. *Immunol. Cell Biol.* 92: 287–97.

205. Samardzic, T., V. Jankovic, S. Stosic-Grujicic, and V. Trajkovic. 2001. STAT1 is required for iNOS activation, but not IL-6 production in murine fibroblasts. *Cytokine* 13: 179–82.

206. Dijkmans, R., and A. Billiau. 1991. Interferon-γ lipopolysaccharide-treated mouse embryonic fibroblasts are killed by a glycolysis L-arginine-dependent process accompanied by depression of mitochondrial respiration. *Eur. J. Biochem.* 202: 151–9.

207. Qiu, H., J. Yang, H. Bai, Y. Fan, S. Wang, X. Han, L. Chen, and X. Yang. 2004. Less inhibition of interferon-gamma to organism growth in host cells may contribute to the high susceptibility of C3H mice to *Chlamydia trachomatis* lung infection. *Immunology* 111: 453–61.

208. Jin, W., and C. Dong. 2013. IL-17 cytokines in immunity and inflammation. *Emerg. Microbes Infect.* 2: e60.

209. Mosolygó, T., J. Korcsik, E. P. Balogh, I. Faludi, D. P. Virók, V. Endrész, and K. Burián. 2013. *Chlamydophila pneumoniae* re-infection triggers the production of IL-17A and IL-17E, important regulators of airway inflammation. *Inflamm. Res.* 62: 451–60.

210. Mosolygó, T., G. Spengler, E. Petra Balogh, V. Endrész, K. Laczi, K. Perei, and K. Burián. 2013. IL-17E production is elevated in the lungs of BALB/c mice in the later stages of *Chlamydia muridarum* infection and re-infection. *In Vivo* 27: 787–792.

211. Wang, C. Q. F., Y. T. Akalu, M. Suarez-Farinas, J. Gonzalez, H. Mitsui, M. A. Lowes, S. J. Orlow, P. Manga, and J. G. Krueger. 2013. IL-17 and TNF synergistically modulate cytokine expression while suppressing melanogenesis: potential relevance to psoriasis. *J. Invest. Dermatol.* 133: 2741–52.

212. Henness, S., C. K. Johnson, Q. Ge, C. L. Armour, J. M. Hughes, and A. J. Ammit. 2004. IL-17A augments TNF-α–induced IL-6 expression in airway smooth muscle by enhancing mRNA stability. *J. Allergy Clin. Immunol.* 114: 958–64.

213. Garg, A. V, M. Ahmed, A. N. Vallejo, A. Ma, and S. L. Gaffen. 2014. The deubiquitinase A20 mediates feedback inhibition of interleukin-17 receptor signaling. *Sci. Signal.* 6: ra44.

214. Moazed, T. C., C. C. Kuo, J. T. Grayston, and L. A. Campbell. 1998. Evidence of systemic dissemination of *Chlamydia pneumoniae* via macrophages in the mouse. *J. Infect. Dis.* 177: 1322–5.

215. Miyairi, I., and G. I. Byrne. 2006. *Chlamydia* and programmed cell death. *Curr. Opin. Microbiol.* 9: 102–8.

216. Perfettini, J. L., V. Hospital, L. Stahl, T. Jungas, P. Verbeke, and D. M. Ojcius. 2003. Cell death and inflammation during infection with the obligate intracellular pathogen, *Chlamydia*. *Biochimie* 85: 763–9.

217. You, Z., X.-B. Shi, G. DuRaine, D. Haudenschild, C. G. Tepper, S. H. Lo, R. Gandour-Edwards, R. W. de Vere White, and A. H. Reddi. 2006. Interleukin-17 receptor-like gene is a novel antiapoptotic gene highly expressed in androgen-independent prostate cancer. *Cancer Res.* 66: 175–83.

218. Silva, M. T., A. Do Vale, and N. M. N. Dos Santos. 2008. Secondary necrosis in multicellular animals: An outcome of apoptosis with pathogenic implications. *Apoptosis* 13: 463–82.

219. Denecker, G., D. Vercammen, M. Steemans, T. Vanden Berghe, G. Brouckaert, G. Van Loo, B. Zhivotovsky, W. Fiers, J. Grooten, W. Declercq, and P. Vandenabeele. 2001. Death receptor-induced apoptotic and necrotic cell death: differential role of caspases and mitochondria. *Cell Death Differ.* 8: 829–40.

220. Fadok, V. A., D. L. Bratton, A. Konowal, P. W. Freed, J. Y. Westcott, and P. M. Henson. 1998. Macrophages that have ingested apoptotic cells *in vitro* inhibit proinflammatory cytokine production through autocrine/paracrine mechanisms involving TGF-β, PGE2, and PAF. *J. Clin. Invest.* 101: 890–8.

221. Albert, M. L., B. Sauter, and N. Bhardwaj. 1998. Dendritic cells acquire antigen from apoptotic cells and induce class I-restricted CTLs. *Nature* 392: 86–89.

222. Jung, S., D. Unutmaz, P. Wong, G.-I. Sano, K. De los Santos, T. Sparwasser, S. Wu, S. Vuthoori, K. Ko, F. Zavala, E. G. Pamer, D. R. Littman, and R. A. Lang. 2002. *In vivo* depletion of CD11c+ dendritic cells abrogates priming of CD8+ T cells by exogenous cell-associated antigens. *Immunity* 17: 211–20.

223. Basu, S., R. J. Binder, R. Suto, K. M. Anderson, and P. K. Srivastava. 2000. Necrotic but not apoptotic cell death releases heat shock proteins, which deliver a partial maturation signal to dendritic cells and activate the NF-κB pathway. *Int. Immunol.* 12: 1539–46.

224. Vromman, F., M. Laverrière, S. Perrinet, A. Dufour, and A. Subtil. 2014. Quantitative monitoring of the *Chlamydia trachomatis* developmental cycle using GFP-expressing bacteria, microscopy and flow cytometry. *PLoS One* 9: e99197.

225. Nagarajan, U. M., J. Sikes, D. Prantner, C. W. Andrews, L. Frazer, A. Goodwin, J. N. Snowden, and T. Darville. 2011. MyD88 deficiency leads to decreased NK Cell gamma interferon production and T cell recruitment during *Chlamydia muridarum* genital tract infection, but a predominant Th1 response and enhanced monocytic inflammation are associated with infection resolution. *Infect. Immun.* 79: 486–98.

226. Scurlock, A. M., L. C. Frazer, C. W. Andrews, C. M. O'Connell, I. P. Foote, S. L. Bailey, K. Chandra-Kuntal, J. K. Kolls, and T. Darville. 2011. Interleukin-17 contributes to generation of Th1 immunity and neutrophil recruitment during *Chlamydia muridarum* genital tract infection but is not required for macrophage influx or normal resolution of infection. *Infect. Immun.* 79: 1349–62.

227. Lu, C., H. Zeng, Z. Li, L. Lei, I.-T. Yeh, Y. Wu, and G. Zhong. 2012. Protective immunity against mouse upper genital tract pathology correlates with high IFNγ but low IL-17 T cell and anti-secretion protein antibody responses induced by replicating chlamydial organisms in the airway. *Vaccine* 30: 475–85.

228. Zhang, X., and M. N. Starnbach. 2015. An excess of the proinflammatory cytokines IFN-γ and IL-12 impairs the development of the memory CD8+ T cell response to *Chlamydia trachomatis*. *J. Immunol.* 195: 1665–75.

229. Nogueira, C. V., X. Zhang, N. Giovannone, E. L. Sennott, and M. N. Starnbach. 2015. Protective immunity against *Chlamydia trachomatis* can engage both CD4+ and CD8+ T cells and bridge the respiratory and genital mucosae. *J. Immunol.* 194: 2319–29.

230. Nagata, T., L. McKinley, J. J. Peschon, J. F. Alcorn, S. J. Aujla, and J. K. Kolls. 2008. Requirement of IL-17RA in Con A induced hepatitis and negative regulation of IL-17 production in mouse T cells. *J. Immunol.* 181: 7473–9.

231. Kumar, P., L. Monin, P. Castillo, W. Elsegeiny, W. Horne, T. Eddens, A. Vikram, M. Good, A. A. Schoenborn, K. Bibby, R. C. Montelaro, D. W. Metzger, A. S. Gulati, and J. K. Kolls. 2016. Intestinal interleukin-17 receptor signaling mediates reciprocal control of the gut microbiota and autoimmune inflammation. *Immunity* 44: 659–671.

232. Johnson, R. M. 2004. Murine oviduct epithelial cell cytokine responses to *Chlamydia muridarum* infection include interleukin-12-p70 secretion. *Infect. Immun.* 72: 3951–60.

233. Chang, S. H., J. M. Reynolds, B. P. Pappu, G. Chen, G. J. Martinez, and C. Dong. 2011. Interleukin-17C promotes Th17 cell responses and autoimmune disease via interleukin-17 receptor E. *Immunity* 35: 611–21.

234. Taube, C., C. Tertilt, G. Gyülveszi, N. Dehzad, K. Kreymborg, K. Schneeweiss, E. Michel, S. Reuter, J.-C. Renauld, D. Arnold-Schild, H. Schild, R. Buhl, and B. Becher. 2011. IL-22 is produced by innate lymphoid cells and limits inflammation in allergic airway disease. *PLoS One* 6: e21799.

235. Monticelli, L. A., G. F. Sonnenberg, M. C. Abt, T. Alenghat, C. G. K. Ziegler, T. A. Doering, J. M. Angelosanto, B. J. Laidlaw, C. Y. Yang, T. Sathaliyawala, M. Kubota, D. Turner, J. M. Diamond, A. W. Goldrath, D. L. Farber, R. G. Collman, E. J. Wherry, and D. Artis. 2011. Innate lymphoid cells promote lung-tissue homeostasis after infection with influenza virus. *Nat. Immunol.* 12: 1045–54.

236. Kim, H. Y., H. J. Lee, Y.-J. Chang, M. Pichavant, S. A. Shore, K. A. Fitzgerald, Y. Iwakura, E. Israel, K. Bolger, J. Faul, R. H. DeKruyff, and D. T. Umetsu. 2014. Interleukin-17-producing innate lymphoid cells and the NLRP3 inflammasome facilitate obesity-associated airway hyperreactivity. *Nat. Med.* 20: 54–61.

237. von Burg, N., S. Chappaz, A. Baerenwaldt, E. Horvath, S. Bose Dasgupta, D. Ashok, J. Pieters, F. Tacchini-Cottier, A. Rolink, H. Acha-Orbea, and D. Finke. 2014. Activated group 3 innate lymphoid cells promote T-cell-mediated immune responses. *Proc. Natl. Acad. Sci. U. S. A.* 111: 12835–40.

238. Sonnenberg, G. F., and D. Artis. 2015. Innate lymphoid cells in the initiation, regulation and resolution of inflammation. *Nat. Med.* 21: 698–708.

239. Gladiator, A., N. Wangler, K. Trautwein-Weidner, and S. LeibundGut-Landmann. 2013. Cutting edge: IL-17-secreting innate lymphoid cells are essential for host defense against fungal infection. *J. Immunol.* 190: 521–5.

240. Hepworth, M. R., L. A. Monticelli, T. C. Fung, C. G. K. Ziegler, S. Grunberg, R. Sinha, A. R. Mantegazza, H.-L. Ma, A. Crawford, J. M. Angelosanto, E. J. Wherry, P. A. Koni, F. D. Bushman, C. O. Elson, G. Eberl, D. Artis, and G. F. Sonnenberg. 2013. Innate lymphoid cells regulate CD4+ T-cell responses to intestinal commensal bacteria. *Nature* 498: 113–7.

241. Mackley, E. C., S. Houston, C. L. Marriott, E. E. Halford, B. Lucas, V. Cerovic, K. J. Filbey, R. M. Maizels, M. R. Hepworth, G. F. Sonnenberg, S. Milling, and D. R. Withers. 2015. CCR7-dependent trafficking of RORγ$^+$ ILCs creates a unique microenvironment within mucosal draining lymph nodes. *Nat. Commun.* 6: 5862.

242. Kinnebrew, M. A., C. G. Buffie, D. E. Gretchen, L. A. Zenewicz, I. Leiner, T. M. Hohl, R. a Flavell, D. R. Littman, and E. G. Pamer. 2013. Intestinal CD103+ CD11b+ lamina propria dendritic cells instruct intestinal epithelial cells to express antimicrobial proteins in response to Toll-like receptor 5 activation. *Immunity* 36: 276–87.

243. Montaldo, E., K. Juelke, and C. Romagnani. 2015. Group 3 innate lymphoid cells (ILC3s): Origin, differentiation, and plasticity in humans and mice. *Eur. J. Immunol.* 45: 2171–82.

244. Schrader, S., A. Klos, S. Hess, H. Zeidler, J. G. Kuipers, and M. Rihl. 2007. Expression of inflammatory host genes in *Chlamydia trachomatis*-infected human monocytes. *Arthritis Res. Ther.* 9: R54.

245. van de Veerdonk, F. L., M. G. Netea, C. A. Dinarello, and L. A. B. Joosten. 2011. Inflammasome activation and IL-1β and IL-18 processing during infection. *Trends Immunol.* 32: 110–116.

246. Gaffen, S. L. 2008. An overview of IL-17 function and signaling. *Cytokine* 43: 402–7.

247. Carrega, P., F. Loiacono, E. Di Carlo, A. Scaramuccia, M. Mora, R. Conte, R. Benelli, G. M. Spaggiari, C. Cantoni, S. Campana, I. Bonaccorsi, B. Morandi, M. Truini, M. C. Mingari, L. Moretta, and G. Ferlazzo. 2015. NCR+ILC3 concentrate in human lung cancer and associate with intratumoral lymphoid structures. *Nat. Commun.* 6: 8280.